Hadronic light-by-light scattering contribution to the muon $g - 2$ from lattice QCD: semi-analytical calculation of the QED kernel

Nils Asmussen,[a] En-Hung Chao,[b] Antoine Gérardin,[c] Jeremy R. Green,[d] Renwick J. Hudspith,[e] Harvey B. Meyer[f,b] and Andreas Nyffeler[*,b]

[a]*Department of Physics and Astronomy, University of Southampton,*
Southampton SO17 1BJ, U.K.

[b]*PRISMA+ Cluster of Excellence & Institut für Kernphysik, Johannes Gutenberg-Universität Mainz,*
D-55099 Mainz, Germany

[c]*Aix-Marseille-Université, Université de Toulon, CNRS, CPT,*
Marseille, France

[d]*Deutsches Elektronen-Synchrotron DESY,*
Platanenallee 6, 15738 Zeuthen, Germany

[e]*GSI Helmholtzzentrum für Schwerionenforschung,*
64291 Darmstadt, Germany

[f]*Helmholtz-Institut Mainz, Johannes Gutenberg-Universität Mainz,*
D-55099 Mainz, Germany

E-mail: asmussen.nils@gmx.de, enchao@uni-mainz.de,
antoine.gerardin@univ-amu.fr, jeremy.green@desy.de,
renwick.james.hudspith@googlemail.com, meyerh@uni-mainz.de,
AndreasNyffeler@gmx.ch

ABSTRACT: Hadronic light-by-light scattering is one of the virtual processes that causes the gyromagnetic factor g of the muon to deviate from the value of two predicted by Dirac's theory. This process makes one of the largest contributions to the uncertainty of the Standard Model prediction for the muon $(g - 2)$. Lattice QCD allows for a first-principles approach to computing this non-perturbative effect. In order to avoid power-law finite-size artifacts generated by virtual photons in lattice simulations, we follow a coordinate-space approach involving a weighted integral over the vertices of the QCD four-point function of the electromagnetic current carried by the quarks. Here we present in detail the semi-analytical calculation of the QED part of the amplitude, employing position-space perturbation theory in continuous, infinite four-dimensional Euclidean space. We also

---

[*]Currently no affiliation.

provide some useful information about a computer code for the numerical implementation of our approach that has been made public at `https://github.com/RJHudspith/KQED`.

Contents

1 Introduction

The anomalous magnetic moment of the muon, $a_\mu \equiv (g-2)_\mu/2$, characterizes its response to a magnetic field, and is one of the most precisely known quantities in fundamental physics. Currently, the experimental world average [1, 2] is in tension with the theoretical evaluation based on the Standard Model (SM) of particle physics. On the basis of the Muon $g-2$

Theory Initiative's 2020 White Paper (WP) [3] with input from refs. [4–23], the tension is at the 4.2σ level. Theoretical and experimental uncertainties are practically equal and just under the level of 0.4 ppm. While a tension between theory and experiment has persisted for about twenty years, the 2021 result of the Fermilab Muon $(g - 2)$ experiment [1] has increased this tension and thereby revived the general interest in possible explanations involving beyond-the-Standard-Model physics, see e.g. [24].

The leading prediction for a_μ in QED is $\frac{\alpha}{2\pi}$ [25], where α is the fine-structure constant. Effects of the strong interaction enter at $O(\alpha^2)$. Due to the low mass scale of the muon, strong-interaction effects in the muon $(g-2)$ must be treated in their full, non-perturbative complexity. As a result, the theory uncertainty of this precision observable is entirely dominated by the hadronic contributions.

The leading hadronic contribution goes under the name of hadronic vacuum polarization (HVP). The situation around the muon $(g - 2)$ has become more intricate with the publication of a lattice-QCD based calculation [26] of the HVP contribution, which finds a larger value than the dispersion-theory based estimate of the WP and would bring the overall theory prediction into far better agreement with the experimental value of a_μ. Thus it will be crucial to resolve the tension between the different determinations of the HVP contribution in order to capitalize on the expected improvements in the experimental determinations of a_μ: a reduction by more than a factor of two is expected from the Fermilab Muon $g - 2$ experiment [27], and further measurements are planned at J-PARC [28] and considered at PSI [29].

An $O(\alpha^3)$ hadronic contribution to a_μ, known as the hadronic light-by-light (HLbL) contribution, also adds significantly to the error budget of the SM prediction. It can be represented as the Feynman diagram depicted in figure 1. In the WP error budget for a_μ, its assigned uncertainty is 0.15 ppm. Therefore, anticipating error reductions in the HVP contribution and in the experimental measurements, it is crucial to further reduce the uncertainty on the HLbL contribution by at least a factor of two.

The HLbL contribution is conceptually more complex than the HVP contribution. On the other hand, being suppressed by an additional power of the fine-structure constant α, the requirements on its relative precision are far less stringent: the uncertainty quoted in the WP corresponds to 20%. In recent years, the HLbL contribution has been evaluated using either dispersive methods, for which a full result can be found in the WP [3] based on refs. [15–21, 23, 30–35], or lattice QCD ([22] and [36]–[37]). Good agreement is found among the three evaluations within the quoted uncertainties.

The purpose of the present paper is to provide a detailed account of the computational strategy underlying our recent calculation [36, 37]. Its full development spanned several years, with progress reported in a number of conferences since 2015 [38–43]. The basic idea is to treat the muon and photon propagators of figure 1 in position-space perturbation theory, in the continuum and in infinite-volume, while the 'hadronic blob' is to be treated in lattice QCD on a spatial torus. Thus much of this paper is concerned with the semi-analytical calculation of the QED part of the amplitude.

The idea to compute the HLbL contribution to a_μ was first proposed in 2005 [44], with a follow-up three years later [45]. These initial methods finally led to the 2014 publica-
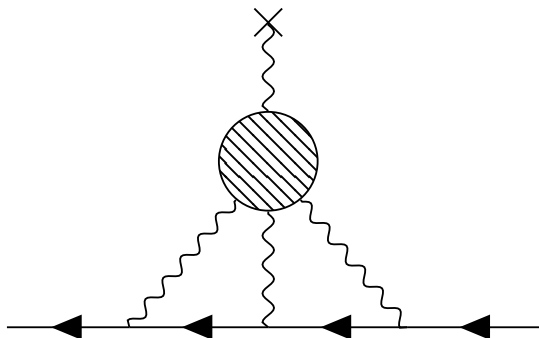
Figure 1. Hadronic light-by-light scattering diagram in the muon $(g-2)$.

tion [46]. In parallel to the development of our strategy, the RBC/UKQCD collaboration then also worked on improving its computational methods [47], with a first exploratory calculation at physical quark masses published in [48]. These methods are based on treating the QED parts of figure 1 within the lattice field theory set up on a finite torus. Starting with ref. [49], the RBC/UKQCD collaboration also developed its own tools to treat the muon and photon propagators in infinite volume. We will return in section 8.1 to some aspects of the cross-fertilization that occurred between the two groups.

It is also worth pointing out other, less direct approaches that have been pursued towards better determining the HLbL contribution to the muon $(g-2)$ using lattice QCD. Of all meson exchanges, the neutral-pion pole contribution is by far the largest, and we have published two lattice calculations of its transition form factor describing its coupling to two (in general) virtual photons [19, 50]. Since the π^0 contribution is the numerically dominant one at long distances, having a dedicated determination thereof also helps control systematic errors at long distances in the direct lattice calculation [51] based on the formalism presented in this paper. As a separate line of study, we have investigated the HLbL scattering amplitude at Euclidean kinematics [52], particularly its eight independent forward-scattering components, which depend on three invariant kinematic variables. Knowing these amplitudes allows one to constrain the contributions of various meson exchanges [52, 53] by parametrizing their transition form factors, information which may subsequently be used to estimate the HLbL contribution to the muon $(g-2)$.

This manuscript is organized as follows. Section 2 presents the general features of our position-space approach and the master-formula for a_μ^{HLbL}. The ingredients necessary for the evaluation of the 'QED kernel' describing all purely QED elements of the amplitude depicted in figure 1 are collected in section 3, at the end of which the averaging over the direction of the muon momentum is performed. A relatively straightforward method of evaluating the final convolution integral yielding the weight functions parametrizing the QED kernel is described in section 4. An alternative, ultimately favored method based on the multipole expansion of the photon propagator in Gegenbauer polynomials is presented in section 5. Some technical aspects of the numerical implementation are given in section 6. Then several models are used in section 7 to compute various contributions to the four-point function of the electromagnetic current in QED and QCD. Since these

– 3 –

contributions to the muon $(g-2)$ have been computed previously (using analytical methods in momentum-space), we use them to perform tests of our position-space QED kernel in section 8. Published results obtained in lattice QCD by the present methods for the quark-connected contribution are also reviewed in that section. Section 9 collects our concluding remarks. The appendices contain additional material useful for numerical implementations, providing in particular the kernel asymptotics for various special kinematic regimes. The final appendix (E) provides some information about a computer code available for the numerical implementation of our approach based on the results of section 5.

2 Master formula for a_μ^{HLbL} in position space

We are interested in the hadronic light-by-light (HLbL) scattering contribution to the anomalous magnetic moment of the muon, see figure 1. The basic idea of our approach is to treat the four-point function of hadronic electromagnetic currents, represented by the blob in figure 1, in lattice QCD regularization, while for the remaining QED part with photons and muons, we use continuum, Euclidean position-space perturbation theory in infinite volume [38–40]. As we will show, this allows a Lorentz covariant, semi-analytical calculation of the QED part which avoids power-law finite-volume corrections $1/L^2$ in a_μ^{HLbL} due to the massless photons. An approach in position space is most natural, since in lattice QCD one obtains the four-point correlation function directly in position space. Furthermore, it will be possible to get directly the HLbL contribution a_μ^{HLbL} as a spatial moment of the four-point correlation function, i.e. no extrapolation of the Pauli form factor $F_2(k^2)$ for $k^2 \to 0$ is needed as tried in earlier attempts in ref. [46].

The HLbL contribution to the muon $(g-2)$ from the light quarks can be obtained from the matrix element of the electromagnetic current

$$j_\rho(x) = \frac{2}{3}(\bar{u}\gamma_\rho u)(x) - \frac{1}{3}(\bar{d}\gamma_\rho d)(x) - \frac{1}{3}(\bar{s}\gamma_\rho s)(x), \tag{2.1}$$

between muon states, which can be parametrized by two form factors (assuming Lorentz symmetry, current conservation as well as parity and charge conjugation invariance)

$$(ie)\langle\mu^-(p')|j_\rho(0)|\mu^-(p)\rangle = -(ie)\bar{u}(p')\Big[\gamma_\rho F_1(k^2) + \frac{\sigma_{\rho\sigma}k_\sigma}{2m}F_2(k^2)\Big]u(p), \tag{2.2}$$

where e is the electric charge of the electron, m is the muon mass, $\sigma_{\rho\sigma} \equiv \frac{i}{2}[\gamma_\rho, \gamma_\sigma]$ and we use γ-matrices in Euclidean space with $\{\gamma_\mu, \gamma_\nu\} = 2\delta_{\mu\nu}$ that are Hermitian, $\gamma_\mu^\dagger = \gamma_\mu$. The on-shell momenta in Euclidean space fulfill $p^2 = p'^2 = -m^2$ and the momentum transfer from the external photon is denoted by $k_\mu = p'_\mu - p_\mu$. The anomalous magnetic moment is then given by the Pauli form factor at vanishing momentum transfer $a_\mu = F_2(0)$.

From the expression for the HLbL diagram in figure 1 in Minkowski space given in ref. [54], we obtain the corresponding result in Euclidean space by performing a Wick

rotation ($\int_q \equiv \int \frac{d^4 q}{(2\pi)^4}$)

$$
\begin{aligned}
(ie)\langle \mu^-(p')|j_\rho(0)|\mu^-(p)\rangle = (-ie)^3\,(ie)^4 \int_{q_1,q_2} &\frac{1}{q_1^2 q_2^2 (q_1 + q_2 - k)^2} \\
\times\, &\frac{-1}{(p'-q_1)^2 + m^2}\,\frac{-1}{(p'-q_1-q_2)^2 + m^2} \\
\times\, &\bar{u}(p')\gamma_\mu(i\slashed{p}' - i\slashed{q}_1 - m)\gamma_\nu(i\slashed{p}' - i\slashed{q}_1 - i\slashed{q}_2 - m)\gamma_\lambda u(p) \\
\times\, &\Pi_{\mu\nu\lambda\rho}(q_1, q_2, k - q_1 - q_2),
\end{aligned} \tag{2.3}
$$

with the QCD four-point correlation function ($\int_x \equiv \int d^4 x$)

$$
\Pi_{\mu\nu\lambda\rho}(q_1, q_2, q_3) = \int_{x,y,z} e^{-i(q_1\cdot x + q_2\cdot y + q_3\cdot z)}\left\langle j_\mu(x) j_\nu(y) j_\lambda(z) j_\rho(0)\right\rangle_{\mathrm{QCD}}. \tag{2.4}
$$

The issue of the Wick rotation in general requires some care. Starting from the time-ordered correlation function with interpolating operators for the muon initial and final states, the standard recipe requires one to Wick rotate the loop momenta, here q_1 and q_2 in eq. (2.3), and the external momenta, here p and p'; see the derivation for a general Feynman diagram in ref. [55]. The expression for the loop integral is initially valid for real Euclidean vectors p, p' and one needs, in principle, to perform an analytic continuation of the final result after all loop integrations have been performed from $p'^2, p^2 > 0$ to $p^2 = p'^2 = -m^2$ to recover the result for an on-shell momentum. In eq. (2.3), we have declared the Euclidean norm of p and p' to be $-m^2$ from the outset, and return to the issue around eq. (2.21) below.

Since the electromagnetic current is conserved, the tensor $\Pi_{\mu\nu\lambda\rho}(q_1, q_2, q_3)$ satisfies the Ward identities (momentum conservation entails $q_1 + q_2 + q_3 + q_4 = 0$)

$$
\{q_{1\mu}; q_{2\nu}; q_{3\lambda}; (q_1 + q_2 + q_3)_\rho\}\,\Pi_{\mu\nu\lambda\rho}(q_1, q_2, q_3) = 0. \tag{2.5}
$$

This implies the relation [56]

$$
\Pi_{\mu\nu\lambda\rho}(q_1, q_2, k - q_1 - q_2) = -k_\sigma \frac{\partial}{\partial k_\rho}\Pi_{\mu\nu\lambda\sigma}(q_1, q_2, k - q_1 - q_2), \tag{2.6}
$$

which allows one to pull out the factor k_σ from the vertex function in eq. (2.3) to obtain the needed form factor $F_2(0)$ with the projection operator [56]

$$
a_\mu^{\mathrm{HLbL}} = F_2(0) = \frac{-i}{48m}\,\mathrm{Tr}\{[\gamma_\rho, \gamma_\sigma](-i\slashed{p} + m)\Gamma_{\rho\sigma}(p,p)(-i\slashed{p} + m)\}\Big|_{p^2 = -m^2}. \tag{2.7}
$$

The HLbL contribution to the vertex function reads for non-vanishing momentum transfer

$$
\begin{aligned}
\Gamma_{\rho\sigma}(p', p) = -e^6 \int_{q_1,q_2} &\frac{1}{q_1^2 q_2^2 (q_1 + q_2 - k)^2}\frac{1}{(p'-q_1)^2 + m^2}\frac{1}{(p'-q_1-q_2)^2 + m^2} \\
\times\, &\Big(\gamma_\mu(i\slashed{p}' - i\slashed{q}_1 - m)\gamma_\nu(i\slashed{p}' - i\slashed{q}_1 - i\slashed{q}_2 - m)\gamma_\lambda\Big) \\
\times\, &\frac{\partial}{\partial k_\rho}\Pi_{\mu\nu\lambda\sigma}(q_1, q_2, k - q_1 - q_2).
\end{aligned} \tag{2.8}
$$

In order go over to a position-space representation for a_μ^{HLbL}, we insert into eq. (2.8) the expression for the four-point function from eq. (2.4) and interchange the integrals over momenta and positions. One can then write the momenta $\slashed{q}_1$ and $\slashed{q}_2$ in the numerator as derivatives with respect to x and y of the exponential function in eq. (2.4) and also perform the derivative with respect to k_ρ to obtain a factor z_ρ.

In this way one gets the following expression for the vertex function at vanishing momentum transfer that enters in the projector in eq. (2.7) in terms of position-space functions

$$\Gamma_{\rho\sigma}(p,p) \;=\; -e^6 \int_{x,y} K_{\mu\nu\lambda}(p,x,y)\, \widehat{\Pi}_{\rho;\mu\nu\lambda\sigma}(x,y), \tag{2.9}$$

with the QED kernel[1]

$$K_{\mu\nu\lambda}(p,x,y) = \gamma_\mu(i\slashed{p} + \slashed{\partial}^{(x)} - m)\gamma_\nu(i\slashed{p} + \slashed{\partial}^{(x)} + \slashed{\partial}^{(y)} - m)\gamma_\lambda\, \mathcal{I}(p,x,y)_{\text{IR reg.}}, \tag{2.10}$$

$$\mathcal{I}(p,x,y)_{\text{IR reg.}} = \int_{q,k} \frac{1}{q^2\,k^2\,(q+k)^2} \frac{1}{(p-q)^2 + m^2} \frac{1}{(p-q-k)^2 + m^2}\, e^{-i(q\cdot x + k\cdot y)}. \tag{2.11}$$

The kernel $K_{\mu\nu\lambda}(p,x,y)$ in eqs. (2.9) and (2.10) is understood to be a function, not a differential operator.

The function

$$\widehat{\Pi}_{\rho;\mu\nu\lambda\sigma}(x,y) \;=\; \int_z iz_\rho \left\langle j_\mu(x)j_\nu(y)j_\sigma(z)j_\lambda(0) \right\rangle_{\text{QCD}} \tag{2.12}$$

in eq. (2.9) is a spatial moment of the four-point function in QCD. Note the order of the indices $\lambda\sigma$ on left-hand side and the order of the currents $j_\sigma(z)j_\lambda(0)$ on the right-hand side. We have frequently used the translation invariance of the four-point function to shift the integration variables x,y or to reverse their direction $z \to -z$. The most important properties of $\widehat{\Pi}$ (Bose and reflection symmetries, transversality from current conservation) are reviewed in subsection 7.1.

Note that the function $\mathcal{I}(p,x,y)_{\text{IR reg.}}$ in eq. (2.11) has a logarithmic infrared divergence for on-shell muon momentum $p^2 = -m^2$ inside the loop integration, i.e. for small q,k with the three massless photon propagators and the two on-shell massive muon propagators. The IR divergence disappears in the kernel $K_{\mu\nu\lambda}(p,x,y)$, after the projection on a_μ^{HLbL} in eq. (2.7), as it should be, since the latter is well defined. After the projection, only terms with derivatives with respect to x and / or y remain, which bring down additional factors of k and / or q from the exponential in eq. (2.11). However, since it is convenient to first compute the scalar function $\mathcal{I}(p,x,y)_{\text{IR reg.}}$, we will regulate the infrared divergence, see details below. After projecting on a_μ^{HLbL} the regulator can be removed.

We insert eq. (2.9) into eq. (2.7), evaluate the trace of the Dirac matrices and obtain the expression

$$a_\mu^{\text{HLbL}} = \frac{me^6}{3} \int_{x,y} \mathcal{L}_{[\rho,\sigma];\mu\nu\lambda}(p,x,y)\, i\widehat{\Pi}_{\rho;\mu\nu\lambda\sigma}(x,y), \tag{2.13}$$

---

[1]Now that the momentum transfer has been set to zero, we use the letter k to denote an integration variable in eq. (2.11).

where the QED kernel is given by

$$
\begin{aligned}
&\mathcal{L}_{[\rho,\sigma];\mu\nu\lambda}(p,x,y) \\
&= \frac{1}{16m^2}\text{Tr}\Big\{(-i\slashed{p}+m)[\gamma_\rho,\gamma_\sigma](-i\slashed{p}+m)K_{\mu\nu\lambda}(p,x,y)\Big\} \quad\quad (2.14) \\
&= -\frac{i}{8m}\text{Tr}\Big\{\big(\slashed{p}[\gamma_\rho,\gamma_\sigma]+2(p_\sigma\gamma_\rho-p_\rho\gamma_\sigma)\big)\gamma_\mu\gamma_\alpha\gamma_\nu\gamma_\beta\gamma_\lambda\Big\}\,\partial_\alpha^{(x)}(\partial_\beta^{(x)}+\partial_\beta^{(y)})\,\mathcal{I} \\
&\quad +\frac{1}{4m}\text{Tr}\Big\{\big(\slashed{p}[\gamma_\rho,\gamma_\sigma]+2(p_\sigma\gamma_\rho-p_\rho\gamma_\sigma)\big)\gamma_\mu\gamma_\alpha\gamma_\nu\Big\}\,p_\lambda\,\partial_\alpha^{(x)}\,\mathcal{I} \\
&\quad +\frac{1}{4m}\text{Tr}\Big\{\big(\slashed{p}[\gamma_\rho,\gamma_\sigma]+2(p_\sigma\gamma_\rho-p_\rho\gamma_\sigma)\big)\gamma_\mu(p_\lambda\gamma_\nu\gamma_\beta-p_\beta\gamma_\nu\gamma_\lambda+p_\nu\gamma_\beta\gamma_\lambda)\Big\}\,(\partial_\beta^{(x)}+\partial_\beta^{(y)})\,\mathcal{I},
\end{aligned}
$$
$$(2.15)$$

and where we used $\slashed{p}\slashed{p}=p^2=-m^2$ and $(-i\slashed{p}+m)(i\slashed{p}+m)=0$. The use of an IR regulator in the function $\mathcal{I}(p,x,y)_{\text{IR reg.}}$ is always understood. As noted above, only terms with derivatives acting on $\mathcal{I}(p,x,y)_{\text{IR reg.}}$ survive after projecting on a_μ^{HLbL}.

It may be worth pointing out some discrete symmetries of the quantities introduced above. First, we note that, for a general vector p,

$$\mathcal{I}(p,x,y)_{\text{IR reg.}} = \mathcal{I}(-p,-x,-y)_{\text{IR reg.}}. \quad\quad (2.16)$$

Second, it is easy to show that

$$\mathcal{I}(p,x,y)_{\text{IR reg.}} = \left(\mathcal{I}(-p^*,x,y)_{\text{IR reg.}}\right)^*, \quad\quad (2.17)$$

$$\mathcal{I}(p,x,y)_{\text{IR reg.}} = \mathcal{I}(p,x,x-y)_{\text{IR reg.}}, \qu\quad (2.18)$$

whence it follows that

$$K_{\lambda\nu\mu}(p,x,x-y) = K_{\mu\nu\lambda}(-p^*,x,y)^\dagger. \qu\quad (2.19)$$

Finally, the latter equation entails the following property for the full kernel,

$$\mathcal{L}_{[\rho,\sigma];\lambda\nu\mu}(p,x,x-y) = -\mathcal{L}_{[\rho,\sigma];\mu\nu\lambda}(-p^*,x,y)^*. \qu\quad (2.20)$$

Our goal is to perform as many integrations of the 8-dimensional integral over x,y in eq. (2.13) as possible (semi-) analytically to have full control over the QED kernel function $\mathcal{L}_{[\rho,\sigma];\mu\nu\lambda}(p,x,y)$. To achieve this, we will rewrite the function $\mathcal{I}(p,x,y)_{\text{IR reg.}}$ in eq. (2.11) in terms of position-space propagators [57–59] and use the method of Gegenbauer polynomials [60–69] to perform the angular integrals and average over the direction of the muon momentum [70] (see also refs. [69, 71]). We will show the details of this calculation in the next sections, but present here first the structure of the final result, our master formula for a_μ^{HLbL} in position space.

As mentioned earlier, we adopt an approach where the Euclidean vector p obeys $p^2 = -m^2$ from the outset, exploiting the fact that the muon is the ground state in the channel of its symmetry. In the context of the use of Gegenbauer polynomials for loop integrals in momentum space in refs. [63, 64] this procedure only works in a straightforward way, if the integrand is a meromorphic function of all the integration variables and all the external invariants, like p^2. Fortunately, in our case one can show that the relevant p-dependent part

of the integrand is a meromorphic function and the analytical continuation to $p^2 = -m^2$ can be performed without problems. Aiming at keeping the absolute size of the imaginary components as small as possible, we thus parametrize the on-shell momentum as follows,

$$p = im\hat{\epsilon}, \quad \hat{\epsilon}^2 = 1, \quad p^2 = -m^2, \tag{2.21}$$

where the unit vector $\hat{\epsilon}$ parametrizes the direction of the muon momentum. From eq. (2.17), for a vector p with purely imaginary components, $\mathcal{I}(p, x, y)_{\text{IR reg.}}$ is real, and so is[2] $\mathcal{L}_{[\rho,\sigma];\mu\nu\lambda}(p, x, y)$. Furthermore, the general property eq. (2.20) becomes

$$\mathcal{L}_{[\rho,\sigma];\lambda\nu\mu}(p, x, x - y) = -\mathcal{L}_{[\rho,\sigma];\mu\nu\lambda}(p, x, y), \qquad p = im\hat{\epsilon}. \tag{2.22}$$

Since a_μ^{HLbL} is a Lorentz scalar, the expression in eq. (2.13) can be averaged over the direction $\hat{\epsilon}$ of the muon momentum ($\int d\Omega_{\hat{\epsilon}} = 2\pi^2$),

$$\bar{\mathcal{L}}_{[\rho,\sigma];\mu\nu\lambda}(x, y) = \frac{1}{2\pi^2} \int d\Omega_{\hat{\epsilon}} \, \mathcal{L}_{[\rho,\sigma];\mu\nu\lambda}(p, x, y) \equiv \left\langle \mathcal{L}_{[\rho,\sigma];\mu\nu\lambda}(p, x, y) \right\rangle_{\hat{\epsilon}}. \tag{2.23}$$

In this way we obtain

$$\begin{aligned}
\bar{\mathcal{L}}_{[\rho,\sigma];\mu\nu\lambda}(x, y) = {} & \mathcal{G}^{\text{I}}_{\delta[\rho,\sigma]\mu\alpha\nu\beta\lambda} \langle \hat{\epsilon}_\delta \partial_\alpha^{(x)} (\partial_\beta^{(x)} + \partial_\beta^{(y)}) \mathcal{I} \rangle_{\hat{\epsilon}} \\
& + m \, \mathcal{G}^{\text{II}}_{\delta[\rho,\sigma]\mu\alpha\nu\beta\lambda} \langle \hat{\epsilon}_\delta \hat{\epsilon}_\beta \, \partial_\alpha^{(x)} \mathcal{I} \rangle_{\hat{\epsilon}} \\
& + m \, \mathcal{G}^{\text{III}}_{\delta[\rho,\sigma]\mu\alpha\nu\beta\lambda} \langle \hat{\epsilon}_\alpha \hat{\epsilon}_\delta (\partial_\beta^{(x)} + \partial_\beta^{(y)}) \mathcal{I} \rangle_{\hat{\epsilon}},
\end{aligned} \tag{2.24}$$

where we have defined

$$\mathcal{G}^{\text{I}}_{\delta[\rho,\sigma]\mu\alpha\nu\beta\lambda} \equiv \frac{1}{8} \text{Tr}\Big\{ \Big(\gamma_\delta[\gamma_\rho, \gamma_\sigma] + 2(\delta_{\delta\sigma}\gamma_\rho - \delta_{\delta\rho}\gamma_\sigma)\Big)\gamma_\mu\gamma_\alpha\gamma_\nu\gamma_\beta\gamma_\lambda \Big\}, \tag{2.25}$$

$$\mathcal{G}^{\text{II}}_{\delta[\rho,\sigma]\mu\alpha\nu\beta\lambda} \equiv -\frac{1}{4} \text{Tr}\Big\{ \Big(\gamma_\delta[\gamma_\rho, \gamma_\sigma] + 2(\delta_{\delta\sigma}\gamma_\rho - \delta_{\delta\rho}\gamma_\sigma)\Big)\gamma_\mu\gamma_\alpha\gamma_\nu \Big\} \, \delta_{\beta\lambda}, \tag{2.26}$$

$$\mathcal{G}^{\text{III}}_{\delta[\rho,\sigma]\mu\alpha\nu\beta\lambda} \equiv -\frac{1}{4} \text{Tr}\Big\{ \Big(\gamma_\delta[\gamma_\rho, \gamma_\sigma] + 2(\delta_{\delta\sigma}\gamma_\rho - \delta_{\delta\rho}\gamma_\sigma)\Big)\gamma_\mu(\delta_{\alpha\lambda}\gamma_\nu\gamma_\beta - \delta_{\alpha\beta}\gamma_\nu\gamma_\lambda + \delta_{\alpha\nu}\gamma_\beta\gamma_\lambda) \Big\}. \tag{2.27}$$

The tensors $\mathcal{G}^{\text{A}}_{\delta[\rho,\sigma]\mu\alpha\nu\beta\lambda}$ are sums of products of Kronecker deltas from the traces of the Dirac matrices in Euclidean space. The QED kernel $\bar{\mathcal{L}}_{[\rho,\sigma];\mu\nu\lambda}(x, y)$ inherits from the kernel $\mathcal{L}_{[\rho,\sigma];\mu\nu\lambda}(p, x, y)$ the antisymmetry property

$$\bar{\mathcal{L}}_{[\rho,\sigma];\lambda\nu\mu}(x, x - y) = -\bar{\mathcal{L}}_{[\rho,\sigma];\mu\nu\lambda}(x, y) \tag{2.28}$$

under the transformation ($\mu \leftrightarrow \lambda$, $y \to x - y$) upon averaging both sides of eq. (2.22) over the direction of the muon momentum.

We thus arrive at our master formula for a_μ^{HLbL} in position space (which we have already presented previously in refs. [38–40])

$$a_\mu^{\text{HLbL}} = \frac{me^6}{3} \int_{x,y} \bar{\mathcal{L}}_{[\rho,\sigma];\mu\nu\lambda}(x, y) \, i\widehat{\Pi}_{\rho;\mu\nu\lambda\sigma}(x, y), \tag{2.29}$$

$$\bar{\mathcal{L}}_{[\rho,\sigma];\mu\nu\lambda}(x, y) = \sum_{\text{A=I,II,III}} \mathcal{G}^{\text{A}}_{\delta[\rho,\sigma]\mu\alpha\nu\beta\lambda} T^{\text{A}}_{\alpha\beta\delta}(x, y), \tag{2.30}$$

$$i\widehat{\Pi}_{\rho;\mu\nu\lambda\sigma}(x, y) = -\int_z z_\rho \left\langle j_\mu(x) \, j_\nu(y) \, j_\sigma(z) \, j_\lambda(0) \right\rangle_{\text{QCD}}. \tag{2.31}$$

---

[2]Indeed, the trace of a product of linear combinations of Euclidean Dirac matrices with real coefficients is real.
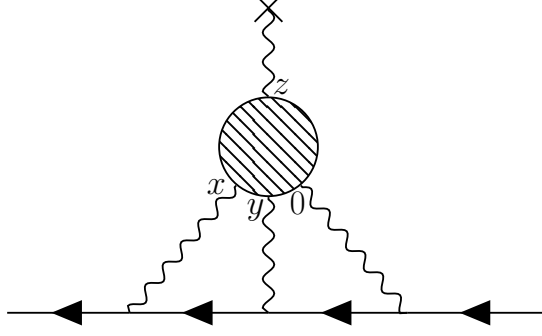
Figure 2. Hadronic light-by-light scattering diagram in the muon $(g - 2)$ with the locations of the vertices $x, y, z, 0$ in the master formula in eq. (2.29).

After contracting the Lorentz indices in eq. (2.29), the integration reduces to a 3-dimensional integral over $|x|, |y|$ and $x \cdot y$. For illustration we depict in figure 2 the HLbL diagram in the muon $(g - 2)$ indicating the positions $x, y, z, 0$ of the four vector currents (attached to the photons) in the master formula in eq. (2.29). We emphasize at this point that the kernel $\bar{\mathcal{L}}$ is far from being unique. A significant amount of freedom remains to adjust the kernel to the needs of practical calculations, without modifying the final value of a_μ^{HLbL}. We return to this aspect in subsection 8.1.

The tensors $T_{\alpha\beta\delta}^{\text{A}}(x, y)$ in eq. (2.30) can be decomposed into a scalar S, a vector V_δ and a tensor part $T_{\beta\delta}$:

$$T_{\alpha\beta\delta}^{\text{I}}(x, y) = \partial_\alpha^{(x)}(\partial_\beta^{(x)} + \partial_\beta^{(y)})V_\delta(x, y), \tag{2.32}$$

$$T_{\alpha\beta\delta}^{\text{II}}(x, y) = m\partial_\alpha^{(x)}\Big(T_{\beta\delta}(x, y) + \frac{1}{4}\delta_{\beta\delta}S(x, y)\Big), \tag{2.33}$$

$$T_{\alpha\beta\delta}^{\text{III}}(x, y) = m(\partial_\beta^{(x)} + \partial_\beta^{(y)})\Big(T_{\alpha\delta}(x, y) + \frac{1}{4}\delta_{\alpha\delta}S(x, y)\Big). \tag{2.34}$$

These parts are given in terms of the function $\mathcal{I}(p, x, y)_{\text{IR reg.}}$ from eq. (2.11) as follows (see eq. (2.24)):

$$S(x, y) = \Big\langle \mathcal{I}(p, x, y)_{\text{IR reg.}} \Big\rangle_{\hat{\epsilon}}, \tag{2.35}$$

$$V_\delta(x, y) = \Big\langle \hat{\epsilon}_\delta \, \mathcal{I}(p, x, y)_{\text{IR reg.}} \Big\rangle_{\hat{\epsilon}}, \tag{2.36}$$

$$T_{\beta\delta}(x, y) = \Big\langle \Big(\hat{\epsilon}_\beta\hat{\epsilon}_\delta - \frac{1}{4}\delta_{\beta\delta}\Big) \mathcal{I}(p, x, y)_{\text{IR reg.}} \Big\rangle_{\hat{\epsilon}}. \tag{2.37}$$

From the property (2.16) of the scalar function $\mathcal{I}(p, x, y)_{\text{IR reg.}}$, it follows that $S(x, y)$ and $T_{\beta\delta}(x, y)$ are even under the simultaneous sign reflection of both their arguments, while $V_\delta(x, y)$ is odd. From here, it follows that the $T_{\alpha\beta\delta}^{\text{A}}(x, y)$ are all odd under $(x, y) \to (-x, -y)$, so that the QED kernel is too,

$$\bar{\mathcal{L}}_{[\rho,\sigma];\mu\nu\lambda}(x, y) = -\bar{\mathcal{L}}_{[\rho,\sigma];\mu\nu\lambda}(-x, -y). \tag{2.38}$$

Since the function $\mathcal{I}(p, x, y)_{\text{IR reg.}}$ is ultraviolet finite by power-counting (including at $x = y = 0$), we conclude that so is the QED kernel, and eq. (2.38) then implies the property

$$\bar{\mathcal{L}}_{[\rho,\sigma];\mu\nu\lambda}(0, 0) = 0. \tag{2.39}$$

The quantity $S(x, y)$ can only be a scalar function $\bar{\mathfrak{g}}^{(0)}$ of the three invariants $|x|, x \cdot y, |y|$; we call this a weight function. The vector and tensor functions will be parametrized by respectively two and three weight functions:

$$S(x, y) = \bar{\mathfrak{g}}^{(0)}(|x|, x \cdot y, |y|), \tag{2.40}$$

$$V_\delta(x, y) = x_\delta \bar{\mathfrak{g}}^{(1)}(|x|, x \cdot y, |y|) + y_\delta \bar{\mathfrak{g}}^{(2)}(|x|, x \cdot y, |y|), \tag{2.41}$$

$$T_{\alpha\beta}(x, y) = \left(x_\alpha x_\beta - \frac{x^2}{4}\delta_{\alpha\beta}\right) \bar{\mathfrak{l}}^{(1)}(|x|, x \cdot y, |y|) + \left(y_\alpha y_\beta - \frac{y^2}{4}\delta_{\alpha\beta}\right) \bar{\mathfrak{l}}^{(2)}(|x|, x \cdot y, |y|)$$
$$+ \left(x_\alpha y_\beta + y_\alpha x_\beta - \frac{x \cdot y}{2}\delta_{\alpha\beta}\right) \bar{\mathfrak{l}}^{(3)}(|x|, x \cdot y, |y|). \tag{2.42}$$

In total, the QED kernel $\bar{\mathcal{L}}_{[\rho,\sigma];\mu\nu\lambda}(x, y)$ in eq. (2.30) is thus parametrized by six weight functions and their derivatives. See appendix A for the explicit expressions of the tensors $T_{\alpha\beta\delta}^{\mathrm{A}}(x, y)$. As we will see in the explicit calculation later, the IR divergence of $\mathcal{I}(p, x, y)_{\mathrm{IR \; reg.}}$ will only be important in the scalar weight function $\bar{\mathfrak{g}}^{(0)}(|x|, x \cdot y, |y|)$, before performing the derivatives in eqs. (2.33) and (2.34).

It is clear that the tensors $S(x, y)$, $V_\delta(x, y)$ and $T_{\beta\delta}(x, y)$ inherit from $\mathcal{I}(p, x, y)_{\mathrm{IR \; reg.}}$ the invariance under $y \to (x - y)$. In turn, their invariance implies the following symmetry properties for the weight functions,

$$\bar{\mathfrak{g}}_*^{(0)} = \bar{\mathfrak{g}}^{(0)}, \tag{2.43}$$

$$\bar{\mathfrak{g}}_*^{(1)} = \bar{\mathfrak{g}}^{(1)} + \bar{\mathfrak{g}}^{(2)}, \tag{2.44}$$

$$\bar{\mathfrak{g}}_*^{(2)} = -\bar{\mathfrak{g}}^{(2)}, \tag{2.45}$$

$$\bar{\mathfrak{l}}_*^{(1)} = \bar{\mathfrak{l}}^{(1)} + \bar{\mathfrak{l}}^{(2)} + 2\bar{\mathfrak{l}}^{(3)}, \tag{2.46}$$

$$\bar{\mathfrak{l}}_*^{(2)} = \bar{\mathfrak{l}}^{(2)}, \tag{2.47}$$

$$\bar{\mathfrak{l}}_*^{(3)} = -\bar{\mathfrak{l}}^{(2)} - \bar{\mathfrak{l}}^{(3)}. \tag{2.48}$$

Unstarred functions have as argument $(|x|, x \cdot y, |y|)$, while starred functions refer to the same weight functions but with argument $(|x|, x \cdot (x - y), |x - y|)$. Furthermore, the rank-three tensors contributing to the QED kernel satisfy[3]

$$T_{\beta\alpha\delta}^{\mathrm{I}}(x, x - y) = T_{\alpha\beta\delta}^{\mathrm{I}}(x, y), \tag{2.49}$$

$$T_{\beta\alpha\delta}^{\mathrm{III}}(x, x - y) = T_{\alpha\beta\delta}^{\mathrm{II}}(x, y). \tag{2.50}$$

We already know that the QED kernel as a whole obeys the antisymmetry property eq. (2.28) under the transformation $(\mu \leftrightarrow \lambda, \; y \to x - y)$. Eq. (2.49), combined with the fact that $\mathcal{G}^{\mathrm{I}}$ is antisymmetric under the simultaneous index exchanges $\mu \leftrightarrow \lambda$ and $\alpha \leftrightarrow \beta$, implies that the contribution to the QED kernel $\mathcal{G}^{\mathrm{I}} T^{\mathrm{I}}$ by itself is antisymmetric under the transformation $(\mu \leftrightarrow \lambda, \; y \to x - y)$.

---

[3]In fact, the contributions $S(x, y)$ and $T_{\beta\delta}(x, y)$ to the rank-three tensors separately satisfy eq. (2.50).
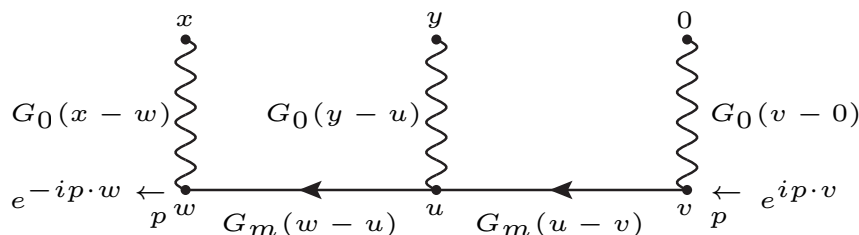
Figure 3. Feynman diagram of the QED part of the HLbL contribution in the muon $g - 2$ in position space, see figure 2, corresponding to the scalar function $\mathcal{I}(p, x, y)_{\text{IR reg.}}$ in eq. (2.11). Note that the arrows on the muon line are only meant for illustration; all propagators are scalar functions. In the derivation, the Euclidean momentum p flowing through the diagram was assumed to be real.

3 Preparatory steps for the calculation of the QED weight functions in position space

In this section, we present some (partly known) results on propagators and their expansion in Gegenbauer polynomials. These preliminaries will allow us to provide the expansion in Gegenbauer polynomials of the function $J(\hat{\epsilon}, u)$, defined in eq. (3.5), which plays a crucial role in the entire calculation. Then, starting in subsection 3.4, we perform the average over the direction of the muon momentum analytically. The final convolution integrals yielding the tensors S, V_δ and $T_{\beta\delta}$ are treated in sections 4 and 5.

3.1 Starting point for the calculation of $\mathcal{I}(p, x, y)_{\text{IR reg.}}$

To obtain a convenient expression for the scalar function $\mathcal{I}(p, x, y)_{\text{IR reg.}}$ in eq. (2.11), we translate the momentum integrals into position-space perturbation theory integrals, where the integration variables correspond to the positions of the vertices, see figure 3.

The relevant Fourier transforms can be performed by using the well-known expressions for the massless and massive propagators in position space [72]:[4]

$$G_0(x - y) = \int_k \frac{e^{ik\cdot(x-y)}}{k^2} = \frac{1}{4\pi^2(x-y)^2} \,, \tag{3.1}$$

$$G_m(x - y) = \int_k \frac{e^{ik\cdot(x-y)}}{k^2 + m^2} = \frac{m}{4\pi^2|x-y|}K_1(m|x-y|) \,, \tag{3.2}$$

where K_1 is a modified Bessel function and we use the conventions from ref. [73]. The propagators in position space are Green's functions of the 'Euclidean Klein-Gordon' equation,

$$(-\triangle^{(x)} + m^2)G_m(x - y) = \delta^{(4)}(x - y), \tag{3.3}$$

and analogously for $m = 0$. Here $\triangle^{(x)} = \sum_{\mu=0}^{3} \partial_\mu^{(x)}\partial_\mu^{(x)}$ is the four-dimensional Laplacian.

These position-space representations of propagators have been used for a long time to evaluate Feynman diagrams, see for instance refs. [57–59, 67, 68]. However, these calculations were mostly dealing with loop integrals, not their Fourier transform as in eq. (2.11);

---

[4]The positions x, y in the definitions of the propagators are generic Euclidean four-vectors and do not correspond to the vertices in the Feynman diagrams in figures 2 and 3.

they involved massless particles (relevant for QCD) and were either aimed at evaluating renormalization constants at higher loop order, or treated Feynman diagrams with a special topology, e.g. of the sun-rise type, where $L+1$ propagators connect the two points x and y in a L-loop diagram. Thus our goal required the development of additional computational methods.

We then obtain as the starting point for the evaluation of the weight-functions of the QED kernel in position space the following representation of the scalar function $\mathcal{I}(p, x, y)_{\text{IR reg.}}$ for $p = im\hat{\epsilon}$:

$$\mathcal{I}(p, x, y)_{\text{IR reg.}} = \int_u G_0(y - u) \, J(\hat{\epsilon}, u) \, J(\hat{\epsilon}, x - u) \,, \tag{3.4}$$

$$J(\hat{\epsilon}, u) = \int_{\tilde{u}} G_0(u - \tilde{u}) e^{m\hat{\epsilon} \cdot \tilde{u}} G_m(\tilde{u}) \,. \tag{3.5}$$

Recall again the need to regulate the IR divergence of the function $\mathcal{I}(p, x, y)_{\text{IR reg.}}$, which is related in position space to the behavior of the integrand in the final integration in eq. (3.4) for large $|u|$, i.e. at long distances. Below we will show that $J(\hat{\epsilon}, u) \sim 1/|u|$ for large $|u|$ and therefore the integral for $\mathcal{I}(p, x, y)_{\text{IR reg.}}$ is logarithmically divergent for large $|u|$, since $\int_u \equiv \int_0^\infty d|u||u|^3 d\Omega_{\hat{u}}$ (with unit-vector $\hat{u} = u/|u|$) and $G_0(y - u) \sim 1/u^2$.

In the derivation of eq. (3.4) we encounter the integral

$$\int_k \frac{e^{ik \cdot x}}{(k - p)^2 + m^2} = e^{ix \cdot p} \, G_m(x) = e^{-m\hat{\epsilon} \cdot x} \, G_m(x) \,. \tag{3.6}$$

The first equality follows, formally, by shifting the integration variable $k \to k - p$. The derivation is formal because with our parametrization of the on-shell momentum $p = im\hat{\epsilon}$ in the integrand, p is a complex Euclidean vector, while the shift in the integration variable assumes that p is a real Euclidean vector. The final result, also used in eq. (3.5), follows by analytical continuation of the expression from a real off-shell vector p to a complex on-shell vector p. The second equality with the on-shell momentum p can be derived directly by using the Schwinger representation of the propagator $((k - p)^2 + m^2)^{-1} = \int_0^\infty d\alpha \exp(-\alpha((k - p)^2 + m^2))$ and then, after the dependence on the components of k_μ has been factorized, performing four simple Gaussian integrals.

Note that although the Feynman diagram from figure 3 is only a tree-level diagram and thus trivial in momentum space, the expression in position space in eq. (3.4) is a non-trivial convolution of propagators and exponentials.

3.2 Gegenbauer method for angular integrals in position space in four dimensions

We summarize first some basic properties of Gegenbauer polynomials which have been used since a long time ago to perform the angular integrations of Feynman loop integrals (hyperspherical approach) in momentum space [63, 64] and in position space [67, 68]. Since we work in $d = 4$ dimensions, we only need the special case of the Gegenbauer polynomials $C_n(\xi) \equiv C_n^{(\alpha=1)}(\xi) \equiv U_n(\xi)$, which are actually equal to the Chebyshev polynomials of the

second kind, see ref. [73].[5] The corresponding generating function is given by

$$\frac{1}{\tau^2 - 2\xi\tau + 1} = \sum_{n=0}^{\infty} \tau^n C_n(\xi), \quad -1 \le \xi \le 1, \quad |\tau| < 1. \tag{3.7}$$

Some low-order Gegenbauer polynomials are given by $C_0(\xi) = 1$, $C_1(\xi) = 2\xi$, $C_2(\xi) = 4\xi^2 - 1$ and therefore $\xi = C_1(\xi)/2$, $\xi^2 = (C_2(\xi) + C_0(\xi))/4$.

Some simple properties of the Gegenbauer polynomials (Chebyshev polynomials of the second kind) are [73]

$$C_n(\cos\theta) = \frac{\sin((n+1)\theta)}{\sin(\theta)}, \tag{3.8}$$

$$C_n(-\xi) = (-1)^n C_n(\xi), \tag{3.9}$$

$$C_n(1) = n+1, \tag{3.10}$$

$$\xi\, C_n(\xi) = \frac{1}{2}\Big[C_{n+1}(\xi) + (1 - \delta_{n0})C_{n-1}(\xi)\Big], \qquad n \ge 0, \tag{3.11}$$

$$\xi^2 C_n(\xi) = \frac{1}{4}\Big[C_{n+2}(\xi) + (2 - \delta_{n0})C_n(\xi) + C_{n-2}(\xi)\Big], \qquad n \ge 0, \tag{3.12}$$

where we adopt in eqs. (3.11) and (3.12) the convention that $C_n(\xi) \equiv 0$ for $n \le -1$. The property (3.9) under parity transformations and the normalization (3.10) follow easily from the generating function in eq. (3.7).

For the evaluation of angular integrals in Feynman diagrams one makes use of the fact that the Gegenbauer polynomials (hyperspherical polynomials) are the polynomials that obey the orthogonality relations

$$\Big\langle C_n(\hat{\epsilon}\cdot\hat{x})\, C_m(\hat{\epsilon}\cdot\hat{y})\Big\rangle_{\hat{\epsilon}} = \frac{\delta_{nm}}{n+1} C_n(\hat{x}\cdot\hat{y}),$$

$$\Big\langle C_n(\hat{\epsilon}\cdot\hat{x})\, C_m(\hat{\epsilon}\cdot\hat{x})\Big\rangle_{\hat{\epsilon}} = \delta_{nm}, \tag{3.13}$$

on the unit sphere, where we denote unit four-vectors as $\hat{x} = x/|x|$, $\hat{y} = y/|y|$.

3.3 Expansion in Gegenbauer polynomials of propagators in position space, of the exponential function and of the function $J(\hat{\epsilon}, y)$

For our goal to perform the angular integrations in the function $\mathcal{I}(p, x, y)_{\text{IR reg.}}$ in eq. (3.4) and the averages in eqs. (2.35), (2.36) and (2.37), it is important to note that if we have a function $f = f(\hat{\epsilon}\cdot x, x^2)$, its dependence on the angle between the vectors $\hat{\epsilon}$ and x can be expanded in Gegenbauer polynomials as follows

$$f(\hat{\epsilon}\cdot x, x^2) = \sum_{n=0}^{\infty} \zeta_n(x^2)\, C_n(\hat{\epsilon}\cdot\hat{x}), \tag{3.14}$$

$$\zeta_n(x^2) = \Big\langle f(\hat{\epsilon}\cdot x, x^2)\, C_n(\hat{\epsilon}\cdot\hat{x})\Big\rangle_{\hat{\epsilon}}, \tag{3.15}$$

where one uses the orthogonality relations in eq. (3.13) to derive the expression for $\zeta_n(x^2)$.

---

[5]Note that in some references $C_n(\xi)$ denotes a dilated Chebyshev polynomial of the first kind.

For later reference we write down the expansions into Gegenbauer polynomials for the massless and massive propagators in position space, the exponential function and the function $J(p, y)$ from eq. (3.5) (again, the vectors x, y in the propagators and in the exponential function are meant to be generic Euclidean four-vectors)

$$4\pi^2 G_0(x - y) \equiv \frac{1}{(x - y)^2} = \sum_{n=0}^{\infty} d_n(x^2, y^2) \, C_n(\hat{x} \cdot \hat{y}), \tag{3.16}$$

$$d_n(x^2, y^2) = \theta(x^2 - y^2) \frac{|y|^n}{|x|^{n+2}} + \theta(y^2 - x^2) \frac{|x|^n}{|y|^{n+2}}, \tag{3.17}$$

$$G_m(x - y) = \sum_{n=0}^{\infty} \gamma_n(x^2, y^2) \, C_n(\hat{x} \cdot \hat{y}), \tag{3.18}$$

$$\gamma_n(x^2, y^2) = \frac{n+1}{2\pi^2 |x||y|} \Big(\theta(x^2 - y^2) \, I_{n+1}(m|y|) \, K_{n+1}(m|x|)$$
$$+ \theta(y^2 - x^2) \, I_{n+1}(m|x|) \, K_{n+1}(m|y|) \Big), \tag{3.19}$$

$$e^{\hat{\epsilon} \cdot x} \equiv e^{x \hat{\epsilon} \cdot \hat{x}} = 2 \sum_{n=0}^{\infty} (n+1) \frac{I_{n+1}(|x|)}{|x|} \, C_n(\hat{\epsilon} \cdot \hat{x}), \qquad x \in \mathbb{R}^4, \tag{3.20}$$

$$J(\hat{\epsilon}, u) = \sum_{n=0}^{\infty} z_n(u^2) \, C_n(\hat{\epsilon} \cdot \hat{u}), \tag{3.21}$$

$$z_n(u^2) = \frac{1}{4\pi^2} \left[I_{n+2}(m|u|) \frac{K_0(m|u|)}{n+1} + I_{n+1}(m|u|) \left(\frac{K_1(m|u|)}{n+1} + \frac{K_0(m|u|)}{m|u|} \right) \right], \tag{3.22}$$

where I_n is another modified Bessel function, see ref. [73]. For integrals involving modified Bessel functions, we have also found the further references [74–77] useful.

The expansion of the massless propagator $G_0(x - y)$ in position space in eqs. (3.16) and (3.17) is formally equal to the corresponding expansion in momentum space and follows immediately from the use of the generating function of the Gegenbauer polynomials in eq. (3.7) to write down the expansion of the massive propagator in Euclidean momentum space and then performing the limit $m \to 0$ [54].

The expansion into Gegenbauer polynomials for the massive propagator $G_m(x - y)$ can be derived as follows. It satisfies the differential equation from eq. (3.3). Since $G_m(x - y)$ is a scalar function, we can choose the coordinate system such that y lies along the positive $\hat{e}_0$ axis, so that x has coordinates $(|x| \cos \phi_1, |x| \sin \phi_1, 0, 0)$ and $\cos \phi_1$ coincides with $\hat{x} \cdot \hat{y}$. The four-dimensional Laplacian operator for a function of $|x|$ and $\cos \phi_1$ reads

$$\triangle^{(x)} = \frac{\partial^2}{\partial |x|^2} + \frac{3}{|x|} \frac{\partial}{\partial |x|} + \frac{1}{|x|^2 \sin^2 \phi_1} \frac{\partial}{\partial \phi_1} \left(\sin^2 \phi_1 \, \frac{\partial}{\partial \phi_1} \right). \tag{3.23}$$

The important fact is that the Gegenbauer polynomials (Chebyshev polynomials of the second kind) are eigenfunctions of the angular part of the Laplacian operator

$$\frac{1}{\sin^2 \phi_1} \frac{\partial}{\partial \phi_1} \left(\sin^2 \phi_1 \, \frac{\partial}{\partial \phi_1} C_n(\cos \phi_1) \right) = -n(n+2) C_n(\cos \phi_1). \tag{3.24}$$

Thus inserting the expansion of $G_m(x-y)$ in eq. (3.18) into the Klein-Gordon equation in eq. (3.3) and applying the differential operator term by term yields the condition

$$\sum_{n=0}^{\infty} \left\{ -\frac{\partial^2}{\partial|x|^2} - \frac{3}{|x|}\frac{\partial}{\partial|x|} + m^2 + \frac{n(n+2)}{|x|^2} \right\} \gamma_n(x^2, y^2) \, C_n(\hat{x} \cdot \hat{y}) = \delta^{(4)}(x-y). \quad (3.25)$$

Using the general expression

$$\delta^{(4)}(x-y) = \frac{1}{|x|^3}\delta(|x|-|y|)\frac{1}{\sin^2\phi_1}\delta(\phi_1-\phi_1^y)\frac{1}{\sin\phi_2}\delta(\phi_2-\phi_2^y)\delta(\phi_3-\phi_3^y), \quad (3.26)$$

we integrate both sides of eq. (3.25) over $\int_0^\pi d\phi_2 \sin\phi_2 \int_0^{2\pi} d\phi_3$ and use the completeness relation of the Gegenbauer polynomials,

$$\frac{2}{\pi}\sum_{n=0}^{\infty} C_n(\cos\phi_1)C_n(\cos\phi_1^y) = \frac{1}{\sin^2\phi_1}\delta(\phi_1-\phi_1^y) \quad (3.27)$$

to obtain

$$4\pi\sum_{n=0}^{\infty}\left\{ -\frac{\partial^2}{\partial|x|^2} - \frac{3}{|x|}\frac{\partial}{\partial|x|} + m^2 + \frac{n(n+2)}{|x|^2}\right\} \gamma_n(x^2, y^2)\, C_n(\hat{x}\cdot\hat{y})$$
$$= \frac{1}{|x|^3}\delta(|x|-|y|)\frac{2}{\pi}\sum_{n=0}^{\infty} C_n(\cos\phi_1^y)\, C_n(\cos\phi_1). \quad (3.28)$$

Choosing again y to lie along the $\hat{e}_0$ direction, we have $\phi_1^y = 0$, $\hat{x}\cdot\hat{y} = \cos\phi_1$ and $C_n(\cos\phi_1^y) = (n+1)$; comparing the series term by term we obtain the differential equation

$$\left\{ -\frac{\partial^2}{\partial|x|^2} - \frac{3}{|x|}\frac{\partial}{\partial|x|} + m^2 + \frac{n(n+2)}{|x|^2}\right\} \gamma_n(x^2, y^2) = \frac{n+1}{2\pi^2|x|^3}\delta(|x|-|y|). \quad (3.29)$$

Two solutions of the homogeneous equation are $K_{n+1}(m|x|)/|x|$ and $I_{n+1}(m|x|)/|x|$. This then leads to the expression for $\gamma_n(x^2, y^2)$ given in eq. (3.19).

We are not aware of any paper, where the expansion into Gegenbauer polynomials of the massive propagator in position space in eqs. (3.18) and (3.19) has been given, even though it is a special case of Gegenbauer's Addition Theorem (see p. 365 of ref. [76]). Note that at $|x| = |y|$, the function $\gamma_n(x^2, y^2)$ is continuous, but not differentiable - there is a cusp. For $m \to 0$ we recover from the expansion of the massive propagator the expansion for the massless propagator.

The expansion into Gegenbauer polynomials for the exponential function in eq. (3.20) follows from the generating function of the Bessel functions I_n and the associated series given in ref. [73]

$$e^{z\cos\theta} = I_0(z) + 2\sum_{n=1}^{\infty} I_n(z)\cos(n\theta), \qquad z \in \mathbb{C}, \quad (3.30)$$

by taking the derivative with respect to θ of both sides of eq. (3.30) and then using eq. (3.8), $z = |x|$ and $\cos\theta = \hat{\epsilon}\cdot\hat{x}$ for $x \in \mathbb{R}^4$. Similar expressions have already been given in refs. [57, 65–68].

For the derivation of the expansion into Gegenbauer polynomials of $J(\hat{\epsilon}, u)$ in eqs. (3.21) and (3.22) we start from the definition of the function in eq. (3.5)

$$J(\hat{\epsilon}, u) = \int_v G_0(u - v)\, e^{m\hat{\epsilon}\cdot v} G_m(v) = \sum_{n=0}^{\infty} z_n(u^2)\, C_n(\hat{\epsilon}\cdot\hat{u}). \qquad (3.31)$$

Inserting the expansions of the massless propagator $G_0(u - v)$ from eqs. (3.16) and (3.17) and of the exponential $e^{m\hat{\epsilon}\cdot v}$ from eq. (3.20), we can use the orthogonality properties of the Gegenbauer polynomials from eq. (3.13) to project on the coefficients $z_n(u^2)$ as in eq. (3.15) to obtain the intermediate result

$$z_n(u^2) = \frac{1}{4\pi^2} \left[\frac{1}{(m|u|)^{n+2}} \int_0^{m|u|} dt\, t^{n+1} I_{n+1}(t) K_1(t) + (m|u|)^n \int_{m|u|}^{\infty} dt\, \frac{I_{n+1}(t)}{t^{n+1}} K_1(t) \right]. \qquad (3.32)$$

For the first integral, we use integration by parts, starting from the observation $K_1(t) = -K_0'(t)$, and then using the well-known identity $\frac{d}{dt}(t^{n+1} I_{n+1}(t)) = t^{n+1} I_n(t)$. We then use the following primitives:

$$\frac{d}{dt}\Big\{ t^{n+2}\Big(K_0(t) I_n(t) + K_1(t) I_{n+1}(t) \Big) \Big\} = 2(n+1) t^{n+1} I_n(t) K_0(t), \qquad (3.33)$$

$$\frac{d}{dt}\Big\{ \frac{1}{t^n}\Big(K_0(t) I_n(t) + K_1(t) I_{n+1}(t) \Big) \Big\} = -\frac{2(n+1)}{t^{n+1}}\, I_{n+1}(t) K_1(t), \qquad (3.34)$$

to obtain the result in eq. (3.22) after some slight rearrangements.

It is worth recording the asymptotics of the coefficients $z_n(u^2)$ for fixed n. Using the known asymptotics of the modified Bessel functions, one finds

$$z_n(u^2) \overset{u^2 \to 0}{=} -\frac{(m|u|)^n}{2^{n+3}\pi^2 \Gamma(n+2)} \left[\log\left(\frac{m|u|}{2}\right) + \gamma_{\mathrm{E}} - \frac{1}{n+1} \right] + \mathrm{O}\left(|u|^{n+2}\right) \qquad (3.35)$$

$$z_n(u^2) \overset{u^2 \to \infty}{=} \frac{n+1}{4\pi^2 m|u|} \Big(\frac{1}{(n+1)^2} - \frac{1}{2m|u|} + \mathrm{O}(u^{-2}) \Big). \qquad (3.36)$$

Furthermore, it is worth noting that

$$\frac{d}{d|u|}(|u| z_n(u^2)) = \frac{(n+1) I_{n+1}(m|u|) K_0(m|u|)}{4\pi^2 m|u|}, \qquad (3.37)$$

and therefore, resumming the expansion in the angular variable using eq. (3.20),

$$\frac{d}{d|u|}(|u| J(\hat{\epsilon}, u)) = \frac{1}{8\pi^2} e^{m\hat{\epsilon}\cdot u} K_0(m|u|). \qquad (3.38)$$

Since $J(\hat{\epsilon}, u)$ is logarithmically divergent for $|u| \to 0$, as can be seen from the definition in eq. (3.5), we have $\lim_{|u|\to 0}(|u| J(\hat{\epsilon}, u)) = 0$. Therefore we can solve this differential equation by simple integration to obtain the integral representation[6]

$$J(\hat{\epsilon}, u) = \frac{1}{8\pi^2 m|u|} \int_0^{m|u|} dt\, e^{t\hat{\epsilon}\cdot\hat{u}}\, K_0(t). \qquad (3.39)$$

From here it is straightforward to obtain the asymptotics of $J(\hat{\epsilon}, u)$ at small and large $|u|$.

---

[6]A very similar function appears in ref. [49].

As already mentioned, around the origin $|u| \to 0$, the function $J(\hat{\epsilon}, u)$ is logarithmically divergent. The precise behavior reads:

$$J(\hat{\epsilon}, u) \overset{|u| \to 0}{\sim} -\frac{1}{16\pi^2} \log(m^2 u^2) + \frac{1}{8\pi^2}(1 - \gamma_{\rm E} + \log(2)) + {\rm O}(|u| \log |u|). \tag{3.40}$$

We note the exactly computable special case if the vector u is collinear with $\hat{\epsilon}$

$$J(\hat{\epsilon}, \pm|u|\hat{\epsilon}) = \frac{1}{8\pi^2}\Big(e^{\pm m|u|}(K_0(m|u|) \pm K_1(m|u|)) \mp \frac{1}{m|u|}\Big). \tag{3.41}$$

In this case, the behavior for large $|u|$ reads

$$J(\hat{\epsilon}, +|u|\hat{\epsilon}) \overset{|u| \to \infty}{\sim} \frac{1}{4\pi\sqrt{2\pi m|u|}}, \qquad\qquad J(\hat{\epsilon}, -|u|\hat{\epsilon}) \overset{|u| \to \infty}{\sim} \frac{1}{8\pi^2 m|u|}. \tag{3.42}$$

For a generic direction of u, we obtain for large $|u|$:

$$J(\hat{\epsilon}, u) \overset{|u| \to \infty}{\sim} \frac{1}{8\pi^2 m|u|}\frac{\pi - \theta}{\sin \theta}, \qquad \cos \theta = \hat{\epsilon} \cdot \hat{u}, \quad 0 < \theta < \pi. \tag{3.43}$$

This behavior at large $|u|$ is obtained from eq. (3.39) by writing the integral $\int_0^{m|u|} = \int_0^\infty - \int_{m|u|}^\infty$. The first term then yields eq. (3.43). The second, using the large-argument expansion of the Bessel function, yields a correction suppressed by $\exp(-2\sin^2(\theta/2)m|u|)$. In particular, the special 'collinear' sector around $\theta = 0$, in which the function $J(\hat{\epsilon}, u)$ only falls off like $(m|u|)^{-1/2}$, has an angular size $\Delta\theta \sim (m|u|)^{-1/2}$.

3.4 Average over the direction of the muon momentum

The product $J(\hat{\epsilon}, u)J(\hat{\epsilon}, x-u)$ can be viewed as a function of $\hat{\epsilon}$ on the unit three-sphere, and can therefore be expanded in scalar, vector, rank-two traceless tensor, etc. components. Computationally, in order to compute S, V_δ and $T_{\beta\delta}$ in eqs. (2.35)–(2.37), it is simpler to first extract these components before performing the convolution with the massless propagator. We therefore introduce the notation

$$s(x, u) = \Big\langle J(\hat{\epsilon}, u)J(\hat{\epsilon}, x - u)\Big\rangle_{\hat{\epsilon}}, \tag{3.44}$$

$$v_\delta(x, u) = \Big\langle \hat{\epsilon}_\delta\, J(\hat{\epsilon}, u)J(\hat{\epsilon}, x - u)\Big\rangle_{\hat{\epsilon}}, \tag{3.45}$$

$$t_{\beta\delta}(x, u) = \Big\langle \Big(\hat{\epsilon}_\beta\hat{\epsilon}_\delta - \frac{1}{4}\delta_{\beta\delta}\Big)J(\hat{\epsilon}, u)J(\hat{\epsilon}, x - u)\Big\rangle_{\hat{\epsilon}}, \tag{3.46}$$

so that

$$S(x, y)_{\rm IR\ reg.} = \int_u G_0(u - y)\, s(x, u), \tag{3.47}$$

$$V_\delta(x, y) = \int_u G_0(u - y)\, v_\delta(x, u), \tag{3.48}$$

$$T_{\beta\delta}(x, y) = \int_u G_0(u - y)\, t_{\beta\delta}(x, u). \tag{3.49}$$

3.5 Calculation of $s(x, u)$

Inserting into eq. (3.44) the expansions of $J(\hat{\epsilon}, u)$ and $J(\hat{\epsilon}, x-u)$ in Gegenbauer polynomials from eq. (3.21) and using the orthogonality relations in eq. (3.13), the angular average yields

$$s(x, u) = \sum_{n=0}^{\infty} z_n(u^2) z_n((x-u)^2) \frac{C_n(\hat{u} \cdot \widehat{x-u})}{n+1}. \tag{3.50}$$

We remark that the symmetry $s(x, u) = s(x, x-u)$, obvious in eq. (3.44), remains manifest in eq. (3.50). At $x = 0$, we have

$$s(0, u) = \sum_{n=0}^{\infty} (-1)^n \, z_n(u^2)^2 \overset{|u| \to \infty}{\sim} \frac{1}{(4\pi^2 m)^2 u^2} \sum_{n=0}^{\infty} \frac{(-1)^n}{(n+1)^2} = \frac{1}{192\pi^2 m^2 u^2}, \tag{3.51}$$

where we used the first term in the large-argument expansion (3.36) of $z_n(u^2)$. Eq. (3.51) provides the leading behavior of $s(x, u)$ at large $|u|$ that will be important to deal with the IR divergence in $S(x, y)$. We remark that the asymptotic prediction of eq. (3.51) for $s(x, u)$ can also be obtained directly from its definition (3.44), employing the asymptotic form (3.43) of the function $J(\hat{\epsilon}, u)$.

3.6 Calculation of $v_\delta(x, u)$

We parametrize the vector components in eq. (3.45) as follows:

$$v_\delta(x, u) = x_\delta \, \mathfrak{f}^{(1)}(x^2, x \cdot u, u^2) + u_\delta \, \mathfrak{f}^{(2)}(x^2, x \cdot u, u^2). \tag{3.52}$$

Multiplying with x_δ and u_δ and solving the system of two equations, we get

$$\begin{pmatrix} \mathfrak{f}^{(1)} \\ \mathfrak{f}^{(2)} \end{pmatrix} = \frac{1}{x^2 u^2 - (x \cdot u)^2} \begin{pmatrix} u^2 & -u \cdot x \\ -u \cdot x & x^2 \end{pmatrix} \begin{pmatrix} \langle (x \cdot \hat{\epsilon}) J(\hat{\epsilon}, u) J(\hat{\epsilon}, x-u) \rangle_{\hat{\epsilon}} \\ \langle (u \cdot \hat{\epsilon}) J(\hat{\epsilon}, u) J(\hat{\epsilon}, x-u) \rangle_{\hat{\epsilon}} \end{pmatrix}. \tag{3.53}$$

Using eq. (3.11) and the orthogonality relations (3.13) we obtain the results

$$\langle (x \cdot \hat{\epsilon}) J(\hat{\epsilon}, u) J(\hat{\epsilon}, x-u) \rangle_{\hat{\epsilon}} = \frac{|u|}{2} \sum_{n=0}^{\infty} (z_{n-1}(u^2) + z_{n+1}(u^2)) \frac{z_n((x-u)^2)}{n+1} C_n(\hat{u} \cdot \widehat{x-u})$$

$$+ \frac{|x-u|}{2} \sum_{n=0}^{\infty} (z_{n-1}((x-u)^2) + z_{n+1}((x-u)^2)) \frac{z_n(u^2)}{n+1} C_n(\hat{u} \cdot \widehat{x-u}), \tag{3.54}$$

$$\langle (u \cdot \hat{\epsilon}) J(\hat{\epsilon}, u) J(\hat{\epsilon}, x-u) \rangle_{\hat{\epsilon}} = \frac{|u|}{2} \sum_{n=0}^{\infty} (z_{n-1}(u^2) + z_{n+1}(u^2)) \frac{z_n((x-u)^2)}{n+1} C_n(\hat{u} \cdot \widehat{x-u}), \tag{3.55}$$

with the convention that $z_n(u^2) = z_n((x-u)^2) = 0$ for $n \leq -1$. In the end we get

$$
\begin{aligned}
\mathfrak{f}^{(1)}(x^2, x \cdot u, u^2) &= \frac{1}{2(x^2 u^2 - (x \cdot u)^2)} \\
&\times \sum_{n=0}^{\infty} \Big(u^2 |x-u| (z_{n-1}((x-u)^2) + z_{n+1}((x-u)^2)) z_n(u^2) \\
&\quad + |u|(u^2 - u \cdot x)(z_{n-1}(u^2) + z_{n+1}(u^2)) z_n((x-u)^2) \Big) \frac{C_n(\hat{u} \cdot \widehat{x-u})}{n+1}, \quad (3.56)
\end{aligned}
$$

$$
\begin{aligned}
\mathfrak{f}^{(2)}(x^2, x \cdot u, u^2) &= \frac{1}{2(x^2 u^2 - (x \cdot u)^2)} \\
&\times \sum_{n=0}^{\infty} \Big(- |x-u| (u \cdot x)(z_{n-1}((x-u)^2) + z_{n+1}((x-u)^2)) z_n(u^2) \\
&\quad + |u|(x^2 - u \cdot x)(z_{n-1}(u^2) + z_{n+1}(u^2)) z_n((x-u)^2) \Big) \frac{C_n(\hat{u} \cdot \widehat{x-u})}{n+1}. \quad (3.57)
\end{aligned}
$$

We now want to study the large-$|u|$ behavior of $\mathfrak{f}^{(i)}(x^2, x \cdot u, u^2)$. Expanding $z_n(u^2)$ and $z_n((x-u)^2)$ for fixed n and large $|u|$, one finds the result in eq. (3.36) and

$$
z_n\left((x-u)^2\right) - z_n(u^2) = \frac{\hat{u} \cdot x}{4\pi^2 m (n+1) u^2} + \mathrm{O}(u^{-3}). \quad (3.58)
$$

We note that

$$
\frac{C_n(\hat{u} \cdot \widehat{x-u})}{n+1} = (-1)^n \left(1 + n(n+2) \left((\hat{x} \cdot \hat{u})^2 - 1 \right) \frac{x^2}{6u^2} \right) + \mathrm{O}(u^{-3}). \quad (3.59)
$$

One then sees that $\langle (u \cdot \hat{\epsilon}) J(\hat{\epsilon}, u) J(\hat{\epsilon}, x - u) \rangle_{\hat{\epsilon}}$ vanishes for $x = 0$. For this reason, we may rewrite

$$
\begin{aligned}
&\langle (u \cdot \hat{\epsilon}) J(\hat{\epsilon}, u) J(\hat{\epsilon}, x - u) \rangle_{\hat{\epsilon}} \quad (3.60) \\
&= \frac{|u|}{2} \sum_{n=0}^{\infty} \left(z_{n-1}(u^2) + z_{n+1}(u^2) \right) (-1)^n \left(z_n\left((x-u)^2 \right) (-1)^n \frac{C_n(\hat{u} \cdot \widehat{x-u})}{n+1} - z_n(u^2) \right).
\end{aligned}
$$

The second factor in the sum is given in leading order by $\frac{\hat{u} \cdot x}{4\pi^2 m (n+1) u^2}$ for large u, and since the series is then still absolutely convergent, one finds that $\langle (u \cdot \hat{\epsilon}) J(\hat{\epsilon}, u) J(\hat{\epsilon}, x - u) \rangle_{\hat{\epsilon}}$ falls off at least as fast as $1/|u|^3$. In fact, at little more work reveals that the coefficient of the $1/|u|^3$ term vanishes. The same argument shows that $\langle (x \cdot \hat{\epsilon}) J(\hat{\epsilon}, u) J(\hat{\epsilon}, x - u) \rangle_{\hat{\epsilon}}$ goes like $|u|^{-3}$ for large $|u|$, thus showing that $\langle \hat{\epsilon}_\delta J(\hat{\epsilon}, u) J(\hat{\epsilon}, x - u) \rangle_{\hat{\epsilon}}$ falls off at least as fast as $|u|^{-3}$ for large $|u|$.

3.7 Calculation of $t_{\alpha\beta}(x, u)$

First, calculate at $x = 0$:

$$
t_{\alpha\beta}(0, u) = \left\langle \left(\hat{\epsilon}_\alpha \hat{\epsilon}_\beta - \frac{1}{4} \delta_{\alpha\beta} \right) J(\hat{\epsilon}, u) J(\hat{\epsilon}, -u) \right\rangle_{\hat{\epsilon}} = \left(u_\alpha u_\beta - \frac{u^2}{4} \delta_{\alpha\beta} \right) b(u^2), \quad (3.61)
$$

Contracting with $u_\alpha u_\beta$ and using the identity from eq. (3.12) and the orthogonality relations (3.13) within the angular average $\langle \dots \rangle_{\hat{\epsilon}}$, we get

$$
\begin{aligned}
b(u^2) &= \frac{1}{3u^2} \sum_{n=0}^{\infty} (-1)^n \left(z_{n-2}(u^2) + z_n(u^2)(1-\delta_{n0}) + z_{n+2}(u^2) \right) z_n(u^2) \quad (3.62) \\
&= \frac{1}{3u^2} \sum_{n=0}^{\infty} (-1)^n z_n(u^2) (z_n(u^2)(1-\delta_{n0}) + 2z_{n+2}(u^2)) \\
&\overset{|u|\to\infty}{\sim} \frac{1}{96\pi^2 m^2 |u|^4} \left(-\frac{1}{\pi^2} + \frac{1}{6} \right). \quad (3.63)
\end{aligned}
$$

For the general case we have with $v = x - u$ the decomposition:

$$
\begin{aligned}
t_{\alpha\beta}(x,u) &= \left(u_\alpha u_\beta - \frac{u^2}{4}\delta_{\alpha\beta} \right) \hat{\mathfrak{h}}^{(1)}(u^2, u\cdot v, v^2) \quad (3.64) \\
&\quad + \left(v_\alpha v_\beta - \frac{v^2}{4}\delta_{\alpha\beta} \right) \hat{\mathfrak{h}}^{(2)}(u^2, u\cdot v, v^2) \\
&\quad + \left(u_\alpha v_\beta + v_\alpha u_\beta - \frac{1}{2}\delta_{\alpha\beta}(u\cdot v) \right) \hat{\mathfrak{h}}^{(3)}(u^2, u\cdot v, v^2).
\end{aligned}
$$

Multiplying with $u_\alpha u_\beta$, $v_\alpha v_\beta$ and $u_\alpha v_\beta + v_\alpha u_\beta$ and solving the system of three equations, we get as intermediate result for the scalar functions $\hat{\mathfrak{h}}^{(k)}$

$$
\begin{pmatrix} \hat{\mathfrak{h}}^{(1)} \\ \hat{\mathfrak{h}}^{(2)} \\ \hat{\mathfrak{h}}^{(3)} \end{pmatrix} = \frac{1}{2D_{u,v}} \begin{pmatrix} 3(v^2)^2 & u^2 v^2 + 2(u\cdot v)^2 & -3v^2(u\cdot v) \\ u^2 v^2 + 2(u\cdot v)^2 & 3(u^2)^2 & -3u^2(u\cdot v) \\ -3v^2(u\cdot v) & -3u^2(u\cdot v) & u^2 v^2 + 2(u\cdot v)^2 \end{pmatrix} \begin{pmatrix} s_1 \\ s_2 \\ s_3 \end{pmatrix} \quad (3.65)
$$

with $D_{u,v} = (u^2 v^2 - (u\cdot v)^2)^2$ and

$$
\begin{aligned}
s_1 &= \langle ((u\cdot\hat{\epsilon})^2 - u^2/4) J(\hat{\epsilon}, u) J(\hat{\epsilon}, v) \rangle_{\hat{\epsilon}} \\
&= \frac{u^2}{4} \sum_{n=0}^{\infty} \left(z_{n-2}(u^2) + z_n(u^2)(1-\delta_{n0}) + z_{n+2}(u^2) \right) z_n(v^2) \cdot \frac{C_n(\hat{u}\cdot\hat{v})}{n+1}, \quad (3.66) \\
s_2 &= \langle ((v\cdot\hat{\epsilon})^2 - v^2/4) J(\hat{\epsilon}, u) J(\hat{\epsilon}, v) \rangle_{\hat{\epsilon}} \\
&= \frac{v^2}{4} \sum_{n=0}^{\infty} z_n(u^2) \left(z_{n-2}(v^2) + z_n(v^2)(1-\delta_{n0}) + z_{n+2}(v^2) \right) \cdot \frac{C_n(\hat{u}\cdot\hat{v})}{n+1}, \quad (3.67) \\
s_3 &= \langle \left(2(\hat{\epsilon}\cdot u)(\hat{\epsilon}\cdot v) - \frac{1}{2}(u\cdot v) \right) J(\hat{\epsilon}, u) J(\hat{\epsilon}, v) \rangle_{\hat{\epsilon}} \\
&= \frac{1}{2} |u||v| \sum_{n=0}^{\infty} \left[(z_{n-1}(u^2) + z_{n+1}(u^2))(z_{n-1}(v^2) + z_{n+1}(v^2)) - (\hat{u}\cdot\hat{v}) z_n(u^2) z_n(v^2) \right] \frac{C_n(\hat{u}\cdot\hat{v})}{n+1}. \\
&\qquad\qquad (3.68)
\end{aligned}
$$

The point now is that $\langle (\hat{\epsilon}_\alpha \hat{\epsilon}_\beta - \frac{1}{4}\delta_{\alpha\beta}) J(\hat{\epsilon}, u) J(\hat{\epsilon}, x-u) \rangle_{\hat{\epsilon}}$ is of order $(1/u^2)$ at large u, but with a tensor structure proportional to $(\hat{u}_\beta \hat{u}_\delta - \frac{1}{4}\delta_{\beta\delta})$. The average over $\hat{u}$ in the next step will cancel this leading contribution, so that $T_{\alpha\beta}(x,y)$ is finite. Anticipating the numerical implementation, we remark that it can be advantageous to subtract a term which vanishes upon the $\hat{u}$ integration and makes the integrand fall off faster at large u.

The leading asymptotic behavior of the scalar functions $s_i(u^2, u \cdot x, x^2)$ for $|u| \to \infty$ is

$$s_1 \sim s_2 \sim -\frac{1}{2} s_3 \overset{|u| \to \infty}{\sim} \frac{1}{128\pi^2 m^2} \left(-\frac{1}{\pi^2} + \frac{1}{6} \right). \tag{3.69}$$

One also finds that, expanding in x around $x = 0$, and for arbitrary $|u|$,

$$s_1 \Big|_{x=0} = s_2 \Big|_{x=0} = -\frac{1}{2} s_3 \Big|_{x=0} = \frac{3}{4} u^4 b(u^2). \tag{3.70}$$

Furthermore, one finds

$$s_1 + s_2 + s_3 = \mathrm{O}(x^2). \tag{3.71}$$

Equations (3.70) and (3.71) can be shown without using the explicit expression of $z_n(u^2)$.

4 Direct evaluation of the final convolution integral

In this section, we treat the final convolution integral yielding the tensors S, V_δ and $T_{\beta\delta}$ (see eqs. (3.47)–(3.49)) by performing two angular integrations analytically, while the third angular integral as well as the integral over the modulus are left to be done numerically. Since this straightforward method leads to some numerical difficulties pointed out below, our final weight functions have been computed with the alternative method presented in section 5. Nevertheless, this method, which was implemented as part of ref. [78], provided important cross-checks (discussed in section 6) for the final QED kernel. The expressions obtained for the weight functions are also used as the starting point for the multipole-expansion method of section 5; see the text around eqs. (5.1)–(5.3).

In order to perform the angular integrations in $\int_u$ in eqs. (3.47)–(3.49), we choose a coordinate system where x is pointing in the direction $\hat{e}_0$ and y is in the $(\hat{e}_0, \hat{e}_1)$ plane and we introduce the angle β between those two vectors

$$x = |x|(1, 0, 0, 0), \tag{4.1}$$

$$y = (y_0, y_1, 0, 0), \qquad y_1 \geq 0, \tag{4.2}$$

$$\hat{x} \cdot \hat{y} = \cos\beta, \qquad 0 \leq \beta \leq \pi, \tag{4.3}$$

$$y_0 = |y| \cos\beta, \tag{4.4}$$

$$y_1 = |y| \sin\beta. \tag{4.5}$$

The vector u is parametrized as follows

$$
\begin{aligned}
u_0 &= |u| \cos\phi_1, \\
u_1 &= |u| \sin\phi_1 \cos\phi_2, \\
u_2 &= |u| \sin\phi_1 \sin\phi_2 \cos\phi_3, \\
u_3 &= |u| \sin\phi_1 \sin\phi_2 \sin\phi_3,
\end{aligned} \tag{4.6}
$$

with $\phi_1, \phi_2 \in [0, \pi]$, $\phi_3 \in [0, 2\pi]$ and the angular integration measure is given by

$$\int d\Omega_{\hat{u}} = \int_0^\pi d\phi_1 \sin^2\phi_1 \int_{-1}^1 d\hat{c}_2 \int_0^{2\pi} d\phi_3 \tag{4.7}$$

where $\hat{c}_2 \equiv \cos\phi_2$.

From the above definitions of the vectors we get

$$x \cdot u = |x||u| \cos \phi_1, \tag{4.8}$$

$$u \cdot y = |u|(y_0 \cos \phi_1 + y_1 \sin \phi_1 \, \hat{c}_2), \tag{4.9}$$

$$(u \cdot y)^2 = u^2(y_0^2 \cos^2 \phi_1 + 2y_0 y_1 \cos \phi_1 \sin \phi_1 \, \hat{c}_2 + y_1^2 \sin^2 \phi_1 \, \hat{c}_2^2), \tag{4.10}$$

$$(u - y)^2 = u^2 - 2u \cdot y + y^2 = y^2 + u^2 - 2|u|y_0 \cos \phi_1 - 2|u|y_1 \sin \phi_1 \, \hat{c}_2. \tag{4.11}$$

We will need the following angular integrals, where $f(x,u) \equiv f(x^2, x \cdot u, u^2) = f(x^2, |x||u| \cos \phi_1, u^2)$ is a generic scalar function of the vectors x and u:

$$\begin{aligned}
\left\langle \frac{1}{(u-y)^2} f(x,u) \right\rangle_{\hat{u}} &\equiv \frac{1}{2\pi^2} \int d\Omega_{\hat{u}} \, \frac{1}{(u-y)^2} \, f(x,u) \\
&= \frac{1}{\pi} \int_0^\pi d\phi_1 \sin^2 \phi_1 f(x^2, |x||u| \cos \phi_1, u^2) \\
&\quad \times \int_{-1}^1 \frac{d\hat{c}_2}{y^2 + u^2 - 2|u|y_0 \cos \phi_1 - 2|u|y_1 \sin \phi_1 \, \hat{c}_2} \\
&= \frac{-1}{2\pi|u||y|\sin\beta} \int_0^\pi d\phi_1 \sin \phi_1 f(x^2, |x||u| \cos \phi_1, u^2) \, \mathrm{Log}, \quad (4.12)
\end{aligned}$$

where we introduced the abbreviation

$$\mathrm{Log} \equiv \ln \left[\frac{y^2 + u^2 - 2|u||y| \cos(\beta - \phi_1)}{y^2 + u^2 - 2|u||y| \cos(\beta + \phi_1)} \right]. \tag{4.13}$$

In a similar way one obtains

$$\left\langle \frac{1}{(u-y)^2} (x \cdot u) f(x,u) \right\rangle_{\hat{u}} = -\frac{|x|}{2\pi|y|\sin\beta} \int_0^\pi d\phi_1 \sin \phi_1 \cos \phi_1 f(x^2, |x||u| \cos \phi_1, u^2) \, \mathrm{Log}, \tag{4.14}$$

$$\begin{aligned}
\left\langle \frac{1}{(u-y)^2} (y \cdot u) f(x,u) \right\rangle_{\hat{u}} &= \frac{-1}{\pi} \int_0^\pi d\phi_1 \sin^2 \phi_1 f(x^2, |x||u| \cos \phi_1, u^2) \\
&\quad \times \left(1 + \frac{y^2 + u^2}{4|u||y|\sin\beta \sin\phi_1} \, \mathrm{Log} \right), \quad (4.15)
\end{aligned}$$

$$\begin{aligned}
\left\langle \frac{(y \cdot u)^2}{(u-y)^2} f(x,u) \right\rangle_{\hat{u}} &= \frac{-1}{8\pi|u||y|\sin\beta} \int_0^\pi d\phi_1 \sin \phi_1 f(x^2, |x||u| \cos \phi_1, u^2) \\
&\quad \times \Big[4|u||y|\sin\beta \sin\phi_1 \left(u^2 + y^2 + 2|u||y| \cos\beta \cos\phi_1 \right) \\
&\quad + (u^2 + y^2)^2 \, \mathrm{Log} \Big]. \quad (4.16)
\end{aligned}$$

The integration over ϕ_3 is always trivial and the integrations over $\hat{c}_2$ lead to simple elementary integrals.

4.1 Calculation of the weight function $\bar{\mathbf{g}}^{(0)}$

Exploiting the behavior of $s(x,u)$ for large $|u|$ from eq. (3.51), we can introduce a fixed vector w and modify the integrand of $S(x,y)$ in eq. (3.47) to get an IR-regulated function

as follows

$$\bar{\mathfrak{g}}^{(0)}(|x|, x \cdot y, |y|) = S(x, y)_{\text{IR reg.}} \equiv \int_u \left(G_0(u-y) \, s(x, u) - \frac{G_0(u)\theta(u^2-w^2)}{192\pi^2 m^2 u^2} \right) \tag{4.17}$$

$$= -\frac{1}{4\pi|y|\sin\beta} \int_0^\infty du \, u^2 \int_0^\pi d\phi_1 \sin\phi_1 \tag{4.18}$$

$$\times \left[\frac{|y|\sin\beta \, \theta(u^2-w^2)}{192\pi m^2 u^3} + \text{Log} \cdot \sum_{n=0}^\infty z_n(u^2) z_n\left((x-u)^2\right) \frac{C_n(\widehat{\hat{u} \cdot x - u})}{n+1} \right],$$

where we used the result from eq. (4.12) for the angular integration. The term with $\theta(u^2-w^2)$ in eq. (4.17) is independent of x and y, therefore it will not affect the final result for the QED kernel, in which only the derivatives of the weight function $\bar{\mathfrak{g}}^{(0)}(|x|, x \cdot y, |y|)$ with respect to x_α and y_α enter; see eq. (2.30), (2.33)–(2.34) and (2.40).

4.2 Calculation of the weight functions $\bar{\mathfrak{g}}^{(1,2)}$

Starting from the definition of $V_\delta(x, y)$ in eq. (2.36), we split off the integration over the length of the vector u and parametrize the angular average as follows:

$$\left\langle \frac{1}{(u-y)^2} \left\langle \hat{\epsilon}_\delta J(\hat{\epsilon}, u) J(\hat{\epsilon}, x-u) \right\rangle_{\hat{\epsilon}} \right\rangle_{\hat{u}} = x_\delta \, \mathfrak{g}_u^{(1)}(x^2, x \cdot y, y^2) + y_\delta \, \mathfrak{g}_u^{(2)}(x^2, x \cdot y, y^2). \tag{4.19}$$

From this we get the vector weight functions in eq. (2.41) via

$$\bar{\mathfrak{g}}^{(i)}(x^2, x \cdot y, y^2) = \frac{1}{2} \int_0^\infty du \, u^3 \mathfrak{g}_u^{(i)}(x^2, x \cdot y, y^2), \quad i = 1, 2. \tag{4.20}$$

Multiplying eq. (4.19) by x_δ and y_δ we then obtain in a similar way as before

$$\begin{pmatrix} \mathfrak{g}_u^{(1)} \\ \mathfrak{g}_u^{(2)} \end{pmatrix} = \frac{1}{x^2 y^2 - (x \cdot y)^2} \begin{pmatrix} y^2 & -x \cdot y \\ -x \cdot y & x^2 \end{pmatrix}$$

$$\times \begin{pmatrix} \left\langle \frac{1}{(u-y)^2} \left(x^2 \, \mathfrak{f}^{(1)}(x, u) + (x \cdot u) \, \mathfrak{f}^{(2)}(x, u) \right) \right\rangle_{\hat{u}} \\ \left\langle \frac{1}{(u-y)^2} \left((x \cdot y) \, \mathfrak{f}^{(1)}(x, u) + (y \cdot u) \, \mathfrak{f}^{(2)}(x, u) \right) \right\rangle_{\hat{u}} \end{pmatrix}. \tag{4.21}$$

Using the results of the angular integrals from eqs. (4.12), (4.14) and (4.15), we get the following results for the weight functions

$$\bar{\mathfrak{g}}^{(2)}(x^2, x \cdot y, y^2) = \frac{1}{8\pi y^2 |x| \sin^3\beta} \int_0^\infty du \, u^2 \int_0^\pi d\phi_1$$

$$\times \left\{ 2\sin\beta + \left(\frac{y^2 + u^2}{2|u||y|} - \cos\beta \cos\phi_1 \right) \frac{\text{Log}}{\sin\phi_1} \right\}$$

$$\times \sum_{n=0}^\infty \left(z_n(u^2) z_{n+1}\left((x-u)^2\right) \left[|x-u|\cos\phi_1 \frac{C_n}{n+1} + (|u|\cos\phi_1 - |x|) \frac{C_{n+1}}{n+2} \right] \right.$$

$$\left. + z_{n+1}(u^2) z_n\left((x-u)^2\right) \left[(|u|\cos\phi_1 - |x|) \frac{C_n}{n+1} + |x-u|\cos\phi_1 \frac{C_{n+1}}{n+2} \right] \right), \tag{4.22}$$

$$\bar{\mathfrak{g}}^{(3)}(x^2, x\cdot y, y^2) = \frac{-1}{8\pi x^2 |y|\sin\beta}\int_0^\infty du\, u^2 \int_0^\pi d\phi_1 \sin\phi_1 \, \text{Log}$$

$$\times \sum_{n=0}^\infty \left(z_n(u^2)z_{n+1}\left((x-u)^2\right)\left(|x-u|\frac{C_n}{n+1}+|u|\frac{C_{n+1}}{n+2}\right)\right.$$

$$\left. + z_{n+1}(u^2)z_n\left((x-u)^2\right)\left(|u|\frac{C_n}{n+1}+|x-u|\frac{C_{n+1}}{n+2}\right)\right), \qquad (4.23)$$

and

$$\bar{\mathfrak{g}}^{(1)}(x^2, x\cdot y, y^2) = \bar{\mathfrak{g}}^{(3)}(x^2, x\cdot y, y^2) - \frac{|y|}{|x|}\cos\beta\,\bar{\mathfrak{g}}^{(2)}(x^2, x\cdot y, y^2). \qquad (4.24)$$

We choose to first compute the scalar function $\bar{\mathfrak{g}}^{(3)}$ because the integrand simplifies and is collinear safe for $\sin\phi_1 \to 0$. The argument of the Gegenbauer polynomials C_n and C_{n+1} is given by

$$\hat{u}\cdot\widehat{x-u} = -\frac{|u|-|x|\cos\phi_1}{|u-x|}. \qquad (4.25)$$

We note that there is a large cancellation inside the curly bracket of eq. (4.22). If we call $A = 2|u||y|/(u^2+y^2)$, such that $0 \le A \le 1$, then Taylor-expanding the logarithm in A shows that the curly bracket is of order A^2 at small A (small A corresponds to both $|u| \ll |y|$ and $|u| \gg |y|$).

4.3 Calculation of the weight functions $\bar{\mathfrak{l}}^{(1,2,3)}$

Upon integrating over the angular variables of u in eq. (2.37), the tensor decomposition reads

$$\left\langle \frac{1}{(u-y)^2}\left\langle\left(\hat{\epsilon}_\alpha\hat{\epsilon}_\beta - \frac{1}{4}\delta_{\alpha\beta}\right)J(\hat{\epsilon},u)\,J(\hat{\epsilon},x-u)\right\rangle_{\hat{\epsilon}}\right\rangle_{\hat{u}}$$

$$= \left(x_\alpha x_\beta - \frac{x^2}{4}\delta_{\alpha\beta}\right)\mathfrak{l}_u^{(1)} + \left(y_\alpha y_\beta - \frac{y^2}{4}\delta_{\alpha\beta}\right)\mathfrak{l}_u^{(2)} + \left(x_\alpha y_\beta + y_\alpha x_\beta - \frac{x\cdot y}{2}\delta_{\alpha\beta}\right)\mathfrak{l}_u^{(3)}. \qquad (4.26)$$

where the scalar functions $\mathfrak{l}_u^{(1)}$ depend on $x^2, x\cdot y, y^2$, as well as on $|u|$. From this we get the tensor weight functions in eq. (2.42) via

$$\bar{\mathfrak{l}}^{(i)}(x^2, x\cdot y, y^2) = \frac{1}{2}\int_0^\infty du\, u^3\, \mathfrak{l}_u^{(i)}(x^2, x\cdot y, y^2), \qquad i = 1, 2, 3. \qquad (4.27)$$

Again, multiplying eq. (4.26) with $x_\alpha x_\beta$, $y_\alpha y_\beta$ and $x_\alpha y_\beta + y_\alpha x_\beta$ and solving as before, the weight functions $\mathfrak{l}_u^{(i)}$ are given by

$$\begin{pmatrix}\mathfrak{l}_u^{(1)}\\\mathfrak{l}_u^{(2)}\\\mathfrak{l}_u^{(3)}\end{pmatrix} = \frac{1}{2D_{x,y}}\begin{pmatrix} 3(y^2)^2 & x^2 y^2 + 2(x\cdot y)^2 & -3y^2(x\cdot y)\\ x^2 y^2 + 2(x\cdot y)^2 & 3(x^2)^2 & -3x^2(x\cdot y)\\ -3y^2(x\cdot y) & -3x^2(x\cdot y) & x^2 y^2 + 2(x\cdot y)^2\end{pmatrix}\begin{pmatrix}v_{1,u}\\v_{2,u}\\v_{3,u}\end{pmatrix}, \qquad (4.28)$$

with $D_{x,y} = (x^2 y^2 - (x \cdot y)^2)^2$ and

$$v_{1,u} = \Big\langle \frac{1}{(u-y)^2} \Big\{ [(u \cdot x)^2 - u^2 x^2/4] \hat{\mathfrak{h}}^{(1)} + [((x-u) \cdot x)^2 - (x-u)^2 x^2/4] \hat{\mathfrak{h}}^{(2)}$$
$$+ [2(u \cdot x)((x-u) \cdot x) - x^2(u \cdot (x-u))/2] \hat{\mathfrak{h}}^{(3)} \Big\} \Big\rangle_{\hat{u}}, \tag{4.29}$$

$$v_{2,u} = \Big\langle \frac{1}{(u-y)^2} \Big\{ [(u \cdot y)^2 - u^2 y^2/4] \hat{\mathfrak{h}}^{(1)} + [((x-u) \cdot y)^2 - y^2(x-u)^2/4] \hat{\mathfrak{h}}^{(2)}$$
$$+ [2(u \cdot y)((x-u) \cdot y) - y^2(u \cdot (x-u))/2] \hat{\mathfrak{h}}^{(3)} \Big\} \Big\rangle_{\hat{u}}, \tag{4.30}$$

$$v_{3,u} = \Big\langle \frac{1}{(u-y)^2} \Big\{ [2(x \cdot u)(y \cdot u) - u^2(x \cdot y)/2] \hat{\mathfrak{h}}^{(1)}$$
$$+ [2(x \cdot (x-u))(y \cdot (x-u)) - (x \cdot y)(x-u)^2/2] \hat{\mathfrak{h}}^{(2)}$$
$$+ [2(u \cdot x)(y \cdot (x-u)) + 2(u \cdot y)(x \cdot (x-u)) - (u \cdot (x-u))(x \cdot y)] \hat{\mathfrak{h}}^{(3)} \Big\} \Big\rangle_{\hat{u}}, \tag{4.31}$$

where the $\hat{\mathfrak{h}}^{(i)}(u^2, u \cdot v, v^2)$ are given in eq. (3.65).

Using the results of the angular integrations in eqs. (4.12), (4.14)–(4.16), we get more explicitly the following intermediate result

$$v_{1,u} = \frac{-x^2}{2\pi uy \sin\beta} \int_0^\pi d\phi_1 \, \sin\phi_1 \, \mathrm{Log} \Big\{ u^2 \Big[\cos^2\phi_1 - \frac{1}{4} \Big] \hat{\mathfrak{h}}^{(1)}$$
$$+ \Big[\frac{3}{4} x^2 - \frac{3}{2} ux \cos\phi_1 + u^2 \Big(\cos^2\phi_1 - \frac{1}{4} \Big) \Big] \hat{\mathfrak{h}}^{(2)}$$
$$+ \Big[\frac{3}{2} ux \cos\phi_1 - 2u^2 \Big(\cos^2\phi_1 - \frac{1}{4} \Big) \Big] \hat{\mathfrak{h}}^{(3)} \Big\}, \tag{4.32}$$

$$v_{2,u} = \frac{-1}{8\pi uy \sin\beta} \int_0^\pi d\phi_1 \, \sin\phi_1 \, \Big[4uy \sin\beta \sin\phi_1 (u^2 + y^2 + 2uy \cos\beta \cos\phi_1)$$
$$+ (u^2 + y^2)^2 \, \mathrm{Log} \Big] \Big\{ \hat{\mathfrak{h}}^{(1)} + \hat{\mathfrak{h}}^{(2)} - 2\hat{\mathfrak{h}}^{(3)} \Big\}$$
$$- \frac{x}{2\pi u \tan\beta} \int_0^\pi d\phi_1 \, \sin\phi_1 \, \Big[4uy \sin\beta \sin\phi_1 + (u^2 + y^2) \, \mathrm{Log} \Big] \Big\{ - \hat{\mathfrak{h}}^{(2)} + \hat{\mathfrak{h}}^{(3)} \Big\}$$
$$- \frac{y}{2\pi u \sin\beta} \int_0^\pi d\phi_1 \, \sin\phi_1 \, \mathrm{Log} \Big\{ [-u^2/4] \, \hat{\mathfrak{h}}^{(1)}$$
$$+ \Big[x^2 \cos^2\beta - \frac{1}{4}(x^2 - 2ux \cos\phi_1 + u^2) \Big] \hat{\mathfrak{h}}^{(2)} - \frac{u}{2} [x \cos\phi_1 - u] \hat{\mathfrak{h}}^{(3)} \Big\}, \tag{4.33}$$

$$v_{3,u} = \frac{-x}{2\pi u \tan\beta} \int_0^\pi d\phi_1 \, \sin\phi_1 \, \mathrm{Log} \, \Big\{ [-u^2/2] \hat{\mathfrak{h}}^{(1)}$$
$$+ [3x^2/2 - xu \cos\phi_1 - u^2/2] \hat{\mathfrak{h}}^{(2)} + [u^2 + ux \cos\phi_1] \hat{\mathfrak{h}}^{(3)} \Big\}$$
$$- \frac{1}{4\pi uy \sin\beta} \int_0^\pi d\phi_1 \, \sin\phi_1 \Big[4uy \sin\beta \sin\phi_1 + (y^2 + u^2) \, \mathrm{Log} \Big]$$
$$\times \Big\{ 2xu \cos\phi_1 \hat{\mathfrak{h}}^{(1)} - 2(x^2 - xu \cos\phi_1) \hat{\mathfrak{h}}^{(2)} + 2(x^2 - 2ux \cos\phi_1) \hat{\mathfrak{h}}^{(3)} \Big\}. \tag{4.34}$$

Similar to eq. (4.27), we define weight functions $\bar{v}^{(i)}$ after the integration of $v_{i,u}$ over the length of the vector u:

$$\bar{v}^{(i)}(x^2, x \cdot y, y^2) = \frac{1}{2} \int_0^\infty du \, u^3 \, v_{i,u}(x^2, x \cdot y, y^2), \qquad i = 1, 2, 3. \tag{4.35}$$

Schematically, we have the following structure,

$$\overrightarrow{\mathfrak{l}}_u = M(x,y) \, N \, M(u, x-u) \, \overrightarrow{s}, \tag{4.36}$$

where $\overrightarrow{\mathfrak{l}}_u$, $\overrightarrow{s} \in \mathbb{R}^3$, the components of $\overrightarrow{s}$ are given by eqs. (3.66)–(3.68), and M is the symmetric 3×3 matrix given in eqs. (3.65) and (4.28), which is a function of two vectors. In particular, $\overrightarrow{\mathfrak{h}} = M(u, x-u) \, \overrightarrow{s}$. The linear operator N corresponds to the relations (4.32)–(4.34), $\overrightarrow{v}_u = N \, \overrightarrow{\mathfrak{h}}$.

The linear operator $M(x,y) \, N \, M(u, x-u)$ leads to fairly long algebraic expressions. We note that the final step, going from the $\overrightarrow{v}_u$ to the $\overrightarrow{\mathfrak{l}}_u$, is a purely algebraic one. If there are linear combinations of the $\overrightarrow{v}_u$ that lead to simpler integrands, those can be used and the linear combinations can be resolved in terms of the $\overrightarrow{\mathfrak{l}}_u$ at the end. We find that the following linear combinations have manageable expressions,[7]

$$\bar{v}^{(1)} = \frac{-1}{4\pi y \sin\beta} \int_0^\infty du \, u^2 \int_0^\pi d\phi_1 \, \sin\phi_1 \, \mathrm{Log} \cdot \left(s_1 + s_2 + s_3\right), \tag{4.37}$$

$$\bar{\mathfrak{l}}^{(4)} \equiv \frac{1}{\sin^2\beta} \left(\bar{v}^{(3)} - \frac{2|y|}{|x|} \cos\beta \, \bar{v}^{(1)} \right) = \frac{1}{4\pi|x|\sin^3\beta} \int_0^\infty du \, u \int_0^\pi d\phi_1$$

$$\times \left\{ 2\sin\beta + \left(\frac{u^2+y^2}{2uy} - \cos\beta \cos\phi_1 \right) \frac{\mathrm{Log}}{\sin\phi_1} \right\}$$

$$\times \left(2(u\cos\phi_1 - x)\, s_1 + 2u\cos\phi_1\, s_2 + (2u\cos\phi_1 - x)\, s_3 \right), \tag{4.38}$$

$$\bar{\mathfrak{l}}^{(2)} = -\frac{1}{64\pi x^2 y^5 \sin^5\beta} \int_0^\infty \frac{du}{u^2} \int_0^\pi \frac{d\phi_1}{\sin^3\phi_1}$$

$$\times \left\{ \left(3u^4 + 8u^2y^2 + 3y^4 + 4u^2y^2\cos(2\beta) - 6uy(u^2+y^2)\cos(\beta - \phi_1) \right.\right.$$

$$\left. + u^2y^2\cos(2(\beta - \phi_1)) + 4u^2y^2\cos(2\phi_1) - 6u^3y\cos(\beta + \phi_1) - 6uy^3\cos(\beta + \phi_1) \right.$$

$$\left.\left. + u^2y^2\cos(2(\beta + \phi_1)) \right) \mathrm{Log} + 12uy\sin\beta\sin\phi_1(u^2+y^2 - 2uy\cos\beta\cos\phi_1) \right\}$$

$$\times \left([2u^2 + 3x^2 - 6ux\cos\phi_1 + u^2\cos(2\phi_1)]\, s_1 + u^2[2 + \cos(2\phi_1)]\, s_2 \right.$$

$$\left. + u[-3x\cos\phi_1 + u(2 + \cos(2\phi_1))]\, s_3 \right). \tag{4.39}$$

Once $\bar{v}^{(1)}$, $\bar{\mathfrak{l}}^{(4)}$ and $\bar{\mathfrak{l}}^{(2)}$ have been computed, $\bar{\mathfrak{l}}^{(1)}$ and $\bar{\mathfrak{l}}^{(3)}$ are recovered by taking successively the linear combinations

$$\bar{\mathfrak{l}}^{(3)} = \frac{1}{2x^2y^2}\bar{\mathfrak{l}}^{(4)} - \frac{y}{x}\cos\beta \, \bar{\mathfrak{l}}^{(2)} \tag{4.40}$$

---

[7]The idea is that instead of directly applying the matrix $M(x,y)$ on $\overrightarrow{v}_u$, we first triangularize the linear system: compute $\bar{\mathfrak{l}}^{(2)}$ and $\bar{\mathfrak{l}}^{(4)} = 2xy^2(y\cos\beta\,\bar{\mathfrak{l}}^{(2)} + x\,\bar{\mathfrak{l}}^{(3)})$ and $\bar{v}^{(1)} = \frac{3}{4}x^4\,\bar{\mathfrak{l}}^{(1)} + x^2y^2(\cos^2\beta - \frac{1}{4})\,\bar{\mathfrak{l}}^{(2)} + \frac{3}{2}x^3y\cos\beta\,\bar{\mathfrak{l}}^{(3)}$.

and

$$\bar{l}^{(1)} = \frac{4}{3x^4} \left(\bar{v}^{(1)} - x^2 y^2 \left(\cos^2 \beta - \frac{1}{4} \right) \bar{l}^{(2)} - \frac{3}{2} x^3 y \cos \beta \, \bar{l}^{(3)} \right). \tag{4.41}$$

Next, we study the behavior of the integrands at large u. The curly bracket in eq. (4.38) is of order $1/u^2$, and the bracket containing the s_i is at most of order $1/u$, based on the properties (3.70)–(3.71). Therefore the integrand in eq. (4.38) is at most of order $1/u^2$ and the integral is absolutely convergent (numerically, it appears to fall off even faster, perhaps as $1/u^3$). Similarly, in eq. (4.39) the curly bracket is of order $1/u$, and the bracket containing the s_i is at most of order unity. Therefore the integrand of eq. (4.39) is at most of order $1/u^3$ and the integral is absolutely convergent.

The case of the integrand in eq. (4.37) is a bit more subtle. It is helpful to consider what happens at either $x = 0$ or $y = 0$ from the beginning. At $y = 0$, starting from eq. (3.64) one finds that

$$T_{\alpha\beta}(x,0) = \frac{4}{3\pi x^2} \left(\hat{x}_\alpha \hat{x}_\beta - \frac{1}{4} \delta_{\alpha\beta} \right) \int_0^\infty du \, u \int_0^\pi d\phi_1 \, \sin^2 \phi_1 \, (s_1 + s_2 + s_3). \tag{4.42}$$

Now, it is obvious that when $x = y = 0$, $\int d^4 u \, G_0(u) \, \langle (\epsilon_\alpha \epsilon_\beta - \frac{1}{4} \delta_{\alpha\beta}) J(\hat{\epsilon}, u) J(\hat{\epsilon}, -u) \rangle_{\hat{\epsilon}}$ vanishes, because $\langle u_\alpha u_\beta - \frac{1}{4} u^2 \delta_{\alpha\beta} \rangle_{\hat{u}} = 0$. How does this result emerge from eq. (4.42) ? We have already seen that $(s_1 + s_2 + s_3)$ vanishes to linear order (included) in $|x|$. One then finds that the quadratic order does not vanish, however it vanishes upon performing the ϕ_1 integral in eq. (4.42),

$$\lim_{x \to 0} \frac{1}{\pi x^2} \int_0^\pi d\phi_1 \, \sin^2 \phi_1 \, (s_1 + s_2 + s_3) = 0. \tag{4.43}$$

It turns out that expanding the summand of the s_i in a Taylor series for small x, the Taylor coefficients fall off with increasing powers of $1/u$. This would be obvious on dimensional grounds if the muon mass did not enter the expression. On close inspection, the only factor that could spoil this property are the factors $z_n(u^2 - 2|u||x|\cos\phi_1 + x^2)$, which are dimensionless functions of $m\sqrt{u^2 - 2|u||x|\cos\phi_1 + x^2}$. However, for large argument these functions go like $z_n(u^2) \sim \frac{1}{4\pi^2(n+1)m|u|}$, so that the dependence on the mass factors out and the dimensional argument applies; note that for this leading behavior, the sum over n is still absolutely convergent. The fact that the Taylor series of $\int_0^\pi d\phi_1 \, \sin^2 \phi_1 \, (s_1 + s_2 + s_3)$ at small $|x|$ starts at order $|x|^3$ (at the earliest) thus implies that the expression is at most of order $|x|^3/(m^2|u|^3)$ at large $|u|$; the integrals over $|u|$ in eq. (4.37) and in eq. (4.42) is then absolutely convergent. For the numerical implementation, one option is then to subtract the $O(x^2)$ term from $(s_1 + s_2 + s_3)$; this has the advantage of making the u-integrand absolutely convergent in the infrared prior to the ϕ_1 integral.

For completeness, let us also treat the case where first x is set to zero. For $x = 0$, we can use eq. (3.61), the expansion of the massless propagator in Gegenbauer polynomials in eqs. (3.16) and (3.17) and the property (3.12) to find

$$T_{\alpha\beta}(0,y) = \frac{1}{6} \left(\hat{y}_\alpha \hat{y}_\beta - \frac{1}{4} \delta_{\alpha\beta} \right) \int_0^\infty du \, u^5 \, b(u^2) \, d_2(u^2, y^2). \tag{4.44}$$

5 Final convolution integral via the multipole expansion of the massless propagator

While the method presented in the previous section can be used to numerically calculate the QED weight functions, certain difficulties arise in special kinematic configurations of the vectors x and y. Especially the regime where x and y are near-collinear can be challenging, in view of the inverse powers of $\sin \beta$ present for instance in eqs. (4.22) or (4.39). Recall the definition $\cos \beta = \hat{x} \cdot \hat{y}$.

We therefore explore a different method to obtain the QED weight functions numerically. The idea is to use the multipole expansion of the massless propagator to obtain the weight functions in the form of a series of polynomials in $\cos \beta$, times a function of $(|x|, |y|)$. The relevant polynomials, as it turns out, are either the Gegenbauer polynomials themselves, or their derivatives.

Let $f(\hat{x} \cdot \hat{u})$ be a smooth test function. Directly integrating the expression $\frac{1}{(u-y)^2} f(\hat{x} \cdot \hat{u})$ over two of the three angles parametrizing u yields a logarithm (see eq. (4.12)), which is found in the expressions for $\bar{\mathfrak{g}}^{(0)}$ (eq. 4.17), $\bar{\mathfrak{g}}^{(3)}$ (eq. 4.23) and $\bar{v}^{(1)}$ (eq. 4.37). As before we will introduce $\cos \phi_1 = \hat{x} \cdot \hat{u}$. If instead one makes use of the multipole expansion of the propagator, as well as of the completeness and orthogonality of the Gegenbauer polynomials, one obtains for the same integral a sum over these polynomials. Matching the two expressions leads to the result

$$-\frac{1}{4|u||y| \sin \beta \sin \phi_1} \operatorname{Log} = \sum_{n=0}^{\infty} \frac{d_n(u^2, y^2)}{n+1} C_n(\cos \beta) C_n(\cos \phi_1), \qquad (5.1)$$

which we will use in the sense of distributions, i.e. inserted in an integral over ϕ_1. The function $d_n(u^2, y^2)$ has been defined in eq. (3.17). Further useful results emerge from integrating the expressions $(\hat{u} \cdot \hat{y}) \frac{f(\hat{x} \cdot \hat{u})}{(u-y)^2}$ and $(\hat{u} \cdot \hat{y})^2 \frac{f(\hat{x} \cdot \hat{u})}{(u-y)^2}$ in the two different ways described above, thus leading to the equalities

$$S_1 \equiv -\frac{1}{4|u||y| \sin \beta} \Big(2 \sin \beta + \Big(\frac{u^2 + y^2}{2|u||y|} - \cos \beta \cos \phi_1 \Big) \frac{\operatorname{Log}}{\sin \phi_1} \Big)$$

$$= \sin^2 \beta \, \sin^2 \phi_1 \sum_{n=1}^{\infty} \frac{d_n(u^2, y^2) \, C_n'(\cos \beta) \, C_n'(\cos \phi_1)}{n(n+1)(n+2)}, \qquad (5.2)$$

$$S_2 \equiv -\frac{1}{8u^3 y^3 \sin \beta \sin \phi_1} \cdot$$

$$\Big\{ \Big(3u^4 + 8u^2 y^2 + 3y^4 + 4u^2 y^2 \cos(2\beta) - 6uy(u^2 + y^2) \cos(\beta - \phi_1) + u^2 y^2 \cos(2(\beta - \phi_1)) $$

$$+ 4u^2 y^2 \cos(2\phi_1) - 6u^3 y \cos(\beta + \phi_1) - 6uy^3 \cos(\beta + \phi_1) + u^2 y^2 \cos(2(\beta + \phi_1)) \Big) \operatorname{Log}$$

$$+ 12uy \sin \beta \sin \phi_1 (u^2 + y^2 - 2uy \cos \beta \cos \phi_1) \Big\}$$

$$= 4 \sin^4 \beta \, \sin^4 \phi_1 \sum_{n=2}^{\infty} \frac{d_n(u^2, y^2) \, C_n''(\cos \beta) C_n''(\cos \phi_1)}{(n-1)n(n+1)(n+2)(n+3)}. \qquad (5.3)$$

Equality (5.2) show that two powers of $\sin^2 \beta$ can be extracted explicitly from the angular integrals for $\bar{\mathfrak{g}}^{(2)}$ (eq. 4.22) and $\bar{\mathfrak{l}}^{(4)}$ (eq. 4.38). Similarly, eq. (5.3) shows that four powers of

$\sin^2 \beta$ can be extracted from the angular integral for $\bar{I}^{(2)}$ (eq. 4.39), allowing one to cancel analytically otherwise numerically problematic inverse powers of $\sin \beta$. In this way, the case where x and y are exactly collinear can be calculated directly, without the use of an extrapolation to $\sin \beta = 0$. The price one pays for this cancellation is that the sum over the derivatives of the Gegenbauer polynomials converges somewhat less rapidly: for instance, $C_n(1) = n + 1$, while $C_n'(1) = \frac{n}{3}(n + 1)(n + 2)$.

5.1 Derivation of eqs. (5.1)–(5.3)

Let $f(\hat{x} \cdot \hat{u})$ be a smooth test function. As given in eq. (4.12), explicit integration over the spherical-coordinate angles ϕ_2 and ϕ_3 yields

$$\left\langle \frac{1}{(u-y)^2} f(\hat{x} \cdot \hat{u}) \right\rangle_{\hat{u}} = -\frac{1}{4|u||y| \sin \beta} \left\langle \frac{\text{Log}}{\sin \phi_1} \cdot f(\cos \phi_1) \right\rangle_{\hat{u}}. \tag{5.4}$$

On the other hand, using the expansion of the massless propagator in eq. (3.16) and of the function f in Gegenbauer polynomials in eq. (3.14), as well as the orthogonality property (3.13), one finds

$$\left\langle \frac{1}{(u-y)^2} f(\hat{x} \cdot \hat{u}) \right\rangle_{\hat{u}} = \sum_{n=0}^{\infty} d_n(u^2, y^2) \frac{C_n(\cos \beta)}{n+1} \left\langle C_n(\cos \phi_1) f(\cos \phi_1) \right\rangle_{\hat{u}}. \tag{5.5}$$

Comparing the expressions yields eq. (5.1).

In the same way, consider the two treatments of the following angular average,

$$\left\langle \frac{\hat{u} \cdot \hat{y} - (\hat{x} \cdot \hat{y})(\hat{x} \cdot \hat{u})}{(u-y)^2} f(\hat{x} \cdot \hat{u}) \right\rangle_{\hat{u}}$$
$$= -\frac{1}{4|u||y| \sin \beta} \left\langle \left(2 \sin \beta + \left(\frac{u^2 + y^2}{2|u||y|} - \cos \beta \cos \phi_1 \right) \frac{\text{Log}}{\sin \phi_1} \right) f(\cos \phi_1) \right\rangle_{\hat{u}}$$
$$= \sum_{n=0}^{\infty} \frac{C_n(\cos \beta)}{n+1} \left\langle C_n(\cos \phi_1) \left(\frac{1}{2}(d_{n+1} + d_{n-1}) - \cos \beta \cos \phi_1 d_n \right) f(\cos \phi_1) \right\rangle_{\hat{u}}. \tag{5.6}$$

We are using the convention $d_n \equiv 0$ for $n < 0$ and the argument of the d_n coefficients is (u^2, y^2) throughout this subsection. Comparing the two equations yields an expression for S_1,

$$S_1 = \sum_{n=0}^{\infty} \frac{C_n(\cos \beta)}{n+1} C_n(\cos \phi_1) \left(\frac{1}{2}(d_{n+1} + d_{n-1}) - \cos \beta \cos \phi_1 d_n \right). \tag{5.7}$$

We can now manipulate the sum in the following way. First apply the cosine factors on the Gegenbauer polynomials, using eq. (3.11),

$$S_1 = \sum_{n=0}^{\infty} \frac{1}{n+1} \Bigg(C_n(\cos \beta) C_n(\cos \phi_1) \frac{1}{2}(d_{n+1} + d_{n-1}) \tag{5.8}$$
$$- \frac{d_n}{4}(C_{n+1}(\cos \beta) + C_{n-1}(\cos \beta))(C_{n+1}(\cos \phi_1) + C_{n-1}(\cos \phi_1)) \Bigg)$$

Next, shift the summation index in the second term so as to factorize $C_n(\cos\phi_1)$, and then collect the terms multiplying d_{n+1} and those multiplying d_{n-1},

$$S_1 = \frac{1}{4}\sum_{n=0}^{\infty}\frac{C_n(\cos\phi_1)}{n+1}\left[\frac{d_{n+1}}{n+2}\Big((n+3)C_n(\cos\beta)-(n+1)C_{n+2}(\cos\beta)\Big)\right. \tag{5.9}$$
$$\left.+\frac{d_{n-1}}{n}\Big((n-1)C_n(\cos\beta)-(n+1)C_{n-2}(\cos\beta)\Big)\right].$$

Note that $\frac{d_{n-1}}{n}$ should be interpreted as zero for $n=0$. Now we notice that the combination appearing in the brackets can be expressed through the derivative of the Gegenbauer polynomials,

$$(n+2)C_{n-1}(z)-nC_{n+1}(z)=2(1-z^2)C_n'(z), \qquad n\geq 0. \tag{5.10}$$

Then shifting again the summation index so as to factorize $C_n'(\cos\beta)$, we arrive at

$$S_1 = \frac{1-\cos^2\beta}{2}\sum_{n=1}^{\infty}d_n\frac{C_n'(\cos\beta)}{n+1}\left(\frac{C_{n-1}(\cos\phi_1)}{n}-\frac{C_{n+1}(\cos\phi_1)}{n+2}\right) \tag{5.11}$$

(we have used the fact that $C_{n=0}'(\cos\beta)=0$ to drop the $n=0$ term); and finally, identifying again the expression for the derivative of C_n in the bracket, we obtain eq. (5.2).

Thirdly, one finds by the same method as above

$$\left\langle\frac{(\hat{u}\cdot\hat{y})^2}{(u-y)^2}f(\hat{x}\cdot\hat{u})\right\rangle_{\hat{u}}$$
$$=-\frac{1}{16u^3y^3\sin\beta}\left\langle\Big(4uy\sin\beta\sin\phi_1(u^2+y^2+2uy\cos\beta\cos\phi_1)+(u^2+y^2)^2\mathrm{Log}\Big)\frac{f(\cos\phi_1)}{\sin\phi_1}\right\rangle_{\hat{u}}$$
$$=\frac{1}{4}\sum_{n=0}^{\infty}\frac{C_n(\cos\beta)}{n+1}(d_{n-2}+(2-\delta_{n0})d_n+d_{n+2})\Big\langle C_n(\cos\phi_1)\,f(\cos\phi_1)\Big\rangle_{\hat{u}}, \tag{5.12}$$

which provides us with a new identity. The specific linear combination appearing in the QED weight function $\overline{\mathrm{I}}^{(2)}$ in eq. (4.39) is

$$S_2 \equiv -\frac{1}{8u^3y^3\sin\beta\sin\phi_1}\cdot$$
$$\left\{\Big(3u^4+8u^2y^2+3y^4+4u^2y^2\cos(2\beta)-6uy(u^2+y^2)\cos(\beta-\phi_1)+u^2y^2\cos(2(\beta-\phi_1))\right.$$
$$+4u^2y^2\cos(2\phi_1)-6u^3y\cos(\beta+\phi_1)-6uy^3\cos(\beta+\phi_1)+u^2y^2\cos(2(\beta+\phi_1))\Big)\mathrm{Log}$$
$$\left.+12uy\sin\beta\sin\phi_1(u^2+y^2-2uy\cos\beta\cos\phi_1)\right\}$$
$$=\sum_{n=0}^{\infty}\frac{C_n(\cos\beta)}{n+1}C_n(\cos\phi_1)\left[2d_n\left(\frac{1}{2}+\cos(2\beta)+\cos(2\phi_1)+\frac{1}{2}\cos(2\beta)\cos(2\phi_1)\right)\right.$$
$$\left.-6\cos\beta\cos\phi_1(d_{n+1}+d_{n-1})+\frac{3}{2}(d_{n+2}+(2-\delta_{n0})d_n+d_{n-2})\right], \tag{5.13}$$

where we have used eqs. (5.1), (5.2) and (5.12) in obtaining the second equality. Manipulations on expression (5.13) similar to those yielding eq. (5.2), including the use of

$$-2\big((n+3)(n-1)+3\delta_{n0}\big)C_n(z)+(n+2)(n+3)C_{n-2}(z)+n(n-1)C_{n+2}(z)$$
$$= 4(1-z^2)^2 C_n''(z), \qquad n \geq 0, \tag{5.14}$$

lead to eq. (5.3).

5.2 Gegenbauer expansion of the QED weight functions

Using the relations above, we provide alternative expressions to compute the six required weight functions and their derivatives. Using eq. (5.1), one derives the following representation for three of the weight functions with argument $(|x|, \hat{c}_\beta, |y|)$, where $\hat{c}_\beta = \cos\beta$,

$$\begin{pmatrix} \bar{\mathfrak{g}}^{(0)} \\ \bar{\mathfrak{g}}^{(3)} \\ \bar{v}^{(1)} \end{pmatrix} = \sum_{n=0}^{\infty} C_n(\hat{c}_\beta) \left[\frac{1}{|y|^{n+2}} \begin{pmatrix} \alpha_{n-}^{(0)} \\ \alpha_{n-}^{(3)} \\ \alpha_{n-}^{(1)} \end{pmatrix} + |y|^n \begin{pmatrix} \alpha_{n+}^{(0)} \\ \alpha_{n+}^{(3)} \\ \alpha_{n+}^{(1)} \end{pmatrix} \right]. \tag{5.15}$$

Here the coefficients $\alpha_{n\pm}^{(k)}$, for $k = 0, 1, 3$, have argument $(|x|, |y|)$, and their functional form is

$$\alpha_{n-}^{(k)}(|x|, |y|) = \frac{1 - \frac{1}{2}\delta_{k3}}{\pi(n+1)} \int_0^{|y|} u^{n+3} du \int_0^\pi d\phi_1 \, \hat{s}_1^2 \, C_n(\hat{c}_1) \, \sigma_k(|x|, \hat{c}_1, |u|), \tag{5.16}$$

$$\alpha_{n+}^{(k)}(|x|, |y|) = \frac{1 - \frac{1}{2}\delta_{k3}}{\pi(n+1)} \int_{|y|}^\infty \frac{du}{u^{n-1}} \int_0^\pi d\phi_1 \, \hat{s}_1^2 \, C_n(\hat{c}_1) \, \sigma_k(|x|, \hat{c}_1, |u|), \tag{5.17}$$

where $\hat{c}_1 = \cos\phi_1$ and $\hat{s}_1 = \sin\phi_1$. The functions $\sigma_k(|x|, \hat{c}_1, |u|)$ appearing in the coefficients $\alpha_{n\pm}^{(k=0,1,3)}$, as well as those appearing in $\beta_{n\pm}^{(k=2,4)}$ and $\gamma_{n\pm}^{(2)}$ below, are given explicitly at the end of this subsection, eqs. (5.24)–(5.31). As a remark, we have already noted that $\bar{\mathfrak{g}}^{(0)}$ contains a logarithmic infrared divergence. In the present representation, that divergence is entirely contained in the coefficient $\alpha_{0+}^{(0)}$, which makes a constant contribution to $\bar{\mathfrak{g}}^{(0)}$, independent of x and y. Since only derivatives of $\bar{\mathfrak{g}}^{(0)}$ with respect to x or y appear in the QED kernel, the coefficient $\alpha_{0+}^{(0)}$ is never actually needed.

Next, starting from eqs. (4.22) and (4.38), and using eq. (5.2), one obtains the representation

$$\begin{pmatrix} \bar{\mathfrak{g}}^{(2)} \\ \bar{\mathfrak{l}}^{(4)}/y^2 \end{pmatrix} = \sum_{n=1}^{\infty} C_n'(\hat{c}_\beta) \left[\frac{1}{|y|^{n+3}} \begin{pmatrix} \beta_{n-}^{(2)} \\ \beta_{n-}^{(4)} \end{pmatrix} + |y|^{n-1} \begin{pmatrix} \beta_{n+}^{(2)} \\ \beta_{n+}^{(4)} \end{pmatrix} \right]. \tag{5.18}$$

with (for $k = 2, 4$)

$$\beta_{n-}^{(k)}(|x|, |y|) = \frac{-(1 - \frac{1}{2}\delta_{k2})}{\pi \, n(n+1)(n+2)} \int_0^{|y|} du \, u^{n+3} \int_0^\pi d\phi_1 \, \hat{s}_1^2 \, C_n'(\hat{c}_1) \, \sigma_k(|x|, \hat{c}_1, |u|), \tag{5.19}$$

$$\beta_{n+}^{(k)}(|x|, |y|) = \frac{-(1 - \frac{1}{2}\delta_{k2})}{\pi \, n(n+1)(n+2)} \int_{|y|}^\infty \frac{du}{u^{n-1}} \int_0^\pi d\phi_1 \, \hat{s}_1^2 \, C_n'(\hat{c}_1) \, \sigma_k(|x|, \hat{c}_1, |u|). \tag{5.20}$$

Finally, using eqs. (4.39) and (5.3), we obtain the form

$$\bar{I}^{(2)}(|x|, \hat{c}_\beta, |y|) = \sum_{n=2}^{\infty} C_n''(\hat{c}_\beta)\Big(\frac{1}{|y|^{n+4}}\gamma_{n-}^{(2)}(|x|, |y|) + |y|^{n-2}\gamma_{n+}^{(2)}(|x|, |y|)\Big), \qquad (5.21)$$

$$\gamma_{n-}^{(2)}(|x|, |y|) = \frac{1}{2\pi\,(n-1)\,n\,(n+1)(n+2)(n+3)} \cdot \qquad (5.22)$$
$$\cdot \int_0^{|y|} du\, u^{n+3} \int_0^\pi d\phi_1\, \hat{s}_1^2\, C_n''(\hat{c}_1)\, \sigma_5(|x|, \hat{c}_1, |u|)$$

$$\gamma_{n+}^{(2)}(|x|, |y|) = \frac{1}{2\pi\,(n-1)\,n\,(n+1)(n+2)(n+3)} \cdot \qquad (5.23)$$
$$\cdot \int_{|y|}^\infty \frac{du}{u^{n-1}} \int_0^\pi d\phi_1\, \hat{s}_1^2\, C_n''(\hat{c}_1)\, \sigma_5(|x|, \hat{c}_1, |u|).$$

We now give the explicit expressions for the sums $\sigma_k(|x|, \hat{c}_1, |u|)$, $k = 0, \ldots, 5$. They involve the modified Bessel functions and the Gegenbauer polynomials. The argument of the C_n and C_n' polynomials is always $(\hat{u} \cdot \widehat{x-u})$; this is only indicated explicitly in the relatively compact expression for σ_0, which in fact coincides with $s(x, u)$. For the weight functions expanded in $C_n(\hat{c}_\beta)$ in eq. (5.15), the sums are

$$\sigma_0 = \sum_{n=0}^{\infty} z_n(u^2)\, z_n((x-u)^2)\, \frac{C_n(\hat{u} \cdot \widehat{x-u})}{n+1}, \qquad (5.24)$$

$$\sigma_3 = \frac{1}{|x|^2} \sum_{n=0}^{\infty} \Big\{ z_n(u^2) z_{n+1}((x-u)^2) \Big[|x-u|\frac{C_n}{n+1} + |u|\frac{C_{n+1}}{n+2}\Big] \qquad (5.25)$$
$$+ z_{n+1}(u^2) z_n((x-u)^2) \Big[|u|\frac{C_n}{n+1} + |x-u|\frac{C_{n+1}}{n+2}\Big] \Big\}$$

$$= \frac{1}{|x|} \sum_{n=0}^{\infty} \Big\{ \frac{z_n(u^2) z_{n+1}((x-u)^2)}{n+2} \Big[\frac{|x|\hat{s}_1^2}{|x-u|}\frac{C_{n+1}'}{n+1} + \hat{c}_1 C_{n+1}\Big] \qquad (5.26)$$
$$+ \frac{z_{n+1}(u^2) z_n((x-u)^2)}{n+1} \Big[-\frac{|x|\hat{s}_1^2}{|x-u|}\frac{C_n'}{n+2} + \hat{c}_1 C_n\Big] \Big\},$$

and

$$\sigma_1 \equiv s_1 + s_2 + s_3 = -\frac{x^2}{4} \sum_{n=0}^{\infty} z_n(u^2) z_n((x-u)^2)\frac{C_n}{n+1} \qquad (5.27)$$

$$+ \frac{u^2}{4} \sum_{n=0}^{\infty} z_n((x-u)^2)\Big(z_{n-2}(u^2) + (2-\delta_{n0}) z_n(u^2) + z_{n+2}(u^2)\Big)\frac{C_n}{n+1}$$

$$+ \frac{(x-u)^2}{4} \sum_{n\geq 0} z_n(u^2)\Big(z_{n-2}((x-u)^2) + (2-\delta_{n0}) z_n((x-u)^2) + z_{n+2}((x-u)^2)\Big)\frac{C_n}{n+1}$$

$$+ \frac{|u||x-u|}{4} \sum_{n=0}^{\infty} \Big\{ \Big(z_n(u^2) z_{n+2}((x-u)^2) + 2 z_n(u^2) z_n((x-u)^2) + z_{n+2}(u^2) z_n((x-u)^2)\Big)\frac{C_{n+1}}{n+2}$$

$$+ \Big(z_{n-2}(u^2) z_n((x-u)^2) + 2 z_n(u^2) z_n((x-u)^2) + z_n(u^2) z_{n-2}((x-u)^2)\Big)\frac{C_{n-1}}{n} \Big\}.$$

For the weight functions expanded in $C'_n(\hat{c}_\beta)$ in eq. (5.18), the sums are

$$\sigma_2 = \frac{1}{|x|} \sum_{n=0}^{\infty} g\{z_n(u^2) z_{n+1}((x-u)^2) \left[|x-u|\hat{c}_1 \frac{C_n}{n+1} + (|u|\hat{c}_1 - |x|) \frac{C_{n+1}}{n+2} \right] \qquad (5.28)$$

$$+ z_{n+1}(u^2) z_n((x-u)^2) \left[(|u|\hat{c}_1 - |x|) \frac{C_n}{n+1} + |x-u|\hat{c}_1 \frac{C_{n+1}}{n+2} \right] g\}$$

$$= \hat{s}_1^2 \sum_{n=0}^{\infty} g\{ \frac{z_n(u^2) z_{n+1}((x-u)^2)}{n+2} \left[\frac{|x|\hat{c}_1}{|x-u|} \frac{C'_{n+1}}{n+1} - C_{n+1} \right] \qquad (5.29)$$

$$- \frac{z_{n+1}(u^2) z_n((x-u)^2)}{n+1} \left[\frac{|x|\hat{c}_1}{|x-u|} \frac{C'_n}{n+2} + C_n \right] g\}.$$

and

$$\sigma_4 = \frac{1}{|u|} \left(\left(2\frac{|u|}{|x|}\hat{c}_1 - 1 \right) \sigma_1 + s_2 - s_1 \right). \qquad (5.30)$$

Finally, the sum appearing in $\bar{\iota}^{(2)}$ is

$$\sigma_5 = \frac{1}{u^2} \left(\frac{|u|}{x^2}(|u|(1+2\hat{c}_1^2) - 3|x|\hat{c}_1)\sigma_1 + 3\frac{|u|}{|x|}\hat{c}_1(s_2 - s_1) + 3s_1 \right). \qquad (5.31)$$

The sums s_1 and s_2 are evaluated as indicated in eqs. (3.66) and (3.67).

For numerical purposes, it is usually preferable to evaluate the derivative of an integrand with respect to a parameter before the integral is performed numerically. Therefore, for completeness, we provide in appendix B the expressions of the $|x|$-derivative of the sums defining the weight functions, namely the $\{\sigma_k\}_{k=0}^5$ as well as s_1 and s_2. In the expressions provided in appendix, the first two derivatives of the functions $z_n(u^2)$ appear. Thanks to eq. (3.37), they can be computed practically in an iterative fashion as follows,

$$\frac{\partial z_n}{\partial |u|} = \frac{n+1}{4\pi^2 m u^2} K_0(mu) I_{n+1}(m|u|) - \frac{z_n(u)}{|u|}, \qquad (5.32)$$

$$\frac{\partial^2 z_n}{\partial |u|^2} = -\frac{3}{u}\left(\frac{\partial z_n}{\partial |u|} \right) + \frac{n(n+2)}{u^2} z_n(u) - \frac{n+1}{2\pi^2 u^2} K_1(m|u|) I_{n+1}(m|u|). \qquad (5.33)$$

Appendix C provides the relevant expressions to obtain the QED weight functions and the full kernel at $x = 0$ or at $y = 0$. The motivation for investigating these special cases is twofold. First, the expressions simplify compared to the general case in that they have one fewer integral or infinite sum. Thus, their evaluation is significantly faster and provides a cross-check for the numerics of the general case, which should approach the special cases in the appropriate limits. Second, when we consider modifications of the QED kernel via subtractions in section 8.1, the kernel at $x = 0$ or $y = 0$ will be needed explicitly. The QED kernel for $y = x$ can be obtained from the case $y = 0$ using the property (2.22).

6 Numerical evaluation of the QED kernel

The basic idea of our approach is to precompute and store the weight functions, since by O(4) symmetry they are functions of three variables. This stands in stark contrast with

the QED kernel itself, which is a function of eight real variables and has 384 independent components. Since up to two derivatives with respect to components of x and y act on the tensors $S(x, y)$, $V_\delta(x, y)$ and $T_{\beta\delta}(x, y)$, chain rules are used to convert these derivatives, when they act on the weight functions, into derivatives with respect to the variables $(|x|, \hat{c}_\beta \equiv \hat{x} \cdot \hat{y}, |y|)$, for instance

$$\partial_\alpha^{(x)} = \hat{x}_\alpha \frac{\partial}{\partial|x|} + \frac{1}{|x|}(\hat{y}_\alpha - \hat{c}_\beta \hat{x}_\alpha)\frac{\partial}{\partial \hat{c}_\beta}. \tag{6.1}$$

The chain-rule based expressions for the tensors $T_{\alpha\beta\delta}^{\mathrm{A}}(x, y)$ in terms of the weight functions are given in appendix A ($A =$ I, II, III). With these rank-three tensors at hand, and with the Dirac traces $\mathcal{G}^A$ computed upon initialization, the QED kernel is obtained via a simple linear combination, eq. (2.30).

We have pursued two strategies to numerically compute the QED weight function. The first is based on eqs. (4.18), (4.22), (4.23), (4.37), (4.38), (4.39), followed by taking the appropriate linear combinations. In this strategy, the weight functions are computed on a three-dimensional grid, each direction representing one of the variables $|x|$, $\hat{c}_\beta$ and $|y|$. While we will not describe this implementation in detail (see [78] for more information), it is worth mentioning that the logarithm appearing in each of the six equations referenced above required a dedicated treatment in the regions where its argument vanishes. The second strategy, which is the one we opted for in our subsequent tests and lattice QCD calculations, consists in calculating the coefficients of the weight-function expansion in Gegenbauer polynomials according to eqs. (5.15), (5.18), (5.21). The coefficients are functions of $|x|$ and $|y|$ and carry an index corresponding to the order of the polynomial in $\hat{c}_\beta$ which they multiply. Implementing both strategies with two independent codes allowed us to have a valuable cross-check of our results. In the following, we describe a sample of the results obtained with the second strategy and the most important technical aspects involved in the numerical calculation. It is worth mentioning at this point the order-of-magnitude computational cost of precomputing the required weight functions provided at [96]: it amounted in total to about three weeks on a dual-core laptop.

The three tensor weight functions as well as the derivatives of the scalar weight function appearing in the kernel $\bar{\mathcal{L}}_{[\rho\sigma];\mu\nu\lambda}(x, y)$ for given values of $|x|$ and $\hat{c}_\beta$ are displayed in figure 4. The result of the numerical integration is shown as a curve. At $y = 0$, we confront the numerical results with the Taylor expansion of the weight functions obtained in appendix C and observe good agreement.[8] In addition, the large-$|y|$ asymptotics for the derivatives of the scalar function $\bar{\mathfrak{g}}^{(0)}$ are determined in appendix D and displayed for $m|y| > 5$ in the three left panels of figure 4. Similarly, figure 5 shows the two vector weight functions. The scalar and tensor weight functions have unit of GeV^{-2}, while the vector ones have unit of GeV^{-1}. It is natural to use the muon mass to build dimensionless combinations. We note that all weight functions are smooth functions of $|y|$, and that they have rather different magnitudes in units of the muon mass. The scalar and the first vector weight function are largest, the other weight functions being at least an order of magnitude smaller. We have

---

[8]For $\bar{\mathfrak{l}}^{(2)}$, we did not derive a prediction at $y = 0$ because it is not needed for the QED kernel.

found this hierarchy to be fairly generic. For the reader's convenience, we have collected a few numerical values of the weight functions in table 1. Quantitative checks have been performed against the weight functions resulting from the first computational strategy described in the previous paragraph. For instance, at the reference point $m_\mu |x| = 0.436$, $\hat{c}_\beta = -0.59375$ and $m_\mu |y| = 0.654$, all derivatives required for the QED kernel have been compared; with m_μ set to unity, the largest absolute difference was found in $\frac{\partial^2 g_1}{\partial |x| \partial \hat{c}_\beta}$, and amounted to 7×10^{-9}.

We next describe some of the numerical techniques we have used to arrive at the results presented in figure 4 and 5. We first note that we have worked in double precision throughout, and have not found it necessary to employ further enhanced arithmetic precision. In the representation of eqs. (5.15), (5.18), (5.21) of the weight functions, one has to carry out a two-dimensional integral of an integrand which is represented as an infinite sum over products of modified Bessel functions and a Gegenbauer polynomial or its derivatives. One integration variable represents the angle between the position vectors x and u, the other is the norm of u. The most important numerical task is thus to evaluate efficiently a sum involving the modified Bessel functions and the Gegenbauer polynomial or its derivatives.

We have evaluated strings of modified Bessel functions (e.g. K_0, K_1, ..., $K_{n_{\max}}$) using routines inspired by those given in [79]. The most important aspect is that the modified Bessel functions of the second kind (K_n) can be evaluated using the recursion relation among them in the direction of increasing index n, while those of the first kind (I_n) must be evaluated in a downward recursion, starting from a sufficiently large n. Since we need these functions for a wide range of n, we store them on the fly during the recursion.

Next, we use the Clenshaw algorithm (see for instance [79]) to perform the sum, exploiting the recursion relations

$$C_{n+1}(z) = 2z C_n(z) - C_{n-1}(z) \qquad (n \geq 1), \qquad (6.2)$$

$$C'_{n+1}(z) = 2z \frac{n+1}{n} C'_n(z) - \frac{n+2}{n} C'_{n-1}(z) \qquad (n \geq 1), \qquad (6.3)$$

$$C''_{n+1}(z) = 2z \frac{n+1}{n-1} C''_n(z) - \frac{n+3}{n-1} C''_{n-1}(z) \qquad (n \geq 2) \qquad (6.4)$$

among the polynomials. Thus none of the C_n, C'_n and C''_n are evaluated explicitly in the calculation of the sums.

We have performed the integration using the integrator `cubature` [80]. This integrator is able to perform numerical integrals on a multi-dimensional rectangular region. For calculating the weight functions, we have mostly used the p-adaptive cubature routine, which uses a tensor product of Clenshaw-Curtis quadrature rules; the degree of the rules is doubled along each dimension until convergence is achieved. An advantage of the `cubature` package is that it allows for a vector of integrands. Since it is the different coefficients $\alpha_m^{(k)}(|x|, |y|)$ ($k = 0, 1, 3$), $\beta_m^{(k)}(|x|, |y|)$ ($j = 2, 4$) and $\gamma_m^{(2)}(|x|, |y|)$ that are being calculated, and that they all involve the same sums (one of the σ_i ($i = 0, \ldots, 5$)), only the Gegenbauer polynomial $C_m(\hat{u} \cdot \hat{x})$ (or its derivative) must be reevaluated for different values of the index m. This saves a significant amount of computations. Because the Gegenbauer polynomial

is strongly oscillating for large m, the calculation of the large-order coefficients to a given relative precision dominates the computing time.

We have turned the integral over $|u|$ from $|y|$ to ∞ into an integral from 0 to $1/|y|$ by making the change of variables $u_1 = 1/|u|$. Given that we want to compute the coefficients of the Gegenbauer-polynomial expansion for all $|y|$, a considerable amount of computing time is saved by simply observing that

$$\alpha_{m-}^{(k)}(|x|, |y| + \Delta|y|) = \alpha_{m-}^{(k)}(|x|, |y|) \qquad (6.5)$$
$$+ \frac{1 - \frac{1}{2}\delta_{k3}}{\pi(m+1)} \int_{|y|}^{|y|+\Delta|y|} u^{m+3} du \int_0^\pi d\phi_1 \, \hat{s}_1^2 \, C_m(\hat{c}_1) \, \sigma_k(|x|, \hat{c}_1, |u|),$$

$$\alpha_{m+}^{(k)}(|x|, |y| - \Delta|y|) = \alpha_{m+}^{(k)}(|x|, |y|) \qquad (6.6)$$
$$+ \frac{1 - \frac{1}{2}\delta_{k3}}{\pi(m+1)} \int_{|y|-\Delta|y|}^{|y|} \frac{du}{u^{m-1}} \int_0^\pi d\phi_1 \, \hat{s}_1^2 \, C_m(\hat{c}_1) \, \sigma_k(|x|, \hat{c}_1, |u|),$$

and similarly for the other coefficients. In this way, the cost of increasing the resolution $1/\Delta|y|$ with which the coefficients are computed is very low. We also recall that the derivative of the coefficients with respect to $|y|$ are needed to obtain the QED kernel. We have used the fact that one can easily obtain these $|y|$-derivatives analytically at practically zero computational cost. Indeed, since

$$\frac{1}{|y|^{m+2}} \frac{\partial}{\partial|y|} \alpha_{m-}^{(k)}(|x|, |y|) + |y|^m \frac{\partial}{\partial|y|} \alpha_{m+}^{(k)}(|x|, |y|) = 0, \qquad (6.7)$$

we have for instance

$$\frac{\partial}{\partial|y|} \bar{\mathfrak{g}}^{(0)} = \sum_{m \geq 0} C_m(\hat{c}_\beta) \left[-(m+2) \frac{1}{|y|^{m+3}} \alpha_{m-}^{(0)} + m|y|^{m-1} \alpha_{m+}^{(0)} \right], \qquad (6.8)$$

and similar expressions apply to all six weight functions. The derivatives with respect to $\hat{c}_\beta$ are of course simply obtained by analytically deriving the Gegenbauer polynomial. Finally, the $|x|$ dependence of the weight functions appears only in the sums $\sigma_k(|x|, \hat{c}_1, |u|)$. Their first $|x|$-derivative is given analytically in appendix B. Only the second $|x|$-derivative of the sums σ_2 and σ_3 was computed numerically by taking a finite difference (with step size $m\delta|x| = 10^{-3}$) of the analytically obtained first derivative.

An important question in the method based on the series in Gegenbauer polynomials is, how many terms are needed to reach a good approximation to the weight function. The answer obviously depends on $|x|$ and $|y|$. Consider the case of the scalar weight function, which is given by the integral of the massless propagator $G_0(y - u)$ multiplied with $s(x, u)$, for fixed vectors x and y. If one used the expansion of $s(x, u)$ in $C_n(\hat{x} \cdot \hat{u})$, together with the expansion of $G_0(y - u)$ in $C_n(\hat{y} \cdot \hat{u})$, the result of the angular integration (see eq. (3.13)) would be to give the expansion of the scalar weight function in $C_n(\hat{x} \cdot \hat{y})$, with coefficients proportional to the product of the coefficients in the two series appearing in the integrand. The expansion of the scalar weight function in $C_n(\hat{x} \cdot \hat{y})$ is precisely the series whose coefficients we compute numerically. Thus, for that series to converge rapidly, it is sufficient that for all u, of the multipole expansion of the massless propagator and the expansion of
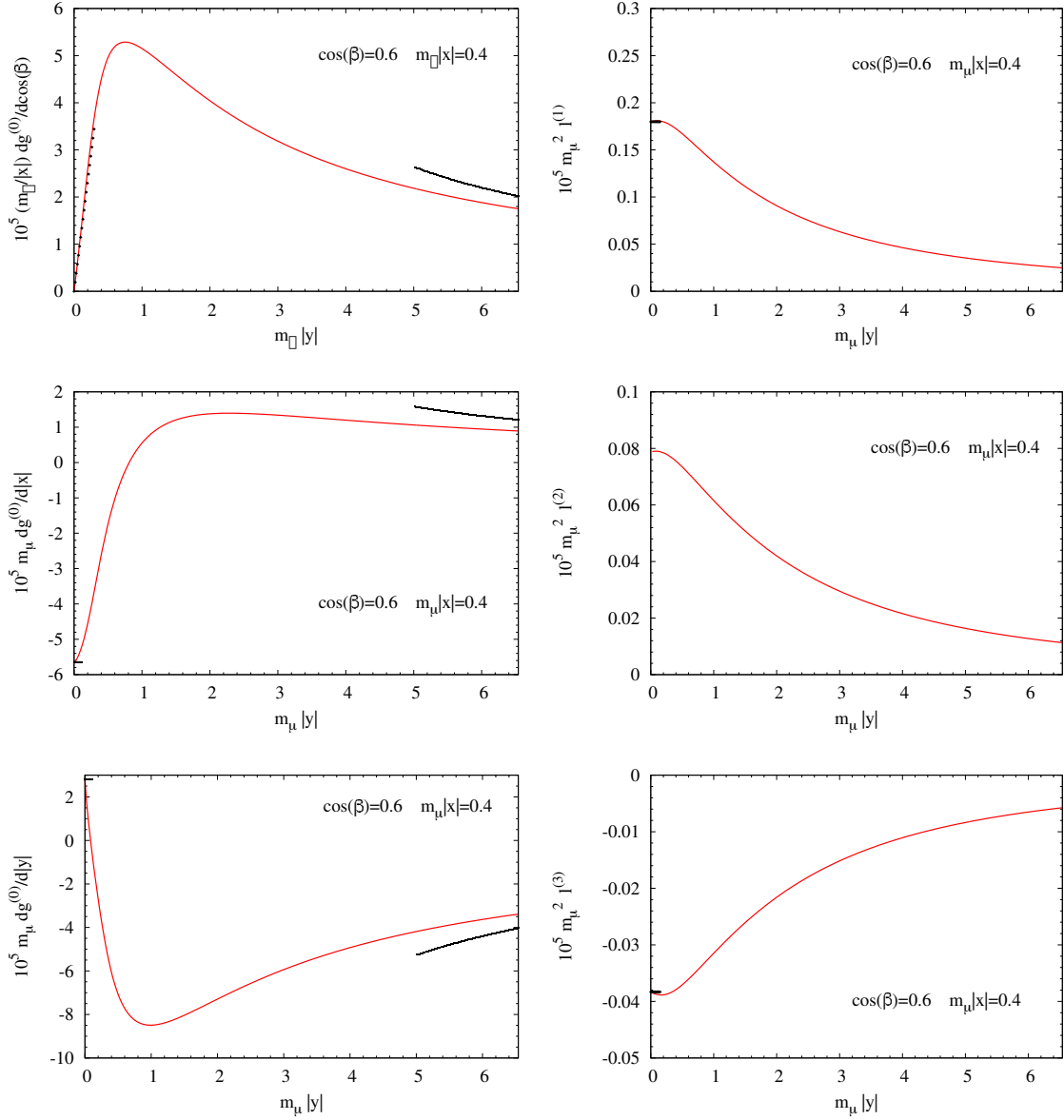
Figure 4. Left panels: the derivatives of the scalar weight function $\bar{\mathfrak{g}}^{(0)}$ appearing in the QED kernel for given values of $|x|$ and $\cos\beta \equiv \hat{x}\cdot\hat{y}$. The analytic predictions for the large-y asymptotics are displayed as thick solid lines. Right panels: the three tensor weight functions $\bar{\mathfrak{l}}^{(1)}$, $\bar{\mathfrak{l}}^{(2)}$, $\bar{\mathfrak{l}}^{(3)}$. The leading term of the Taylor expansion around the origin, which is $\mathrm{O}(|y|^0)$ except for the top left panel, is indicated for all cases but $\bar{\mathfrak{l}}^{(2)}$; note that the latter weight function is multiplied by a tensor of order $|y|^2$ in the QED kernel.
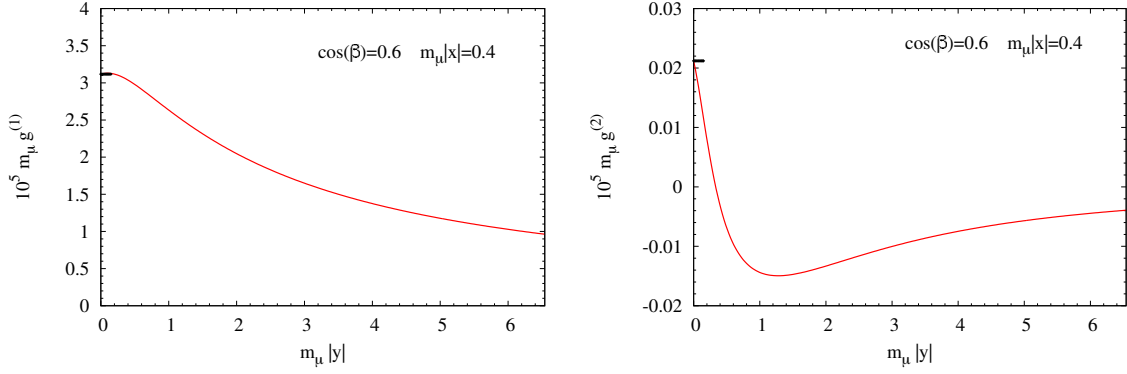
Figure 5. The vector weight functions $\bar{\mathfrak{g}}^{(1)}$ and $\bar{\mathfrak{g}}^{(2)}$ appearing in the QED kernel for given values of $|x|$ and $\hat{c}_\beta \equiv \hat{x} \cdot \hat{y}$, the muon mass being denoted by m_μ. The leading term of the Taylor expansion around the origin $(\mathrm{O}(|y|^0))$ is indicated as a short horizontal line.

$10^5 \times$ weight fct.	$|y| = 0.532889$	$|y| = 0.872000$	$|y| = 2.39800$
$d\bar{\mathfrak{g}}^{(0)}/d\cos\beta$	2.023	2.099	1.465
$d\bar{\mathfrak{g}}^{(0)}/d|x|$	-1.489	0.2071	1.393
$d\bar{\mathfrak{g}}^{(0)}/d|y|$	-7.317	-8.443	-6.713
$\bar{\mathfrak{g}}^{(1)}$	2.958	2.723	1.870
$\bar{\mathfrak{g}}^{(2)}$	-0.007883	-0.01357	-0.01197
$\bar{\mathfrak{l}}^{(1)}$	0.1653	0.1448	0.07812
$\bar{\mathfrak{l}}^{(2)}$	0.07271	0.06462	0.03633
$\bar{\mathfrak{l}}^{(3)}$	-0.03674	-0.03297	-0.01867

Table 1. The weight functions (multiplied by 10^5) for $|x| = 0.4$, $\cos\beta = 0.6$ and three different values of $|y|$. The muon mass is set to unity throughout this table.

$s(x, u)$ in $C_n(\hat{x} \cdot \hat{u})$, at least one converges rapidly. The multipole expansion of $G_0(y - u)$ converges poorly when $|u| = |y|$; the expansion of $s(x, u)$ in $C_n(\hat{x} \cdot \hat{u})$ converges poorly when $|u| = |x|$. Thus to guarantee that the series in $C_n(\hat{x} \cdot \hat{y})$ converges rapidly, one must avoid the case $|x| \approx |y|$. The latter condition however defines a surface of codimension one in the space of (x, y), and the poor convergence thus affects a substantial fraction of the sampled (x, y) points. However, we can use the symmetry (2.43) to compute the weight function with the argument y exchanged for $(x - y)$, which in general will improve the convergence of the series in $C_n(\hat{x} \cdot \hat{y})$, since the value of $|x|$ is then substantially different from $|x - y|$. The only case where the convergence cannot be improved by using the symmetry property of the weight function is when the points $(0, x, y)$ form an equilateral triangle. The condition for this to happen however is a subset of codimension two. Thus if the convergence of the series cannot be controlled in a region $||x| - |y|| < \Delta$ and $||x| - |x - y|| < \Delta$, an integral over the QED kernel with a function which is smooth for an equilateral-triangle constellation of $(0, x, y)$ will suffer an error of order Δ^2. To guarantee an accurate computation of

the QED kernel in the equilateral-triangle constellation, additional computations would be required. In the practical applications of the QED kernel, we have not found it necessary to improve further the quality of its evaluation for an overall accuracy on a_μ^{HLbL} on the order of one percent. The considerations above apply to all weight functions, and the symmetry relations (2.43)–(2.48) can be exploited to always compute the weight functions with the most favorable arguments for the purpose of the expansion in Gegenbauer polynomials.

Some trial-and-error was necessary to find out an appropriate extent and step size[9] for the grid in $|x|$ and $|y|$. Both variables were sampled up to $|x|_{\text{max}} = |y|_{\text{max}} = 6.54m^{-1}$. For the variable $m|y|$, which is cheap to sample finely, we use a step size of $\delta_{\text{g}} = 0.0242222$. For the variable $m|x|$, we use the same fine step size for small $m|x|$ up to $m|x| = 0.363333$, and a step size three times bigger for the larger $m|x|$. The number of coefficients of the Gegenbauer-polynomial expansion computed for a given pair $(|x|, |y|)$ was chosen[10] to be $(8 + \text{floor}(5m|x|))$. For $m|y| < \delta_{\text{g}}$, we use the Taylor-expansion given in appendix C in order to interpolate the QED kernel between the point at $m|y| = 0$ and the first point of the grid at $m|y| = \delta_{\text{g}}$. We proceed similarly in the case $m|x| < \delta_{\text{g}}$. The large-$|y|$ asymptotics derived in appendix D were not used in the numerical implementation, they only served to acquire a qualitative understanding of the large-distance behavior of the QED kernel.

As sketched at the beginning of this section, given precomputed coefficients of the Gegenbauer polynomial expansion of the weight functions on a grid in $|x|$ and $|y|$, the remaining computational tasks to obtain the QED kernel at a given (x, y) point are: to evaluate the sums yielding the weight functions (again using the Clenshaw algorithm), interpolate the weight functions (and their derivatives), apply the chain rules to obtain the $T_{\alpha\beta\delta}^{(\text{A})}$ tensors and finally to perform the contraction of these with the $\mathcal{G}_{\delta[\rho,\sigma]\mu\alpha\nu\beta\lambda}^{\text{A}}$ tensors. We have written a code in the C programming language to perform these tasks. Some implementation details and a link to the code can be found in appendix E.

7 Example calculations of the four-point amplitude $i\widehat{\Pi}$

In this section we derive explicit expressions for $i\widehat{\Pi}_{\rho;\mu\nu\lambda\sigma}(x, y)$ in several models that are relevant for understanding the corresponding tensor in QCD. Our primary goal is to use these four-point functions to test (in section 8) the validity of the coordinate-space approach to a_μ^{HLbL} developed here. In addition, we will gain insight into the shape and range of the integrand, information which is valuable in preparing the lattice-QCD calculation.

But first, we review the most important properties of the tensor $i\widehat{\Pi}_{\rho;\mu\nu\lambda\sigma}(x, y)$.

---

[9]The required extent of the grid is dictated by the physics entering the correlation function $i\widehat{\Pi}$; it was chosen large enough for the π^0 exchange to be reproduced with subpercent precision at $m_\pi = 135\,\text{MeV}$. The step size should be small enough that the achieved precision on the grid points does not get 'spoiled' entirely by the interpolation. Since the weight functions vary more rapidly at small arguments $|x|$ and $|y|$, a relatively small step size was chosen in this region.

[10]The stability of the resulting weight functions was tested by varying the number of terms in the Gegenbauer-polynomial series.

7.1 General properties of $i\widehat{\Pi}$

The rank-five tensor has the Bose symmetries

$$\widehat{\Pi}_{\rho;\mu\nu\lambda\sigma}(x,y) = \widehat{\Pi}_{\rho;\nu\mu\lambda\sigma}(y,x) = \widehat{\Pi}_{\rho;\lambda\nu\mu\sigma}(-x, y-x). \tag{7.1}$$

Combining the two generators of Bose symmetries from eq. (7.1), we obtain a finite symmetry group with 3! elements. Note that while the first equality in eq. (7.1) follows immediately from the definition of $\widehat{\Pi}$, the second one requires translation symmetry and the property that

$$\int d^4 z \, \langle j_\mu(x) j_\nu(y) j_\sigma(z) j_\lambda(0) \rangle = 0, \tag{7.2}$$

which holds in infinite volume as a consequence of the observation that a conserved current can be written as a total divergence,

$$j_\sigma(z) = \partial_\alpha^{(z)}(z_\sigma j_\alpha(z)), \tag{7.3}$$

and Gauss's theorem.

The tensor $\widehat{\Pi}$ has the further discrete symmetry

$$\widehat{\Pi}_{\rho;\mu\nu\lambda\sigma}(-x,-y) = -\widehat{\Pi}_{\rho;\mu\nu\lambda\sigma}(x,y) \tag{7.4}$$

as a consequence of the space and Euclidean-time reversal symmetries of QCD. Current conservation implies

$$\partial_\mu^{(x)}\widehat{\Pi}_{\rho;\mu\nu\lambda\sigma}(x,y) = 0, \tag{7.5}$$

$$\partial_\nu^{(y)}\widehat{\Pi}_{\rho;\mu\nu\lambda\sigma}(x,y) = 0, \tag{7.6}$$

$$(\partial_\lambda^{(x)} + \partial_\lambda^{(y)})\widehat{\Pi}_{\rho;\mu\nu\lambda\sigma}(x,y) = 0. \tag{7.7}$$

For the last result, we have again assumed infinite volume and translation symmetry, and made use of eq. (7.2). For the same reasons, we have the properties

$$\int_x \widehat{\Pi}_{\rho;\mu\nu\lambda\sigma}(x,y) = \int_y \widehat{\Pi}_{\rho;\mu\nu\lambda\sigma}(x,y) = 0, \tag{7.8}$$

which will be exploited in the numerical tests of section 8.1. These properties hold in the continuum formulation of QED or QCD. In a theory like scalar QED (see subsection 7.4 below), the appropriate contact terms, as predicted by the Ward identities of current conservation, must be included into the definition of $i\widehat{\Pi}$ in order for eq. (7.8) to be satisfied.

We finally give the representation of $i\widehat{\Pi}$ in terms of the Euclidean momentum-space HLbL amplitude. The latter is related to the position-space four-point function of the electromagnetic current via a triple Fourier transform,

$$\left\langle j_\mu(x) j_\nu(y) j_\sigma(z) j_\lambda(0) \right\rangle = \int_{q_1,q_2,q_3} e^{i(q_1 \cdot x + q_2 \cdot y + q_3 \cdot z)} \Pi_{\mu\nu\sigma\lambda}(q_1,q_2,q_3). \tag{7.9}$$

The quantity of interest, $i\widehat{\Pi}_{\rho;\mu\nu\lambda\sigma}(x,y)$, can then be calculated using the equation

$$i\widehat{\Pi}_{\rho;\mu\nu\lambda\sigma}(x,y) = -i \int_{q_1,q_2} e^{i(q_1 \cdot x + q_2 \cdot y)} \frac{\partial}{\partial q_{3\rho}} \Pi_{\mu\nu\sigma\lambda}(q_1,q_2,q_3)\Big|_{q_3=0}. \tag{7.10}$$

This relation is particularly useful when form factors are introduced to describe the coupling of mesons to photons, as in the case of the pion-pole contribution.

7.2 Pion-pole contribution to hadronic light-by-light scattering in the VMD model

As a starting point for calculating the contribution of the pion pole, we take the Minkowski-space expression for the HLbL amplitude given in [54]. To convert it to Euclidean space, we use the prescription given in [53], whereby we arrive at

$$
\begin{aligned}
\Pi_{\mu\nu\sigma\lambda}(q_1, q_2, q_3)\Big|_{\pi_0} &= \frac{\mathcal{F}(-q_1^2, -q_2^2)\mathcal{F}(-q_3^2, -(q_1+q_2+q_3)^2)}{(q_1+q_2)^2 + m_\pi^2} \epsilon_{\mu\nu\alpha\beta}\, q_{1\alpha}\, q_{2\beta}\, \epsilon_{\sigma\lambda\gamma\delta}\, q_{3\gamma}\, (q_1+q_2)_\delta \\
&+ \frac{\mathcal{F}(-q_1^2, -(q_1+q_2+q_3)^2)\mathcal{F}(-q_2^2, -q_3^2)}{(q_2+q_3)^2 + m_\pi^2} \epsilon_{\mu\lambda\alpha\beta}\, q_{1\alpha}\, (q_2+q_3)_\beta\, \epsilon_{\nu\sigma\gamma\delta}\, q_{2\gamma}\, q_{3\delta} \\
&+ \frac{\mathcal{F}(-q_1^2, -q_3^2)\mathcal{F}(-q_2^2, -(q_1+q_2+q_3)^2)}{(q_1+q_3)^2 + m_\pi^2} \epsilon_{\mu\sigma\alpha\beta}\, q_{1\alpha}\, q_{3\beta}\, \epsilon_{\nu\lambda\gamma\delta}\, q_{2\gamma}\, (q_1+q_3)_\delta.
\end{aligned}
\tag{7.11}
$$

From here the required derivative $\frac{\partial}{\partial q_{3\rho}}\Pi_{\mu\nu\sigma\lambda}(q_1, q_2, q_3)|_{q_3=0}$ is obtained straightforwardly. Before Fourier transforming it with respect to q_1 and q_2, we choose a specific parametrization of the form factor.

7.2.1 Vector-meson dominance parametrization of the form factor

In the following, we use the vector-meson dominance (VMD) model for the transition form factor,

$$
\mathcal{F}(-q_1^2, -q_2^2) = \frac{c_\pi}{(q_1^2 + m_V^2)(q_2^2 + m_V^2)},
\tag{7.12}
$$

its normalization $c_\pi = -\frac{N_c m_V^4}{12\pi^2 F_\pi}$ being determined by the axial anomaly. Inserting this form into the expression for $\frac{\partial}{\partial q_{3\rho}}\Pi_{\mu\nu\sigma\lambda}(q_1, q_2, q_3)|_{q_3=0}$, and the latter into (7.10), and rewriting the expression using coordinate-space propagators, one finds the master expression

$$
\begin{aligned}
i\widehat{\Pi}_{\rho;\mu\nu\lambda\sigma}(x, y) = \quad & \frac{c_\pi^2}{m_V^2(m_V^2 - m_\pi^2)} \frac{\partial}{\partial x_\alpha} \frac{\partial}{\partial y_\beta} \Big\{ \epsilon_{\mu\nu\alpha\beta}\epsilon_{\sigma\lambda\rho\gamma}\Big(\frac{\partial}{\partial x_\gamma} + \frac{\partial}{\partial y_\gamma}\Big) K_\pi(x, y) \\
& + \epsilon_{\mu\lambda\alpha\beta}\epsilon_{\nu\sigma\gamma\rho}\frac{\partial}{\partial y_\gamma} K_\pi(y - x, y) + \epsilon_{\mu\sigma\alpha\rho}\epsilon_{\nu\lambda\beta\gamma}\frac{\partial}{\partial x_\gamma} K_\pi(x, x - y)\Big\},
\end{aligned}
\tag{7.13}
$$

where

$$
K_\pi(x, y) \equiv \int_u \Big(G_{m_\pi}(u) - G_{m_V}(u)\Big)G_{m_V}(x - u)G_{m_V}(y - u) = K_\pi(y, x).
\tag{7.14}
$$

We remind the reader that we denote by G_M the scalar propagator with mass M; see eq. (3.2).

Thus the main task is to compute the scalar function $K_\pi(x, y)$, which depends on three scalar quantities, $|x|$, $\cos\beta \equiv \hat{x}\cdot\hat{y}$ and $|y|$. The three derivatives that must be applied onto the function $K_\pi(x, y)$ are computed using a lengthy chain rule.

The goal is therefore to compute $K_\pi(x, y)$ and the derivatives with respect to the scalar variables analytically as far as possible. Using the expansion of the scalar propagator in Gegenbauer polynomials and exploiting their orthogonality property, one obtains immediately an expansion of $K_\pi(x, y)$ in $C_n(\hat{x}\cdot\hat{y})$. Via the change of integration variable $u \to x - u$

in eq. (7.14) and the subsequent Gegenbauer expansion of the propagators, one arrives at the alternative expansion

$$K_\pi(x,y) = \sum_{n \geq 0} C_n(\widehat{x-y} \cdot \hat{x}) \, b_n(|x|, |x-y|), \tag{7.15}$$

$$b_n(|x|, |x-y|) = \frac{2\pi^2}{n+1} \int_0^\infty d|u| \, |u|^3 G_{m_V}(u) \, \delta\gamma_n(x^2, u^2) \, \gamma_n((x-y)^2, u^2), \tag{7.16}$$

with $\delta\gamma_n(x^2, u^2) = \gamma_n(x^2, u^2)|_{m_\pi} - \gamma_n(x^2, u^2)|_{m_V}$ the difference of the expansion coefficients of two massive propagators with different masses in Gegenbauer polynomials; see eq. (3.19) for the explicit expression for $\gamma_n(x^2, u^2)$. Because the difference of two propagators is only logarithmically divergent at the origin, the convergence of the multipole expansion is improved. A further, analogous expression for $K_\pi(x,y)$ expanded in $C_n(\widehat{x-y} \cdot \hat{y})$ is obtained by interchanging x and y on the right-hand side of eq. (7.15).

An important consideration in the evaluation of $K_\pi(x,y)$, very similar to the discussion in the penultimate paragraph of section 6, is the following. For the sum in eq. (7.15) to be rapidly convergent, at least one of the $\delta\gamma_n(x^2, u^2)$ and $\gamma_n((x-y)^2, u^2)$ should decrease rapidly with n, for all u. This works when the ratio of $|x|$ and $|x-y|$ is not too close to unity. If this is not the case, the expansion in $C_n(\widehat{x-y} \cdot \hat{y})$ can be used. The only problematic constellation is when the points $(0, x, y)$ form an equilateral triangle; in this case, a more sophisticated technique would be required. However, in an integral over x at fixed y for instance, this case represents a set of codimension 2. In practice, this means that if the sum, truncated at $n_{\max}$, does not provide an accurate estimate of $K_\pi(x,y)$ in a range $|x| = |y|(1 \pm \epsilon)$ and $\cos\beta = \frac{\pi}{3}(1 \pm \epsilon)$, where ϵ shrinks when $n_{\max}$ increases, the error on the resulting integral is of order ϵ^2, since the integrand is regular in the equilateral constellation. In our numerical implementation, we chose $n_{\max} = 64$.

Explicitly, the form of the coefficients is

$$b_n(|x|, \Delta) \stackrel{\Delta \leqq |x|}{=} \frac{(n+1)m_V}{8\pi^4 |x| \Delta} \tag{7.17}$$

$$\Big\{ K_{n+1}(m_V \Delta) \Big(K_{n+1}(m_\pi |x|) G_n^1(m_\pi, m_V, \Delta) - K_{n+1}(m_V |x|) G_n^1(m_V, m_V, \Delta) \Big)$$

$$+ I_{n+1}(m_V \Delta) \Big(K_{n+1}(m_\pi |x|)(G_n^2(m_\pi, m_V, \Delta) - G_n^2(m_\pi, m_V, |x|))$$

$$- K_{n+1}(m_V |x|)(G_n^2(m_V, m_V, \Delta) - G_n^2(m_V, m_V, |x|)) \Big)$$

$$+ I_{n+1}(m_V \Delta) \Big(I_{n+1}(m_\pi |x|) G_n^3(m_\pi, m_V, |x|) - I_{n+1}(m_V |x|) G_n^3(m_V, m_V, |x|) \Big) \Big\},$$

$$b_n(|x|, \Delta) \stackrel{|x| \leqq \Delta}{=} \frac{(n+1)m_V}{8\pi^4 |x| \Delta} \tag{7.18}$$

$$\Big\{ K_{n+1}(m_V \Delta) \Big(K_{n+1}(m_\pi |x|) G_n^1(m_\pi, m_V, |x|) - K_{n+1}(m_V |x|) G_n^1(m_V, m_V, |x|) \Big)$$

$$+ K_{n+1}(m_V \Delta) \Big(I_{n+1}(m_\pi |x|)(G_n^2(m_V, m_\pi, |x|) - G_n^2(m_V, m_\pi, \Delta))$$

$$- I_{n+1}(m_V |x|)(G_n^2(m_V, m_V, |x|) - G_n^2(m_V, m_V, \Delta)) \Big)$$

$$+ I_{n+1}(m_V \Delta) \Big(I_{n+1}(m_\pi |x|) G_n^3(m_\pi, m_V, \Delta) - I_{n+1}(m_V |x|) G_n^3(m_V, m_V, \Delta) \Big) \Big\}$$

with

$$G_n^1(m_1, m_2, |x|) = \int_0^{|x|} du \, K_1(m_V u) I_{n+1}(m_1 u) I_{n+1}(m_2 u), \tag{7.19}$$

$$G_n^2(m_1, m_2, |x|) = \int_{|x|}^{s} du \, K_1(m_V u) I_{n+1}(m_1 u) K_{n+1}(m_2 u), \tag{7.20}$$

$$G_n^3(m_1, m_2, |x|) = \int_{|x|}^{\infty} du \, K_1(m_V u) K_{n+1}(m_1 u) K_{n+1}(m_2 u). \tag{7.21}$$

As a reminder, I_n and K_n denote the modified Bessel functions. Note that the dependence of G_n^2 on the upper limit s of integration drops out in the functions b_n. In our approach to the numerical implementation, the values of the functions $G_n^{1,2,3}$ are computed and stored on a regular one-dimensional grid. Then, when the function $K_\pi(x, y)$ and its derivatives are needed at a certain target point, the more favorable expansion in $C_n(\widehat{x - y} \cdot \hat{x})$ and $C_n(\widehat{x - y} \cdot \hat{y})$ is chosen, and an interpolation is performed in the variables $|x|$ and $|x - y|$, at the target value of $\cos\alpha = \widehat{x - y} \cdot \hat{x}$. A chain rule relates the derivatives with respect to one of the variables $(|x|, \cos\beta, |y|)$ to those with respect to one of the variables $(|x|, \cos\alpha, |x - y|)$. With up to three derivatives involved, the chain rule is best generated with a symbolic manipulation program. A further element used in the evaluation of the derivatives is based on the observation

$$(-\triangle^{(y)} + M_V^2)K_\pi(x, y) = G_{m_V}(x - y)\Big(G_{m_\pi}(y) - G_{m_V}(y)\Big). \tag{7.22}$$

This equation is used to express the second and higher derivatives with respect to $|y|$ in terms of the derivatives with respect to $\cos\beta$ of the same order and in terms of lower derivatives.

7.2.2 Tests performed

From the momentum-space expression

$$K_\pi(x, y) = (m_V^2 - m_\pi^2) \int_{q_1, q_2} \frac{e^{i(q_1 \cdot x + q_2 \cdot y)}}{[(q_1 + q_2)^2 + m_\pi^2](q_1^2 + m_V^2)(q_2^2 + m_V^2)[(q_1 + q_2)^2 + m_V^2]}, \tag{7.23}$$

one easily obtains

$$\int_{x,y} K_\pi(x, y) = \frac{m_V^2 - m_\pi^2}{m_\pi^2 m_V^6}, \tag{7.24}$$

which provides a test of the numerical implementation of $K_\pi(x, y)$. More differential information can also be obtained,

$$\int_y K_\pi(x, y) = \frac{1}{m_V^2}\Big(\frac{1}{m_V^2 - m_\pi^2}(G_{m_\pi}(x) - G_{m_V}(x)) - \frac{K_0(m_V|x|)}{8\pi^2}\Big). \tag{7.25}$$

Also, using integration by parts and the result (7.24), one shows that

$$\int_{x,y} \delta_{\mu\nu} x_\lambda (x_\rho y_\sigma - y_\rho x_\sigma) i\widehat{\Pi}_{\rho;\mu\nu\lambda\sigma}(x, y) = -\int_{x,y} \delta_{\mu\nu} y_\lambda (x_\rho y_\sigma - y_\rho x_\sigma) i\widehat{\Pi}_{\rho;\mu\nu\lambda\sigma}(x, y)$$

$$= \frac{1}{2} \int_{x,y} (\delta_{\nu\lambda} x_\mu - \delta_{\mu\lambda} y_\nu)(x_\rho y_\sigma - y_\rho x_\sigma) i\widehat{\Pi}_{\rho;\mu\nu\lambda\sigma}(x, y) = \frac{3}{\pi^4 m_\pi^2 F_\pi^2}. \tag{7.26}$$

The three integrals test respectively the third, second and first term of eq. (7.13), which contains three terms in total.

7.3 Lepton-loop contribution to light-by-light scattering in QED

In this subsection, we present the perturbative calculation of the fermion loop contribution to $i\widehat{\Pi}_{\rho;\mu\nu\lambda\sigma}(x,y)$.

7.3.1 The coordinate-space four-point function of the electromagnetic current

We start out by writing out the expression for the quark-connected contribution of the unintegrated coordinate-space four-point function of the electromagnetic current, valid in an arbitrary $U(N_c)$ gauge field background. We note the important property

$$S(x,y) = \gamma_5 S(y,x)^\dagger \gamma_5 \tag{7.27}$$

of the fermion propagator, where the dagger acts on the Dirac indices. This property holds in an arbitrary background gauge field.

Performing the six fully-connected Wick contractions, we note that due to the property (7.27) they pair up, corresponding to the fermion number flowing in opposite directions. One obtains

$$\langle j_\mu(x)\, j_\nu(y)\, j_\sigma(z)\, j_\lambda(0)\rangle = -2\mathrm{Re}\{I^{(1)}_{\mu\nu\sigma\lambda}(x,y,z,0) + I^{(2)}_{\mu\nu\sigma\lambda}(x,y,z,0) + I^{(3)}_{\mu\nu\sigma\lambda}(x,y,z,0)\}, \tag{7.28}$$

with

$$I^{(1)}_{\mu\nu\sigma\lambda}(x,y,z,w) = \mathrm{Tr}\{\gamma_\mu S(x,y)\gamma_\nu S(y,z)\gamma_\sigma S(z,w)\gamma_\lambda S(w,x)\}, \tag{7.29}$$

$$I^{(2)}_{\mu\nu\sigma\lambda}(x,y,z,w) = \mathrm{Tr}\{\gamma_\mu S(x,y)\gamma_\nu S(y,w)\gamma_\lambda S(w,z)\gamma_\sigma S(z,x)\} = I^{(1)}_{\mu\nu\lambda\sigma}(x,y,w,z), \tag{7.30}$$

$$I^{(3)}_{\mu\nu\sigma\lambda}(x,y,z,w) = \mathrm{Tr}\{\gamma_\lambda S(w,y)\gamma_\nu S(y,z)\gamma_\sigma S(z,x)\gamma_\mu S(x,w)\} = I^{(1)}_{\lambda\nu\sigma\mu}(w,y,z,x). \tag{7.31}$$

7.3.2 Vanishing background gauge field: the QED case

Recall the free Dirac fermion propagator $S(x,y)$ in Euclidean position space,

$$S(w+x,w) \equiv \int \frac{d^4p}{(2\pi)^4}\, \frac{-ip_\mu\gamma_\mu + m}{p^2 + m^2}\, e^{ip\cdot x} = \frac{m^2}{4\pi^2|x|}\Big[\gamma_\mu x_\mu \frac{K_2(m|x|)}{|x|} + K_1(m|x|)\Big], \tag{7.32}$$

with

$$S(w+x,w) = \frac{x_\mu\,\gamma_\mu}{2\pi^2(x^2)^2} \qquad (m=0) \tag{7.33}$$

in the massless case. In the free theory, the propagator is actually Hermitian with respect to the Dirac indices, so that the general property (7.27) holds even without the dagger. From here on, the expressions in this section assume a single fermion flavor with unit electric charge. Thus the calculation can be interpreted as a treatment of the contribution of a lepton of mass m to light-by-light scattering in a_μ. Also, in a vanishing background field, we note the translation-invariance property

$$I^{(j)}_{\mu\nu\sigma\lambda}(x,y,z,w) = I^{(j)}_{\mu\nu\sigma\lambda}(x-w,y-w,z-w,0), \qquad j=1,2,3, \tag{7.34}$$

which can be combined with the Bose symmetry of the photons to write

$$I^{(2)}_{\mu\nu\sigma\lambda}(x,y,z,0) = I^{(1)}_{\mu\nu\lambda\sigma}(x,y,0,z) = I^{(1)}_{\mu\nu\lambda\sigma}(x-z,y-z,-z,0), \qquad (7.35)$$

$$I^{(3)}_{\mu\nu\sigma\lambda}(x,y,z,0) = I^{(1)}_{\lambda\nu\sigma\mu}(0,y,z,x) = I^{(1)}_{\lambda\nu\sigma\mu}(-x,y-x,z-x,0). \qquad (7.36)$$

Furthermore, the expression inside the curly bracket in eq. (7.28) is already real. In the free massless case, one thus obtains

$$I^{(1)}_{\mu\nu\sigma\lambda}(x,y,z,0) = \frac{(-x_\alpha)(x-y)_\beta(y-z)_\gamma z_\delta}{(2\pi^2)^4|x|^4|x-y|^4|y-z|^4|z|^4}\mathrm{Tr}\{\gamma_\alpha\gamma_\mu\gamma_\beta\gamma_\nu\gamma_\gamma\gamma_\sigma\gamma_\delta\gamma_\lambda\}, \qquad (7.37)$$

$$I^{(2)}_{\mu\nu\sigma\lambda}(x,y,z,0) = \frac{y_\alpha(-z_\beta)(z-x)_\gamma(x-y)_\delta}{(2\pi^2)^4|y|^4|z|^4|x-z|^4|x-y|^4}\mathrm{Tr}\{\gamma_\nu\gamma_\alpha\gamma_\lambda\gamma_\beta\gamma_\sigma\gamma_\gamma\gamma_\mu\gamma_\delta\}, \qquad (7.38)$$

$$I^{(3)}_{\mu\nu\sigma\lambda}(x,y,z,0) = \frac{(y-z)_\alpha(z-x)_\beta\,x_\gamma\,(-y_\delta)}{(2\pi^2)^4|y-z|^4|z-x|^4|x|^4|y|^4}\mathrm{Tr}\{\gamma_\nu\gamma_\alpha\gamma_\sigma\gamma_\beta\gamma_\mu\gamma_\gamma\gamma_\lambda\gamma_\delta\}. \qquad (7.39)$$

In the free massive case, the result is

$$I^{(1)}_{\mu\nu\sigma\lambda}(x,y,z,0) = \left(\frac{m}{2\pi}\right)^8 \Big[$$
$$\frac{(-x_\alpha)(x-y)_\beta(y-z)_\gamma z_\delta\;K_2(m|x|)K_2(m|x-y|)K_2(m|y-z|)K_2(m|z|)}{|x|^2|x-y|^2|y-z|^2|z|^2}\;\cdot$$

$$\cdot\,\mathrm{Tr}\{\gamma_\alpha\gamma_\mu\gamma_\beta\gamma_\nu\gamma_\gamma\gamma_\sigma\gamma_\delta\gamma_\lambda\} \qquad (7.40)$$

$$+\frac{K_1(m|x|)K_1(m|x-y|)K_1(m|y-z|)K_1(m|z|)}{|x||x-y||y-z||z|}\mathrm{Tr}\{\gamma_\mu\gamma_\nu\gamma_\sigma\gamma_\lambda\}$$

$$+\frac{(-x_\alpha)(x-y)_\beta\;K_2(m|x|)K_2(m|x-y|)K_1(m|y-z|)K_1(m|z|)}{|x|^2|x-y|^2|y-z||z|}\mathrm{Tr}\{\gamma_\alpha\gamma_\mu\gamma_\beta\gamma_\nu\gamma_\sigma\gamma_\lambda\}$$

$$+\frac{(-x_\alpha)(y-z)_\gamma\;K_2(m|x|)K_1(m|x-y|)K_2(m|y-z|)K_1(m|z|)}{|x|^2|x-y||y-z|^2|z|}\mathrm{Tr}\{\gamma_\alpha\gamma_\mu\gamma_\nu\gamma_\gamma\gamma_\sigma\gamma_\lambda\}$$

$$+\frac{(-x_\alpha)z_\delta\;K_2(m|x|)K_1(m|x-y|)K_1(m|y-z|)K_2(m|z|)}{|x|^2|x-y||y-z||z|^2}\mathrm{Tr}\{\gamma_\alpha\gamma_\mu\gamma_\nu\gamma_\sigma\gamma_\delta\gamma_\lambda\}$$

$$+\frac{(x-y)_\beta(y-z)_\gamma\;K_1(m|x|)K_2(m|x-y|)K_2(m|y-z|)K_1(m|z|)}{|x||x-y|^2|y-z|^2|z|}\mathrm{Tr}\{\gamma_\mu\gamma_\beta\gamma_\nu\gamma_\gamma\gamma_\sigma\gamma_\lambda\}$$

$$+\frac{(x-y)_\beta z_\delta\;K_1(m|x|)K_2(m|x-y|)K_1(m|y-z|)K_2(m|z|)}{|x||x-y|^2|y-z||z|^2}\mathrm{Tr}\{\gamma_\mu\gamma_\beta\gamma_\nu\gamma_\sigma\gamma_\delta\gamma_\lambda\}$$

$$+\frac{(y-z)_\gamma z_\delta\;K_1(m|x|)K_1(m|x-y|)K_2(m|y-z|)K_2(m|z|)}{|x||x-y||y-z|^2|z|^2}\mathrm{Tr}\{\gamma_\mu\gamma_\nu\gamma_\gamma\gamma_\sigma\gamma_\delta\gamma_\lambda\}\Big].$$

To evaluate the coordinate-space four-point function, it is thus sufficient to program the function $I^{(1)}_{\mu\nu\sigma\lambda}(x,y,z,0)$, and call it three times to compute the four-point function $\langle j_\mu(x)\,j_\nu(y)\,j_\sigma(z)\,j_\lambda(0)\rangle$. As for the Dirac traces, it is straightforward to compute and store the 65536 components of $\mathrm{Tr}\{\gamma_\alpha\gamma_\mu\gamma_\beta\gamma_\nu\gamma_\gamma\gamma_\sigma\gamma_\delta\gamma_\lambda\}$ once for all times.

7.3.3 Calculation of $i\widehat{\Pi}_{\rho;\mu\nu\lambda\sigma}(x,y)$

From eq. (7.28), in order to compute

$$i\widehat{\Pi}_{\rho;\mu\nu\lambda\sigma}(x,y) = 2\int_z z_\rho\,\mathrm{Re}\{I^{(1)}_{\mu\nu\sigma\lambda}(x,y,z,0) + I^{(2)}_{\mu\nu\sigma\lambda}(x,y,z,0) + I^{(3)}_{\mu\nu\sigma\lambda}(x,y,z,0)\}, \quad (7.41)$$

it is sufficient to compute the two integrals

$$\widehat{\Pi}^{(1)}_{\rho;\mu\nu\lambda\sigma}(x,y) \equiv 2\,\mathrm{Re}\int d^4z\; z_\rho\, I^{(1)}_{\mu\nu\sigma\lambda}(x,y,z,0), \tag{7.42}$$

$$\Pi^{(r,1)}_{\mu\nu\lambda\sigma}(x,y) \equiv 2\,\mathrm{Re}\int d^4z\; I^{(1)}_{\mu\nu\sigma\lambda}(x,y,z,0). \tag{7.43}$$

Indeed, for the second term, we make use of the property

$$I^{(2)}_{\mu\nu\sigma\lambda}(x,y,z,0) = I^{(1)}_{\mu\nu\lambda\sigma}(x,y,0,z) = I^{(1)}_{\nu\lambda\sigma\mu}(y,0,z,x) = I^{(1)}_{\nu\lambda\sigma\mu}(y-x,-x,z-x,0) \tag{7.44}$$

(where we have performed a cyclic permutation of the arguments in the second equality), from which there follows

$$2\int d^4z\; z_\rho\, I^{(2)}_{\mu\nu\sigma\lambda}(x,y,z,0) = 2\int d^4z\; (z_\rho+x_\rho)I^{(1)}_{\nu\lambda\sigma\mu}(y-x,-x,z,0) \tag{7.45}$$
$$= \widehat{\Pi}^{(1)}_{\rho;\nu\lambda\mu\sigma}(y-x,-x) + x_\rho\,\Pi^{(r,1)}_{\nu\lambda\mu\sigma}(y-x,-x).$$

Similarly, the third term can be expressed as

$$I^{(3)}_{\mu\nu\sigma\lambda}(x,y,z,0) = I^{(1)}_{\lambda\nu\sigma\mu}(0,y,z,x) = I^{(1)}_{\lambda\nu\sigma\mu}(-x,y-x,z-x,0), \tag{7.46}$$

so that

$$2\int d^4z\; z_\rho\, I^{(3)}_{\mu\nu\sigma\lambda}(x,y,z,0) = 2\int d^4z\; (z_\rho+x_\rho)I^{(1)}_{\lambda\nu\sigma\mu}(-x,y-x,z,0) \tag{7.47}$$
$$= \widehat{\Pi}^{(1)}_{\rho;\lambda\nu\mu\sigma}(-x,y-x) + x_\rho\,\Pi^{(r,1)}_{\lambda\nu\mu\sigma}(-x,y-x).$$

Thus $i\widehat{\Pi}_{\rho;\mu\nu\lambda\sigma}(x,y)$ can be expressed through the functions $\widehat{\Pi}^{(1)}_{\rho;\mu\nu\lambda\sigma}(x,y)$ and $\Pi^{(r,1)}_{\nu\lambda\mu\sigma}(x,y)$ via

$$i\widehat{\Pi}_{\rho;\mu\nu\lambda\sigma}(x,y) = \widehat{\Pi}^{(1)}_{\rho;\mu\nu\lambda\sigma}(x,y) \tag{7.48}$$
$$+\widehat{\Pi}^{(1)}_{\rho;\nu\lambda\mu\sigma}(y-x,-x) + x_\rho\,\Pi^{(r,1)}_{\nu\lambda\mu\sigma}(y-x,-x)$$
$$+\widehat{\Pi}^{(1)}_{\rho;\lambda\nu\mu\sigma}(-x,y-x) + x_\rho\,\Pi^{(r,1)}_{\lambda\nu\mu\sigma}(-x,y-x).$$

It remains to perform the required integrals. The result is

$$
\widehat{\Pi}^{(1)}_{\rho;\mu\nu\lambda\sigma}(x,y) \tag{7.49}
$$
$$
= 2\Big(\frac{m}{2\pi}\Big)^8 \Big[\frac{(-x_\alpha)(x-y)_\beta K_2(m|x|)K_2(m|x-y|)}{|x|^2|x-y|^2} \cdot f_{\rho\delta\gamma}(y) \cdot \mathrm{Tr}\{\gamma_\alpha\gamma_\mu\gamma_\beta\gamma_\nu\gamma_\gamma\gamma_\sigma\gamma_\delta\gamma_\lambda\}
$$
$$
+ \frac{K_1(m|x|)K_1(m|x-y|)}{|x||x-y|} \cdot f_{\rho\delta\gamma}(y) \cdot \mathrm{Tr}\{\gamma_\mu\gamma_\nu\gamma_\gamma\gamma_\sigma\gamma_\delta\gamma_\lambda\}
$$
$$
+ \frac{K_1(m|x|)K_1(m|x-y|)}{|x||x-y|}\, g_\rho(y) \cdot \mathrm{Tr}\{\gamma_\mu\gamma_\nu\gamma_\sigma\gamma_\lambda\}
$$
$$
+ \frac{(-x_\alpha)(x-y)_\beta\, K_2(m|x|)K_2(m|x-y|)}{|x|^2|x-y|^2} g_\rho(y) \cdot \mathrm{Tr}\{\gamma_\alpha\gamma_\mu\gamma_\beta\gamma_\nu\gamma_\sigma\gamma_\lambda\}
$$
$$
+ \frac{(-x_\alpha)\, K_2(m|x|)K_1(m|x-y|)}{|x|^2|x-y|} h_{\rho\gamma}(y) \cdot \mathrm{Tr}\{\gamma_\alpha\gamma_\mu\gamma_\nu\gamma_\gamma\gamma_\sigma\gamma_\lambda\}
$$
$$
+ \frac{(x-y)_\beta\, K_1(m|x|)K_2(m|x-y|)}{|x||x-y|^2} h_{\rho\gamma}(y) \cdot \mathrm{Tr}\{\gamma_\mu\gamma_\beta\gamma_\nu\gamma_\gamma\gamma_\sigma\gamma_\lambda\}
$$
$$
+ \frac{(-x_\alpha)\, K_2(m|x|)K_1(m|x-y|)}{|x|^2|x-y|} \hat{f}_{\rho\delta}(y) \cdot \mathrm{Tr}\{\gamma_\alpha\gamma_\mu\gamma_\nu\gamma_\sigma\gamma_\delta\gamma_\lambda\}
$$
$$
+ \frac{(x-y)_\beta\, K_1(m|x|)K_2(m|x-y|)}{|x||x-y|^2} \hat{f}_{\rho\delta}(y) \cdot \mathrm{Tr}\{\gamma_\mu\gamma_\beta\gamma_\nu\gamma_\sigma\gamma_\delta\gamma_\lambda\} \Big] \tag{7.50}
$$

and

$$
\Pi^{(r,1)}_{\mu\nu\lambda\sigma}(x,y) \tag{7.51}
$$
$$
= 2\Big(\frac{m}{2\pi}\Big)^8 \Big[\frac{(-x_\alpha)(x-y)_\beta\, K_2(m|x|)K_2(m|x-y|)}{|x|^2|x-y|^2} \cdot l_{\gamma\delta}(y) \cdot \mathrm{Tr}\{\gamma_\alpha\gamma_\mu\gamma_\beta\gamma_\nu\gamma_\gamma\gamma_\sigma\gamma_\delta\gamma_\lambda\}
$$
$$
+ \frac{K_1(m|x|)K_1(m|x-y|)}{|x||x-y|} \cdot p(|y|) \cdot \mathrm{Tr}\{\gamma_\mu\gamma_\nu\gamma_\sigma\gamma_\lambda\}
$$
$$
+ \frac{(-x_\alpha)(x-y)_\beta\, K_2(m|x|)K_2(m|x-y|)}{|x|^2|x-y|^2} \cdot p(|y|) \cdot \mathrm{Tr}\{\gamma_\alpha\gamma_\mu\gamma_\beta\gamma_\nu\gamma_\sigma\gamma_\lambda\}
$$
$$
+ \frac{(-x_\alpha)\, K_2(m|x|)K_1(m|x-y|)}{|x|^2|x-y|} \cdot q_\gamma(y) \cdot \mathrm{Tr}\{\gamma_\alpha\gamma_\mu\gamma_\nu\gamma_\gamma\gamma_\sigma\gamma_\lambda\}
$$
$$
+ \frac{(x-y)_\beta\, K_1(m|x|)K_2(m|x-y|)}{|x||x-y|^2} \cdot q_\gamma(y) \cdot \mathrm{Tr}\{\gamma_\mu\gamma_\beta\gamma_\nu\gamma_\gamma\gamma_\sigma\gamma_\lambda\}
$$
$$
+ \frac{(-x_\alpha)\, K_2(m|x|)K_1(m|x-y|)}{|x|^2|x-y|} \cdot q_\delta(y) \cdot \mathrm{Tr}\{\gamma_\alpha\gamma_\mu\gamma_\nu\gamma_\sigma\gamma_\delta\gamma_\lambda\}
$$
$$
+ \frac{(x-y)_\beta\, K_1(m|x|)K_2(m|x-y|)}{|x||x-y|^2} \cdot q_\delta(y) \cdot \mathrm{Tr}\{\gamma_\mu\gamma_\beta\gamma_\nu\gamma_\sigma\gamma_\delta\gamma_\lambda\}
$$
$$
+ \frac{K_1(m|x|)K_1(m|x-y|)}{|x||x-y|} \cdot l_{\gamma\delta}(y) \cdot \mathrm{Tr}\{\gamma_\mu\gamma_\nu\gamma_\gamma\gamma_\sigma\gamma_\delta\gamma_\lambda\} \Big].
$$

The functions appearing in the expressions above are

$$\hat{f}_{\rho\delta}(y) \equiv \int_z z_\rho z_\delta \frac{K_1(m|y-z|)}{|y-z|} \frac{K_2(m|z|)}{|z|^2} = \frac{\pi^2}{m^3}\Big\{\hat{y}_\rho\hat{y}_\delta\, m|y|K_1(m|y|) + \delta_{\rho\delta}K_0(m|y|)\Big\},$$
(7.52)

$$f_{\rho\delta\gamma}(y) \equiv \int_z z_\rho z_\delta (y-z)_\gamma \frac{K_2(m|y-z|)}{|y-z|^2} \frac{K_2(m|z|)}{|z|^2} = -\frac{1}{m}\frac{\partial}{\partial y_\gamma}\hat{f}_{\rho\delta}(y)$$
(7.53)

$$= \frac{\pi^2}{m^3}\Big\{\hat{y}_\gamma\hat{y}_\delta\hat{y}_\rho\, m|y|K_2(m|y|) + (\delta_{\rho\delta}\hat{y}_\gamma - \delta_{\gamma\rho}\hat{y}_\delta - \delta_{\gamma\delta}\hat{y}_\rho)\, K_1(m|y|)\Big\},$$
(7.54)

$$g_\rho(y) \equiv \int d^4z\, z_\rho \frac{K_1(m|y-z|)}{|y-z|} \frac{K_1(m|z|)}{|z|} = \frac{\pi^2}{m^2}y_\rho\, K_0(m|y|),$$
(7.55)

$$h_{\rho\gamma}(y) \equiv \int d^4z\, z_\rho (y-z)_\gamma \frac{K_2(m|y-z|)}{|y-z|^2} \frac{K_1(m|z|)}{|z|} = -\frac{1}{m}\frac{\partial}{\partial y_\gamma}g_\rho(y)$$
(7.56)

$$= \frac{\pi^2}{m^3}\Big(\hat{y}_\gamma\hat{y}_\rho\, m|y|\, K_1(m|y|) - \delta_{\gamma\rho}K_0(m|y|)\Big),$$
(7.57)

$$l_{\gamma\delta}(y) \equiv \int d^4z\, z_\delta(y-z)_\gamma \frac{K_2(m|y-z|)K_2(m|z|)}{|y-z|^2|z|^2}$$
(7.58)

$$= \frac{2\pi^2}{m^2}\Big(\hat{y}_\gamma\hat{y}_\delta\, K_2(m|y|) - \delta_{\gamma\delta}\frac{K_1(m|y|)}{m|y|}\Big),$$
(7.59)

$$p(|y|) \equiv \int d^4z\, \frac{K_1(m|y-z|)}{|y-z|}\frac{K_1(m|z|)}{|z|} = \frac{2\pi^2}{m^2}\, K_0(m|y|),$$
(7.60)

$$q_\gamma(y) \equiv \int d^4z\,(y-z)_\gamma \frac{K_2(m|y-z|)}{|y-z|^2}\frac{K_1(m|z|)}{|z|} = -\frac{y_\gamma}{m|y|}p'(|y|) = \frac{2\pi^2}{m^2}\,\hat{y}_\gamma\, K_1(m|y|).$$
(7.61)

The integrals are performed by using the Gegenbauer expansion of the massive scalar propagator, eq. (3.18). Then, in the case of $p(|y|)$, which is proportional to the convolution of two scalar propagators, one makes use of the integrals [77][11]

$$\int_0^r dz\, z K_\lambda(mz)\, I_\lambda(mz) = \frac{r^2}{2}\left[\left(1 + \frac{\lambda^2}{m^2r^2}\right)I_\lambda(mr)K_\lambda(mr) - I'_\lambda(mr)K'_\lambda(mr)\right] - \frac{\lambda}{2m^2},$$
(7.62)

$$\int_r^\infty dz\, z K_\lambda(mz)^2 = \frac{r^2}{2}(K'_\lambda(mr))^2 - \frac{1}{2}\left(r^2 + \frac{\lambda^2}{m^2}\right)K_\lambda(mr)^2.$$
(7.63)

In other radial integrals, one can first reduce the order of the Bessel functions using integration by parts.

7.4 Pion-loop contribution to light-by-light scattering in scalar QED

In this subsection we present in some detail the calculation of the charged-pion-loop contribution to $i\widehat{\Pi}$ in the framework of scalar QED. In this framework, the pions are approximated as point particles; it should be noted that the absence of form factors associated with the

---

[11]In eq. (7.62), $\text{Re}(\lambda) > -1$ is assumed and in eq. (7.63), $\text{Re}(m) > 0$ is assumed. The prime denotes the derivatives of the Bessel function with respect to their argument, e.g. $K'_0(mr) = -K_1(mr)$.

$\gamma\pi\pi$ vertex leads to an a_μ^{HLbL} contribution almost three times larger than the dispersively evaluated "pion box" (see ref. [17]).

Since some expressions are quite long and only one mass appears in the entire calculation, we denote the pion propagator simply by G rather than G_{m_π}. Also, the position-space vectors of the four vertices of the light-by-light amplitude will generally be denoted by (X^1, X^2, X^3, X^4), rather than $(x, y, z, 0)$, in order to notationally exploit the high degree of permutation symmetry of the amplitude.

The Euclidean Lagrangian for a massive complex scalar field minimally coupled to an external gauge field is

$$\mathcal{L} = (\partial_\mu + ieA_\mu)\phi^*(\partial_\mu - ieA_\mu)\phi + m_\pi^2\phi^*\phi. \tag{7.64}$$

It is convenient to introduce the generating functional

$$Z[A_\mu] = \int D\phi D\phi^* \; e^{-S[\phi,\phi^*,A_\mu]}. \tag{7.65}$$

We want to compute the connected four-point function of the gauge field $A_\mu(x)$,

$$\tilde{\Pi}_{\mu_1\mu_2\mu_3\mu_4}(X^1, X^2, X^3, X^4) \equiv \left.\frac{\delta^4 \log Z}{\delta A_{\mu_1}(X^1)\delta A_{\mu_2}(X^2)\delta A_{\mu_3}(X^3)\delta A_{\mu_4}(X^4)}\right|_{A_\mu=0}. \tag{7.66}$$

Its relation to the desired function $i\widehat{\Pi}$ is given below in eq. (7.86).

Let

$$j_\mu(x) = i(\phi^*\partial_\mu\phi - \phi\partial_\mu\phi^*) \tag{7.67}$$

be the electromagnetic current (in units of e) associated with the complex scalar field ϕ. We split up the calculation of $\tilde{\Pi}$ into three contributions,

$$\tilde{\Pi}_{\mu_1\mu_2\sigma\mu_3}(X^1, X^2, z, X^3) = \sum_{n=0,1,2} \tilde{\Pi}^{(n)}_{\mu_1\mu_2\sigma\mu_3}(X^1, X^2, z, X^3), \tag{7.68}$$

where $\tilde{\Pi}^{(n)}$ is the contribution to $\tilde{\Pi}$ resulting from n insertions of the Lagrangian term $\Delta\mathcal{L} = e^2\phi^*\phi A_\mu A_\mu$ and $(4 - 2n)$ insertions of the electromagnetic current.

7.4.1 Four-point function of the current

As the main contribution to the four-point function of the gauge field $A_\mu(x)$, we compute the four-point function of the electromagnetic current

$$\tilde{\Pi}^{(0)}_{\mu_1\mu_2\mu_3\mu_4}(X^1, X^2, X^3, X^4) \equiv \left\langle j_{\mu_1}(X^1)j_{\mu_2}(X^2)j_{\mu_3}(X^3)j_{\mu_4}(X^4)\right\rangle \tag{7.69}$$

$$= \sum_{\mathrm{A=I,II,III}} \tilde{\Pi}^{(0),\mathrm{A}}_{\mu_1\mu_2\mu_3\mu_4}(X^1, X^2, X^3, X^4). \tag{7.70}$$

There are 16 individual four-point functions generated by the two terms of each current. Each one gives rise to 6 Wick contractions. Thus there are 96 Wick contractions in total.

The three types of terms that we distinguish in eq. (7.70) differ by the number of derivatives acting on ϕ and on the ϕ^* respectively,

$$\tilde{\Pi}^{(0),\mathrm{I}}_{\mu_1\mu_2\mu_3\mu_4}(X^1,X^2,X^3,X^4) = \Big\langle \prod_{k=1}^4 \phi(X^k)^* \partial_{\mu_k}\phi(X^k) \Big\rangle + \big\langle \text{herm. conjug.}\big\rangle, \quad (7.71)$$

$$\tilde{\Pi}^{(0),\mathrm{II}}_{\mu_1\mu_2\mu_3\mu_4}(X^1,X^2,X^3,X^4) = -\sum_{l=1}^4 \Big\{ \Big\langle \phi(X^l)\partial_{\mu_l}\phi(X^l)^* \prod_{k\neq l}^4 \phi(X^k)^* \partial_{\mu_k}\phi(X^k) \Big\rangle \quad (7.72)$$

$$+ \big\langle \text{herm. conjug.}\big\rangle \Big\},$$

$$\tilde{\Pi}^{(0),\mathrm{III}}_{\mu_1\mu_2\mu_3\mu_4}(X^1,X^2,X^3,X^4) = \sum_{k<l}^4 \Big\langle \phi(X^k)\partial_{\mu_k}\phi(X^k)^* \cdot \phi(X^l)\partial_{\mu_l}\phi(X^l)^* \cdot \quad (7.73)$$

$$\cdot \prod_{j\neq k,l}^4 \phi(X^j)^* \partial_{\mu_j}\phi(X^j) \Big\rangle.$$

We note that $\tilde{\Pi}^{(0),\mathrm{I,II,III}}$ contain respectively 12, 48 and 36 Wick contractions.

We set $(X^3,\mu_3) := (z,\sigma)$ and then $(X^4,\mu_4) := (X^3,\mu_3)$, and write out the z-dependence explicitly, since we want to integrate over z at a later stage. We use the group of permutations $\mathcal{S}_n$, which contains $n!$ elements. The result of the Wick contractions is

$$\tilde{\Pi}^{(0),\mathrm{I}}_{\mu_1\mu_2\sigma\mu_3}(X^1,X^2,z,X^3) = 2\sum_{\pi\in\mathcal{S}_3} \partial_\sigma^z G(z-X^{\pi(3)})\, \partial_{\mu_{\pi(3)}}^{X^{\pi(3)}} G(X^{\pi(3)}-X^{\pi(2)}) \quad (7.74)$$

$$\partial_{\mu_{\pi(2)}}^{X^{\pi(2)}} G(X^{\pi(2)}-X^{\pi(1)})\, \partial_{\mu_{\pi(1)}}^{X^{\pi(1)}} G(X^{\pi(1)}-z),$$

and

$$\tilde{\Pi}^{(0),\mathrm{II}}_{\mu_1\mu_2\sigma\mu_3}(X^1,X^2,z,X^3) = 2\sum_{\pi\in\mathcal{S}_3} \Big\{ \quad (7.75)$$

$$\partial_\sigma^z \partial_{\mu_{\pi(3)}}^z G(z-X^{\pi(3)})\, G(X^{\pi(3)}-X^{\pi(2)})\, \partial_{\mu_{\pi(2)}}^{X^{\pi(2)}} G(X^{\pi(2)}-X^{\pi(1)})\, \partial_{\mu_{\pi(1)}}^{X^{\pi(1)}} G(X^{\pi(1)}-z)$$

$$+\partial_{\mu_{\pi(3)}}^{X^{\pi(3)}} \partial_\sigma^{X^{\pi(3)}} G(X^{\pi(3)}-z)\, G(z-X^{\pi(2)})\, \partial_{\mu_{\pi(2)}}^{X^{\pi(2)}} G(X^{\pi(2)}-X^{\pi(1)})\, \partial_{\mu_{\pi(1)}}^{X^{\pi(1)}} G(X^{\pi(1)}-X^{\pi(3)})$$

$$+\partial_{\mu_{\pi(3)}}^{X^{\pi(3)}} \partial_{\mu_{\pi(2)}}^{X^{\pi(3)}} G(X^{\pi(3)}-X^{\pi(2)})\, G(X^{(2)}-z)\, \partial_\sigma^z G(z-X^{\pi(1)}) \partial_{\mu_{\pi(1)}}^{X^{\pi(1)}} G(X^{\pi(1)}-X^{\pi(3)})$$

$$+\partial_{\mu_{\pi(3)}}^{X^{\pi(3)}} \partial_{\mu_{\pi(2)}}^{X^{\pi(3)}} G(X^{\pi(3)}-X^{\pi(2)})\, G(X^{\pi(2)}-X^{\pi(1)})\, \partial_{\mu_{\pi(1)}}^{X^{\pi(1)}} G(X^{\pi(1)}-z)\, \partial_\sigma^z G(z-X^{\pi(3)}) \Big\},$$

as well as

$$\tilde{\Pi}^{(0),\mathrm{III}}_{\mu_1\mu_2\sigma\mu_3}(X^1,X^2,z,X^3) = 2\sum_{\pi\in\mathcal{S}_3} \Big\{ \quad (7.76)$$

$$\partial_\sigma^z \partial_{\mu_{\pi(3)}}^z G(z-X^{\pi(3)})\, \partial_{\mu_{\pi(1)}}^{X^{\pi(1)}} \partial_{\mu_{\pi(2)}}^{X^{\pi(1)}} G(X^{\pi(1)}-X^{\pi(2)})\, G(X^{\pi(3)}-X^{\pi(1)})\, G(X^{\pi(2)}-z)$$

$$+\partial_{\mu_{\pi(3)}}^z G(z-X^{\pi(3)})\, \partial_\sigma^{X^{\pi(2)}} \partial_{\mu_{\pi(2)}}^{X^{\pi(2)}} G(X^{\pi(2)}-z)\, \partial_{\mu_{\pi(1)}}^{X^{\pi(1)}} G(X^{\pi(1)}-X^{\pi(2)})\, G(X^{\pi(3)}-X^{\pi(1)})$$

$$+\partial_\sigma^{X^{\pi(1)}} G(X^{\pi(1)}-z)\, \partial_{\mu_{\pi(1)}}^{X^{\pi(3)}} \partial_{\mu_{\pi(3)}}^{X^{\pi(3)}} G(X^{\pi(3)}-X^{\pi(1)})\, \partial_{\mu_{\pi(2)}}^{X^{\pi(2)}} G(X^{\pi(2)}-X^{\pi(3)})\, G(z-X^{\pi(2)}) \Big\}.$$

7.4.2 One-tadpole contributions

Now to the contributions of the four-point function of $A_\mu(x)$ involving exactly one tadpole, coming from the term $\Delta\mathcal{L} = e^2\phi^*\phi A_\mu A_\mu$ in the Lagrangian. Note that a factor two appears because the term is quadratic in A_μ.

$$\tilde{\Pi}^{(1)}_{\mu_1\mu_2\mu_3\mu_4}(X^1, X^2, X^3, X^4) = -2\sum_{k<l}\delta_{\mu_k\mu_l}\delta(X^k - X^l)\left\langle\phi^*(X^k)\phi(X^k)\prod_{j\neq k,l}j_{\mu_j}(X^j)\right\rangle$$

$$= 2\sum_{k<l}\delta_{\mu_k\mu_l}\delta(X^k - X^l)\left\{\left\langle\phi^*(X^k)\phi(X^k)\prod_{j\neq k,l}\phi(X^j)^*\partial_{\mu_j}\phi(X^j)\right\rangle + \left\langle\text{herm. conjug.}\right\rangle\right.$$

$$\left. -\left\langle\phi^*(X^k)\phi(X^k)\sum_{j\neq k,l}\phi(X^j)^*\partial_{\mu_j}\phi(X^j)\Big(\phi(X^m)\partial_{\mu_m}\phi(X^m)^*\Big)_{m=10-(j+k+l)}\right\rangle\right\}. \quad (7.77)$$

Disregarding the overall factor of two, there are six permutations ($k < l$) and each gives rise to eight Wick contractions, yielding a total of 48 such contractions. Now set $(X^3, \mu_3) := (z, \sigma)$ and $(X^4, \mu_4) := (X^3, \mu_3)$. There are three permutations in which z appears in the delta function, and three where it does not.

$$\tilde{\Pi}^{(1)}_{\mu_1\mu_2\sigma\mu_3}(X^1, X^2, z, X^3) = 2\sum_{\pi\in\mathcal{S}_3}\left\{\delta_{\sigma\mu_{\pi(1)}}\delta(z - X^{\pi(1)})\right. \quad (7.78)$$

$$\cdot\Big(\partial^{X^{\pi(3)}}_{\mu_{\pi(3)}}G(X^{\pi(3)} - X^{\pi(2)})\,G(X^{\pi(1)} - X^{\pi(3)})\,\partial^{X^{\pi(2)}}_{\mu_{\pi(2)}}G(X^{\pi(2)} - X^{\pi(1)})$$

$$+G(X^{\pi(1)} - X^{\pi(2)})\,\partial^{X^{\pi(3)}}_{\mu_{\pi(3)}}G(X^{\pi(3)} - X^{\pi(1)})\,\partial^{X^{\pi(2)}}_{\mu_{\pi(2)}}G(X^{\pi(2)} - X^{\pi(3)})$$

$$+\partial^{X^{\pi(3)}}_{\mu_{\pi(3)}}\partial^{X^{\pi(3)}}_{\mu_{\pi(2)}}G(X^{\pi(3)} - X^{\pi(2)})\,G(X^{\pi(1)} - X^{\pi(3)})\,G(X^{\pi(2)} - X^{\pi(1)})$$

$$+\partial^{X^{\pi(1)}}_{\mu_{\pi(2)}}G(X^{\pi(1)} - X^{\pi(2)})\,\partial^{X^{\pi(3)}}_{\mu_{\pi(3)}}G(X^{\pi(3)} - X^{\pi(1)})\,G(X^{\pi(2)} - X^{\pi(3)})\Big)$$

$$+\delta_{\mu_{\pi(1)}\mu_{\pi(2)}}\delta(X^{\pi(1)} - X^{\pi(2)})$$

$$\cdot\Big(\partial^{X^{\pi(3)}}_{\mu_{\pi(3)}}G(X^{\pi(3)} - z)\,G(X^{\pi(1)} - X^{\pi(3)})\,\partial^z_\sigma G(z - X^{\pi(1)})$$

$$+G(X^{\pi(1)} - z)\,\partial^{X^{\pi(3)}}_{\mu_{\pi(3)}}G(X^{\pi(3)} - X^{\pi(1)})\,\partial^z_\sigma G(z - X^{\pi(3)})$$

$$+\partial^{X^{\pi(3)}}_{\mu_{\pi(3)}}\partial^{X^{\pi(3)}}_\sigma G(X^{\pi(3)} - z)\,G(X^{\pi(1)} - X^{\pi(3)})\,G(z - X^{\pi(1)})$$

$$+\partial^{X^{\pi(1)}}_\sigma G(X^{\pi(1)} - z)\,\partial^{X^{\pi(3)}}_{\mu_{\pi(3)}}G(X^{\pi(3)} - X^{\pi(1)})\,G(z - X^{\pi(3)})\Big)\right\}.$$

7.4.3 Two-tadpole contributions

Finally, the contribution containing two tadpoles has the form

$$\tilde{\Pi}^{(2)}_{\mu_1\mu_2\mu_3\mu_4}(X^1, X^2, X^3, X^4) \quad (7.79)$$

$$= 4\sum_{l=1}^{3}\delta_{\mu_4\mu_l}\,\delta(X^4 - X^l)\,\delta_{\mu_j\mu_k}\,\delta(X^j - X^k)\Big\langle(\phi^*\phi)(X^4)\,(\phi^*\phi)(X^l)\Big\rangle,$$

where it is understood that (j, k, l) form a permutation of $(1, 2, 3)$. The expression can also be written as

$$\tilde{\Pi}^{(2)}_{\mu_1\mu_2\mu_3\mu_4}(X^1, X^2, X^3, X^4) \quad (7.80)$$

$$= 2\sum_{\pi\in\mathcal{S}_3}\delta_{\mu_4\mu_{\pi(1)}}\,\delta(X^4 - X^{\pi(1)})\,\delta_{\mu_{\pi(2)}\mu_{\pi(3)}}\,\delta(X^{\pi(2)} - X^{\pi(3)})\Big\langle(\phi^*\phi)(X^4)\,(\phi^*\phi)(X^{\pi(2)})\Big\rangle,$$

Performing the contractions, one obtains

$$\tilde{\Pi}^{(2)}_{\mu_1\mu_2\sigma\mu_3}(X^1, X^2, z, X^3) \tag{7.81}$$
$$= 2\sum_{\pi\in\mathcal{S}_3} \delta_{\sigma\mu_{\pi(1)}}\, \delta(z - X^{\pi(1)})\, \delta_{\mu_{\pi(2)}\mu_{\pi(3)}}\, \delta(X^{\pi(2)} - X^{\pi(3)})G(X^{\pi(1)} - X^{\pi(2)})^2.$$

7.4.4 Test of the Ward identity

The Ward identity for current conservation reads

$$\partial^z_\sigma(\tilde{\Pi}^{(0)}_{\mu_1\mu_2\sigma\mu_3} + \tilde{\Pi}^{(1)}_{\mu_1\mu_2\sigma\mu_3} + \tilde{\Pi}^{(2)}_{\mu_1\mu_2\sigma\mu_3})(X^1, X^2, z, X^3) = 0. \tag{7.82}$$

Taking into account the Green's function property (3.3) of the scalar propagator as well as the identity $\delta'(z - x_1)f(z) = \delta'(z - x_1)f(x_1) - \delta(z - x_1)f'(x_1)$, a straightforward but tedious calculation yields

$$\partial^z_\sigma \tilde{\Pi}^{(0)}_{\mu_1\mu_2\sigma\mu_3}(X^1, X^2, z, X^3) = -2\sum_{\pi\in\mathcal{S}_3} \partial^z_{\mu_{\pi(1)}}\delta(z - X^{\pi(1)})\Big\{ \tag{7.83}$$
$$G(X^{\pi(1)} - X^{\pi(2)})\, \partial^{X^2}_{\mu_2}G(X^2 - X^3)\, \partial^{X^3}_{\mu_3}G(X^{\pi(3)} - X^{\pi(1)})$$
$$+G(X^{\pi(1)} - X^{\pi(2)})\, \partial^{X^2}_{\mu_{\pi(2)}}G(X^{\pi(2)} - X^{\pi(3)})\, \partial^{X^3}_{\mu_{\pi(3)}}G(X^{\pi(3)} - X^{\pi(1)})$$
$$+\partial^{X^{\pi(1)}}_{\mu_{\pi(3)}}G(X^{\pi(1)} - X^{\pi(3)})\, \partial^{X^2}_{\mu_{\pi(2)}}G(X^{\pi(2)} - X^{\pi(1)})\, G(X^{\pi(3)} - X^{\pi(2)})$$
$$+\partial^{X^{\pi(3)}}_{\mu_{\pi(3)}}\partial^{X^{\pi(3)}}_{\mu_{\pi(2)}}G(X^{\pi(3)} - X^{\pi(2)})\, G(X^{\pi(1)} - X^{\pi(3)})\, G(X^{\pi(2)} - X^{\pi(1)})\Big\}.$$

Similarly, using again eq. (3.3), one finds

$$\partial^z_\sigma \tilde{\Pi}^{(1)}_{\mu_1\mu_2\sigma\mu_3}(X^1, X^2, z, X^3) = 2\sum_{\pi\in\mathcal{S}_3}\Big\{\partial^z_{\mu_{\pi(1)}}\delta(z - X^{\pi(1)}) \tag{7.84}$$
$$\cdot\Big(\partial^{X^{\pi(3)}}_{\mu_{\pi(3)}}G(X^{\pi(3)} - X^{\pi(2)})\, G(X^{\pi(1)} - X^{\pi(3)})\, \partial^{X^{\pi(2)}}_{\mu_{\pi(2)}}G(X^{\pi(2)} - X^{\pi(1)})$$
$$+G(X^{\pi(1)} - X^{\pi(2)})\, \partial^{X^{\pi(3)}}_{\mu_{\pi(3)}}G(X^{\pi(3)} - X^{\pi(1)})\, \partial^{X^{\pi(2)}}_{\mu_{\pi(2)}}G(X^{\pi(2)} - X^{\pi(3)})$$
$$+\partial^{X^{\pi(3)}}_{\mu_{\pi(3)}}\partial^{X^{\pi(3)}}_{\mu_{\pi(2)}}G(X^{\pi(3)} - X^{\pi(2)})\, G(X^{\pi(1)} - X^{\pi(3)})\, G(X^{\pi(2)} - X^{\pi(1)})$$
$$+\partial^{X^{\pi(1)}}_{\mu_{\pi(2)}}G(X^{\pi(1)} - X^{\pi(2)})\, \partial^{X^{\pi(3)}}_{\mu_{\pi(3)}}G(X^{\pi(3)} - X^{\pi(1)})\, G(X^{\pi(2)} - X^{\pi(3)})\Big)$$
$$-\delta_{\mu_{\pi(1)}\mu_{\pi(2)}}\delta(X^{\pi(1)} - X^{\pi(2)})\, \partial^z_{\mu_{\pi(3)}}\delta(X^{\pi(3)} - z)\, G(X^{\pi(3)} - X^{\pi(1)})^2\Big\}.$$

Finally,

$$\partial^z_\sigma \tilde{\Pi}^{(2)}_{\mu_1\mu_2\sigma\mu_3}(X^1, X^2, z, X^3) = \tag{7.85}$$
$$= 2\sum_{\pi\in\mathcal{S}_3} \partial^z_{\mu_{\pi(1)}}\delta(z - X^{\pi(1)})\, \delta_{\mu_{\pi(2)}\mu_{\pi(3)}}\, \delta(X^{\pi(2)} - X^{\pi(3)})G(X^{\pi(1)} - X^{\pi(3)})^2.$$

Thus one verifies that the Ward identity eq. (7.82) is satisfied: the terms with two delta functions cancel between $\tilde{\Pi}^{(1)}$ and $\tilde{\Pi}^{(2)}$, while the terms with a single delta function cancel between $\tilde{\Pi}^{(0)}$ and $\tilde{\Pi}^{(1)}$.

7.4.5 The expression for $i\widehat{\Pi}_{\rho;\mu_1\mu_2\mu_3\sigma}(X^1, X^2)$

We recall the relation

$$i\widehat{\Pi}_{\rho;\mu_1\mu_2\mu_3\sigma}(X^1, X^2) = -\int d^4z \, z_\rho \, \tilde{\Pi}_{\mu_1\mu_2\sigma\mu_3}(X^1, X^2, z, X^3)\Big|_{X^3=0}, \tag{7.86}$$

and decompose the rank-five tensor according to

$$i\widehat{\Pi}_{\rho;\mu_1\mu_2\mu_3\sigma}(X^1, X^2) = \sum_{n=0,1,2} i\widehat{\Pi}^{(n)}_{\rho;\mu_1\mu_2\mu_3\sigma}(X^1, X^2), \tag{7.87}$$

$$i\widehat{\Pi}^{(n)}_{\rho;\mu_1\mu_2\mu_3\sigma}(X^1, X^2) \equiv -\int d^4z \, z_\rho \, \tilde{\Pi}^{(n)}_{\mu_1\mu_2\sigma\mu_3}(X^1, X^2, z, X^3)\Big|_{X^3=0}. \tag{7.88}$$

We will make use of the integral

$$H_\rho(X^1, X^3) = \int d^4z \, z_\rho \, G(z - X^3) \, G(z - X^1) \tag{7.89}$$

$$= \left(\frac{m_\pi}{4\pi^2}\right)^2 \left[g_\rho(X^3 - X^1) + X^1_\rho \, p(|X^3 - X^1|)\right], \tag{7.90}$$

where

$$g_\rho(y) \equiv \int d^4z \, z_\rho \, \frac{K_1(m_\pi|y - z|)}{|y - z|} \, \frac{K_1(m_\pi|z|)}{|z|} = \frac{\pi^2}{m_\pi^2} y_\rho \, K_0(m_\pi|y|), \tag{7.91}$$

$$p(|y|) \equiv \int d^4z \, \frac{K_1(m_\pi|y - z|)}{|y - z|} \frac{K_1(m_\pi|z|)}{|z|} = \frac{2\pi^2}{m_\pi^2} \, K_0(m_\pi|y|). \tag{7.92}$$

Simplifying, one finds

$$H_\rho(X^1, X^3) = \frac{1}{16\pi^2} K_0(m_\pi|X^3 - X^1|) \, (X^1_\rho + X^3_\rho). \tag{7.93}$$

What is needed in the following is the antisymmetrized derivative

$$\partial^{X^3}_{[\sigma} H_{\rho]}(X^1, X^3) = -\frac{1}{4} G(X^3 - X^1) \, [X^1_\rho, X^3_\sigma], \tag{7.94}$$

where we have introduced the notation $[X^1_\rho, X^3_\sigma] \equiv X^1_\rho X^3_\sigma - X^3_\rho X^1_\sigma$.

A straightforward but lengthy calculation then leads to the expressions

$$i\widehat{\Pi}^{(0)}_{[\rho;\mu_1\mu_2\mu_3\sigma]}(X^1,X^2) \tag{7.95}$$

$$= \sum_{\pi\in\mathcal{S}_3}\Big\{ G(X^{\pi(3)}-X^{\pi(2)})\,\partial^{X^{\pi(2)}}_{\mu_{\pi(2)}}G(X^{\pi(2)}-X^{\pi(1)})\,\partial^{X^{\pi(1)}}_{\mu_{\pi(1)}}\partial^{X^{\pi(3)}}_{\mu_{\pi(3)}}G(X^{\pi(1)}-X^{\pi(3)})\,[X^{\pi(1)}_\rho,X^{\pi(3)}_\sigma]$$

$$+G(X^{\pi(3)}-X^{\pi(2)})\,\partial^{X^{\pi(2)}}_{\mu_{\pi(2)}}G(X^{\pi(2)}-X^{\pi(1)})\,G(X^{\pi(1)}-X^{\pi(3)})(\delta_{\mu_{\pi(1)}\rho}\delta_{\sigma\mu_{\pi(3)}}-\delta_{\rho\mu_{\pi(3)}}\delta_{\sigma\mu_{\pi(1)}})$$

$$+G(X^{\pi(3)}-X^{\pi(2)})\,\partial^{X^{\pi(2)}}_{\mu_{\pi(2)}}G(X^{\pi(2)}-X^{\pi(1)})\,\partial^{X^{\pi(1)}}_{\mu_{\pi(1)}}G(X^{\pi(1)}-X^{\pi(3)})\,(\delta_{\sigma\mu_{\pi(3)}}X^{\pi(1)}_\rho-\delta_{\rho\mu_{\pi(3)}}X^{\pi(1)}_\sigma)$$

$$+G(X^{\pi(3)}-X^{\pi(2)})\,\partial^{X^{\pi(2)}}_{\mu_{\pi(2)}}G(X^{\pi(2)}-X^{\pi(1)})\,\partial^{X^{\pi(3)}}_{\mu_{\pi(3)}}G(X^{\pi(1)}-X^{\pi(3)})\,(\delta_{\rho\mu_{\pi(1)}}X^{\pi(3)}_\sigma-\delta_{\sigma\mu_{\pi(1)}}X^{\pi(3)}_\rho)$$

$$+\frac{1}{2}\partial^{X^{\pi(2)}}_{\mu_{\pi(2)}}G(X^{\pi(2)}-X^{\pi(1)})\,\partial^{X^{\pi(1)}}_{\mu_{\pi(1)}}G(X^{\pi(1)}-X^{\pi(3)})\partial^{X^{\pi(3)}}_{\mu_{\pi(3)}}G(X^{\pi(2)}-X^{\pi(3)})\,[X^{\pi(3)}_\rho,X^{\pi(1)}_\sigma-X^{\pi(2)}_\sigma]$$

$$+\frac{1}{2}\partial^{X^{\pi(3)}}_{\mu_{\pi(3)}}G(X^{\pi(3)}-X^{\pi(2)})\,\partial^{X^{\pi(2)}}_{\mu_{\pi(2)}}G(X^{\pi(2)}-X^{\pi(1)})G(X^{\pi(3)}-X^{\pi(1)})(\delta_{\sigma\mu_{\pi(1)}}X^{\pi(3)}_\rho-\delta_{\rho\mu_{\pi(1)}}X^{\pi(3)}_\sigma)$$

$$+\frac{1}{2}G(X^{\pi(3)}-X^{\pi(2)})\,\partial^{X^{\pi(2)}}_{\mu_{\pi(2)}}G(X^{\pi(2)}-X^{\pi(1)})\partial^{X^{\pi(1)}}_{\mu_{\pi(1)}}G(X^{\pi(3)}-X^{\pi(1)})(\delta_{\sigma\mu_{\pi(3)}}X^{\pi(2)}_\rho-\delta_{\rho\mu_{\pi(3)}}X^{\pi(2)}_\sigma)$$

$$+\partial^{X^{\pi(3)}}_{\mu_{\pi(3)}}\partial^{X^{\pi(3)}}_{\mu_{\pi(2)}}G(X^{\pi(3)}-X^{\pi(2)})\,G(X^{\pi(2)}-X^{\pi(1)})\,\partial^{X^{\pi(1)}}_{\mu_{\pi(1)}}G(X^{\pi(1)}-X^{\pi(3)})\,[X^{\pi(1)}_\rho,X^{\pi(2)}_\sigma-X^{\pi(3)}_\sigma]$$

$$+\partial^{X^{\pi(3)}}_{\mu_{\pi(3)}}\partial^{X^{\pi(3)}}_{\mu_{\pi(2)}}G(X^{\pi(3)}-X^{\pi(2)})\,G(X^{\pi(2)}-X^{\pi(1)})\,G(X^{\pi(1)}-X^{\pi(3)})(\delta_{\sigma\mu_{\pi(1)}}X^{\pi(3)}_\rho-\delta_{\rho\mu_{\pi(1)}}X^{\pi(3)}_\sigma)\Big\},$$

$$i\widehat{\Pi}^{(1)}_{[\rho;\mu_1\mu_2\mu_3\sigma]}(X^1,X^2)+i\widehat{\Pi}^{(2)}_{[\rho;\mu_1\mu_2\mu_3\sigma]}(X^1,X^2)=\sum_{\pi\in\mathcal{S}_3}\Big\{(\delta_{\rho\mu_{\pi(1)}}X^{\pi(1)}_\sigma-\delta_{\sigma\mu_{\pi(1)}}X^{\pi(1)}_\rho) \tag{7.96}$$

$$\cdot\Big(2G(X^{\pi(1)}-X^{\pi(2)})\,\partial^{X^{\pi(3)}}_{\mu_{\pi(3)}}G(X^{\pi(3)}-X^{\pi(1)})\,\partial^{X^{\pi(2)}}_{\mu_{\pi(2)}}G(X^{\pi(2)}-X^{\pi(3)})$$

$$+\partial^{X^{\pi(1)}}_{\mu_{\pi(2)}}G(X^{\pi(1)}-X^{\pi(2)})\,\partial^{X^{\pi(3)}}_{\mu_{\pi(3)}}G(X^{\pi(3)}-X^{\pi(1)})\,G(X^{\pi(2)}-X^{\pi(3)})$$

$$+\partial^{X^{\pi(3)}}_{\mu_{\pi(3)}}\partial^{X^{\pi(3)}}_{\mu_{\pi(2)}}G(X^{\pi(3)}-X^{\pi(2)})\,G(X^{\pi(1)}-X^{\pi(3)})\,G(X^{\pi(2)}-X^{\pi(1)})$$

$$+\delta_{\mu_{\pi(2)}\mu_{\pi(3)}}\delta(X^{\pi(2)}-X^{\pi(3)})\,G(X^{\pi(2)}-X^{\pi(1)})^2\Big)$$

$$+\delta_{\mu_{\pi(2)}\mu_{\pi(3)}}\delta(X^{\pi(2)}-X^{\pi(3)})\,G(X^{\pi(2)}-X^{\pi(1)})^2(\delta_{\sigma\mu_{\pi(1)}}X^{\pi(2)}_\rho-\delta_{\rho\mu_{\pi(1)}}X^{\pi(2)}_\sigma)\Big\}.$$

The setting of X^3 to zero is implied in the two equations above (see eq. (7.86)). In summary, the charged-pion-loop contribution to the function $i\widehat{\Pi}$ is given by eqs. (7.87), (7.95) and (7.96).

A final step is required if one wants to perform numerical integrations over $i\widehat{\Pi}$ in order to obtain a_μ^{HLbL}, namely to isolate the delta-function-like contributions, which we also call contact contributions. The last two terms of eq. (7.96) are explicitly contact contributions. Eq. (7.95), however, also contributes contact terms, because second derivatives of the scalar propagator appear. Using the defining property (3.3) of the propagator, these second-derivative terms can be written as

$$\partial_\mu\partial_\nu G(x)=\Big(\delta_{\mu\nu}-4\frac{x_\mu x_\nu}{x^2}\Big)\frac{G'(x)}{|x|}+\frac{x_\mu x_\nu}{x^2}\,m_\pi^2\,G(x)-\frac{1}{4}\delta_{\mu\nu}\,\delta(x), \tag{7.97}$$

where $G'(x)=\frac{d}{d|x|}G(x)=\frac{-m_\pi^2}{4\pi^2}\frac{K_2(m_\pi|x|)}{|x|}$. We have taken into account the fact that, applied to smooth test functions, $\Big(\delta_{\mu\nu}-4\frac{x_\mu x_\nu}{x^2}\Big)\delta(x)=0$, so that $\frac{x_\mu x_\nu}{x^2}\delta(x)$ can be substituted by $\frac{1}{4}\delta_{\mu\nu}\delta(x)$. Collecting all the contributions proportional to a delta function in

$i\widehat{\Pi}_{[\rho;\mu_1\mu_2\mu_3\sigma]}(X^1, X^2)$, we find in total

$$
\begin{aligned}
i\widehat{\Pi}_{[\rho;\mu_1\mu_2\mu_3\sigma]}(X^1, X^2)_{\text{contact}} = \frac{3}{2}\Big[& \delta_{\mu_2\mu_3}\,\delta(X^2)\,G(X^1)^2\,(\delta_{\rho\mu_1}X^1_\sigma - \delta_{\sigma\mu_1}X^1_\rho) \qquad (7.98) \\
& -\delta_{\mu_1\mu_2}\,\delta(X^1 - X^2)\,G(X^2)^2\,(\delta_{\rho\mu_3}X^2_\sigma - \delta_{\sigma\mu_3}X^2_\rho) \\
& +\delta_{\mu_1\mu_3}\,\delta(X^1)\,G(X^2)^2\,(\delta_{\rho\mu_2}X^2_\sigma - \delta_{\sigma\mu_2}X^2_\rho)\Big].
\end{aligned}
$$

We note that these terms are integrable; for instance, the first term goes like $1/|X^1|^3$ for small $|X^1|$.

8 Applications and tests of the QED kernel

In this section, we combine the QED kernel as computed in section 5 with the four-point functions $i\widehat{\Pi}$ given explicitly in section 7 in order to check whether the coordinate-space method developed here reproduces known results. Furthermore, the method is tested for the case that the QED fermion loop is computed on the lattice, reproducing the known result after taking the continuum limit. Finally, in subsection 8.4 an overview of results obtained for the fully connected part of the lattice QCD four-point function is presented.

8.1 Improved kernels

The master formula, given by eq. (2.29), can be written in a slightly different way to optimize the lattice QCD calculation. First, as already noted in ref. [49], the QED weight function is not uniquely defined. This freedom can be used to obtained a better behaved integrand with smaller statistical and systematic uncertainties. As shown below, it turns out to be a crucial ingredient for practical lattice QCD calculations. The idea is to remove large fluctuations or large cancellations in the integrand that do not affect the central value in the continuum and infinite volume but increase the statistical error and/or systematic effects in the estimator. Second, a naive implementation of the master formula in lattice QCD calculations is rather expensive. But the numerical cost can be considerably reduced by using a different formula, equivalent in the infinite volume limit. These two improvements are discussed next.

In the continuum and in infinite volume, the conservation of the electromagnetic current implies eq. (7.8), namely that the integral of the four-point function $i\widehat{\Pi}_{\rho;\mu\nu\lambda\sigma}(x, y)$ over x without any x-dependent weight-factor vanishes. The same observation applies to the integral over the coordinate-vector y. Therefore, in infinite volume, any function which depends only on x or y can be added to the QED kernel without affecting the final result. On the infinite lattice, and with Wilson fermions, this property still holds at finite lattice spacing if one uses the conserved vector current, see eq. (8.10b). When using local vector currents, the result holds once the continuum limit has been taken. We will consider four
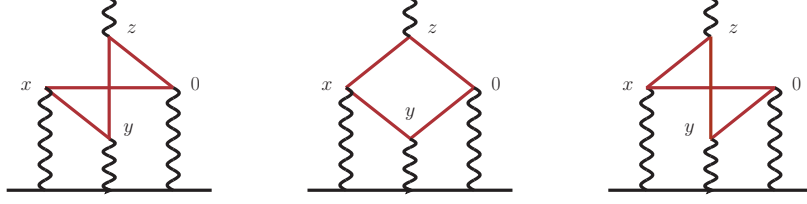
Figure 6. Wick contractions for the connected contribution in Method 1.

kernels $\overline{\mathcal{L}}^{(n)}$ which differ only by such subtractions,

$$\overline{\mathcal{L}}^{(0)}_{[\rho,\sigma],\mu\nu\lambda}(x,y) = \overline{\mathcal{L}}_{[\rho,\sigma],\mu\nu\lambda}(x,y)\,, \tag{8.1a}$$

$$\overline{\mathcal{L}}^{(1)}_{[\rho,\sigma],\mu\nu\lambda}(x,y) = \overline{\mathcal{L}}_{[\rho,\sigma],\mu\nu\lambda}(x,y) - \frac{1}{2}\overline{\mathcal{L}}_{[\rho,\sigma],\mu\nu\lambda}(x,x) - \frac{1}{2}\overline{\mathcal{L}}_{[\rho,\sigma],\mu\nu\lambda}(y,y)\,, \tag{8.1b}$$

$$\overline{\mathcal{L}}^{(2)}_{[\rho,\sigma],\mu\nu\lambda}(x,y) = \overline{\mathcal{L}}_{[\rho,\sigma],\mu\nu\lambda}(x,y) - \overline{\mathcal{L}}_{[\rho,\sigma],\mu\nu\lambda}(0,y) - \overline{\mathcal{L}}_{[\rho,\sigma],\mu\nu\lambda}(x,0)\,, \tag{8.1c}$$

$$\overline{\mathcal{L}}^{(3)}_{[\rho,\sigma],\mu\nu\lambda}(x,y) = \overline{\mathcal{L}}_{[\rho,\sigma],\mu\nu\lambda}(x,y) - \overline{\mathcal{L}}_{[\rho,\sigma],\mu\nu\lambda}(x,x) + \overline{\mathcal{L}}_{[\rho,\sigma],\mu\nu\lambda}(0,x) - \overline{\mathcal{L}}_{[\rho,\sigma],\mu\nu\lambda}(0,y)\,. \tag{8.1d}$$

In addition to vanishing when both arguments vanish,

$$\overline{\mathcal{L}}^{(n)}_{[\rho,\sigma],\mu\nu\lambda}(0,0) = 0, \qquad (n = 0,1,2,3), \tag{8.2}$$

(see eq. (2.39) for the non-trivial cases $n = 0$ and $n = 2$), the subtracted kernels vanish in various special configurations,

$$\overline{\mathcal{L}}^{(1)}(x,x) = 0\,, \quad \overline{\mathcal{L}}^{(2)}(x,0) = \overline{\mathcal{L}}^{(2)}(0,y) = 0\,, \quad \overline{\mathcal{L}}^{(3)}(x,0) = \overline{\mathcal{L}}^{(3)}(x,x) = 0\,. \tag{8.3}$$

In [43, 51] we introduced a kernel tuneable by an arbitrary parameter Λ that approaches $\overline{\mathcal{L}}^{(0)}$ when $\Lambda \to \infty$ and $\overline{\mathcal{L}}^{(2)}$ when $\Lambda \to 0$,

$$\begin{aligned}\overline{\mathcal{L}}^{(\Lambda)}_{[\rho,\sigma];\mu\nu\lambda}(x,y) = &\ \overline{\mathcal{L}}_{[\rho,\sigma];\mu\nu\lambda}(x,y) \\ &- \partial_\mu^{(x)}(x_\alpha e^{-\Lambda m^2 x^2/2})\overline{\mathcal{L}}_{[\rho,\sigma];\alpha\nu\lambda}(0,y) - \partial_\nu^{(y)}(y_\alpha e^{-\Lambda m^2 y^2/2})\overline{\mathcal{L}}_{[\rho,\sigma];\mu\alpha\lambda}(x,0),\end{aligned} \tag{8.4}$$

as we empirically found that with $\overline{\mathcal{L}}^{(2)}$ and $\overline{\mathcal{L}}^{(3)}$, the integrand was too long-ranged, while with $\overline{\mathcal{L}}^{(0)}$ and $\overline{\mathcal{L}}^{(1)}$ it was too peaked at short distances. In our most recent works [36, 37], we presented results exclusively with $\Lambda = 0.4$.

For each quark flavour f, the quark-connected part of the hadronic four-point function Π involves three different Wick contractions. Each of those appears twice, with opposite fermion-number flow, resulting in a purely real contribution; see eq. (7.28) and figure 6. Computing explicitly all three contractions, and using the master formula given by eq. (2.29), amounts to what we call Method 1 [51]. To estimate all three contractions, we first compute point-to-all propagators with sources located at the origin and at the site y. Then, we perform sequential inversions using the propagators, summed over z and with the weight factor z_ρ, as sequential sources to finally contract both results and summing

over x. Since one needs to anti-symmetrize between ρ and σ, it amounts to 6 sequential inversions for each primary inversion.

Alternatively, we could choose the first Wick contraction, $I^{(1)}_{\mu\nu\sigma\lambda}(x, y, z, w)$ of eq. (7.29) corresponding to the leftmost diagram in figure 6, as a reference and swap the vertices at the level of the muon line — an idea that was already exploited in [47]. Defining the gauge-field average of the three Wick contractions as follows,

$$\widetilde{\Pi}^{(j)}_{\mu\nu\sigma\lambda}(x, y, z) \equiv \langle -2 \operatorname{Re} I^{(j)}_{\mu\nu\sigma\lambda}(x, y, z, 0) \rangle, \qquad (j = 1, 2, 3), \tag{8.5}$$

we obtain the Method 2 [51] estimator ($A = 0, 1, 2, 3$ or Λ)

$$
\begin{aligned}
a^{\mathrm{HLbL}}_{\mu} = -\frac{me^6}{3} \int d^4 y \int d^4 x \\
\Big\{ \Big(\overline{\mathcal{L}}^{(A)}_{[\rho,\sigma],\mu\nu\lambda}(x, y) + \overline{\mathcal{L}}^{(A)}_{[\rho,\sigma],\nu\mu\lambda}(y, x) - \overline{\mathcal{L}}^{(A)}_{[\rho,\sigma],\lambda\nu\mu}(x, x - y) \Big) \int d^4 z\, z_\rho\, \widetilde{\Pi}^{(1)}_{\mu\nu\sigma\lambda}(x, y, z) \\
+ \overline{\mathcal{L}}^{(A)}_{[\rho,\sigma],\lambda\nu\mu}(x, x - y)\, x_\rho \int d^4 z\, \widetilde{\Pi}^{(1)}_{\mu\nu\sigma\lambda}(x, y, z) \Big\}.
\end{aligned}
\tag{8.6}
$$

For the quark-connected contribution, and with $A \doteq \Lambda$, this equation is the starting point for all our lattice-QCD results in refs. [36, 37], as well as the final results in ref. [51]. The advantage of this representation is that all propagators can be expressed in terms of the two point-to-all propagators with sources located at the origin and on site y by exploiting the γ_5-hermiticity relation (7.27). Eq. (8.6) can be proven starting from the master formula (2.29) and using the identities

$$\widetilde{\Pi}^{(2)}_{\mu\nu\sigma\lambda}(x, y, z) = \widetilde{\Pi}^{(1)}_{\nu\mu\sigma\lambda}(y, x, z), \tag{8.7a}$$

$$\widetilde{\Pi}^{(3)}_{\mu\nu\sigma\lambda}(x, y, z) = \widetilde{\Pi}^{(1)}_{\lambda\nu\sigma\mu}(-x, y - x, z - x) \tag{8.7b}$$

as well as eq. (2.38). In practice, we reduce the master formulae to a one-dimensional integral over the variable $|y|$; the integrand then differs between Method 1 and Method 2, even in the continuum limit. The advantage of Method 2 is that only one additional propagator needs to be computed for each value of y: for N values of $|y|$, the number of quark propagators that need to be computed is $N + 1$ compared to $7(N + 1)$ for Method 1, where sequential inversions are used. In addition, combining all possible pairs of quark propagators allows one to compute $\mathrm{O}(N^2)$ independent data, which may include multiple statistical samples of the same $|y|$.

In general, the last term in eq. (8.6) does not vanish, in spite of eq. (7.2) holding, because $\Pi^{(1)}_{\mu\nu\sigma\lambda}(x, y, z)$ is only one of three contributing Wick contractions to the four-point function. In fact, as a Ward identity following from current conservation, one can show that

$$\int d^4 z\, \widetilde{\Pi}^{(1)}_{\mu\nu\sigma\lambda}(x, y, z) = (-2y_\sigma) \left\langle \operatorname{Re} \operatorname{Tr}\{\gamma_\mu S(x, y)\gamma_\nu S(y, 0)\gamma_\lambda S(0, x)\} \right\rangle. \tag{8.8}$$

However, for a pseudoscalar-pole contribution, this term vanishes,

$$\int d^4 z\, \Pi^{(1);\pi^0}_{\mu\nu\sigma\lambda}(x, y, z) = 0, \tag{8.9}$$
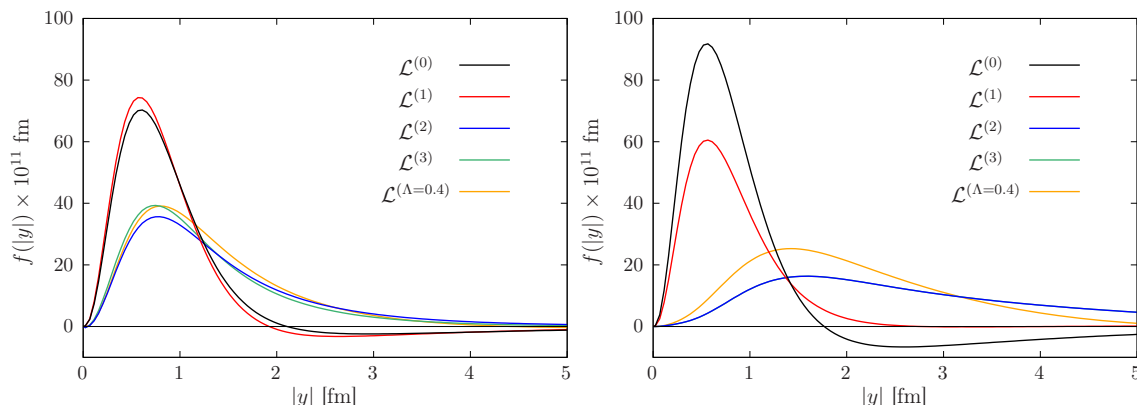
Figure 7. The integrand with respect to the variable $|y|$ leading to a_μ^{HLbL} for the neutral pion-pole with a VMD form factor and a pion mass of $135\,\text{MeV}$. The integrals over $|x|$ and $\cos\beta$ have already been performed at this stage. The different curves correspond to the kernels introduced in eq. (8.1) and eq. (8.4). Left: Method 1. Right: Method 2. Note that for method 2, the kernel $\overline{\mathcal{L}}^{(2)}$ and $\overline{\mathcal{L}}^{(3)}$ yield identical curves.

because[12] the Fourier-transform of $\Pi_{\mu\nu\sigma\lambda}^{(1);\pi^0}(x,y,z)$ contains an explicit factor of q_3, the momentum dual to z. As a consequence, we expect smaller finite-size effect on this term.

In summary, Method 2 is numerically far cheaper to apply. It leads to a mild broadening of the overall integrand in $|y|$ (see figure 7, as well as figures 18 and 19 of ref. [51]), which a suitable tuning of the parameter Λ can counteract. Thus the combination of Method 2 and the kernel $\overline{\mathcal{L}}^{(\Lambda)}$ was invaluable to our lattice QCD results in refs. [36, 37, 51].

8.2 Tests in the continuum

As a first check of our master formula, and to gain some insight on the shape of the integrand, we compute several contributions to a_μ^{LbL} using the expressions for $\widehat{\Pi}$ derived in the previous section, and compare them with the known results obtained in momentum space.

8.2.1 The pion-pole contribution to a_μ^{HLbL}

The pion-pole contribution is estimated using the expression of $\widehat{\Pi}$ derived in section 7.2, assuming a VMD transition form factor. We note that, when using Method 2, one needs to find the correct mapping between the three contractions in momentum space (see eq. (7.11)) and the reference contraction in position space. This can be done using partially-quenched chiral perturbation theory and we refer the reader to ref. [36] for more details. After integration over $|x|$ and $\cos\beta$, the integrand, as a function of $|y|$, is displayed in figure 7 for both Methods 1 and 2 and all four kernels $\overline{\mathcal{L}}^{(n)}$ with a pion mass of $m_\pi = 135\,\text{MeV}$. For pion masses in the range [135 - 600] MeV, we reproduce the results, obtained from the

---

[12]As noted in [36, 43], the quark-level Wick contraction $\Pi_{\mu\nu\sigma\lambda}^{(1)}(x,y,z)$ does not contain the diagram in which the π^0 propagates between the pair $(0, y)$ and the pair (x, z) of vertices, which corresponds to the third (and last) term in eq. (7.11). The first two terms, which do contribute, vanish at $q_3 = 0$, leading to the conclusion (8.9).

m_π [MeV]	a_μ^{HLbL} [70]	Method 1	deviation	Method 2	deviation
135	57.00	57.21	$+0.37\%$	57.33	$+0.57\%$
200	42.84	42.91	$+0.16\%$	42.83	-0.02%
300	29.64	29.63	-0.03%	29.64	$+0.00\%$
400	21.75	21.71	-0.18%	21.71	-0.18%
600	13.10	13.07	-0.22%	13.07	-0.22%

Table 2. Results for the pion-pole contribution to a_μ^{HLbL} in units of 10^{-11} assuming a VMD transition form factor as discussed in the text. We use $m_V = 775.49$ MeV and $F_\pi = 92.4$ MeV. The results are obtained using the standard kernel $\overline{\mathcal{L}}^{(0)}$ and for both methods 1 and 2. We also provide the deviation to the results obtained from the expressions in ref. [70].
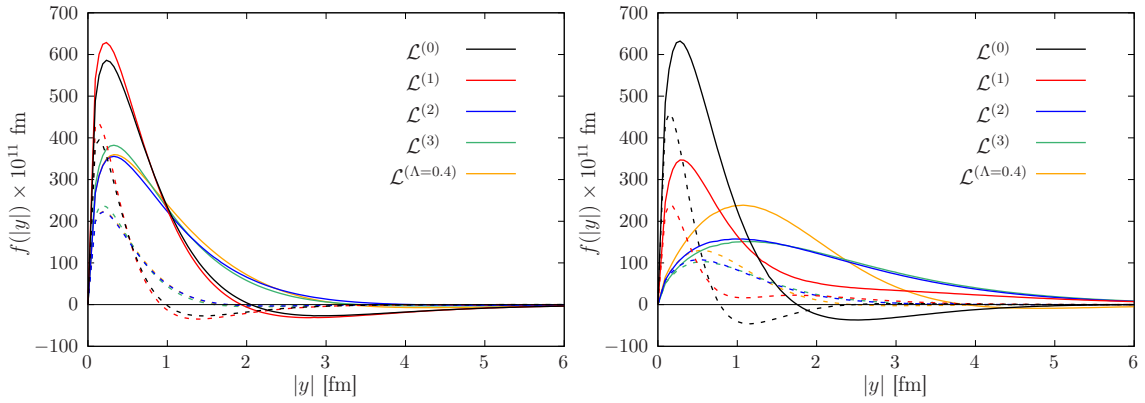
Figure 8. The integrand with respect to the variable $|y|$ leading to a_μ^{LbL} for the lepton-loop contribution with $m_l/m = 1$ (full lines) and $m_l/m = 2$ (dashed lines). The integrals over $|x|$ and $\cos\beta$ have already been performed at this stage. The different curves correspond to the kernels introduced in eq. (8.1) and eq. (8.4). Left: Method 1. Right: Method 2.

three-dimensional integral representation in momentum space in ref. [70], at the percent level. The results are summarized in table 2. Using the standard kernel, one observes that this contribution is remarkably long-range with a negative tail at large $|y|$. In particular, one needs a very large lattice $L \gg 5$ fm to capture the negative tail at the physical pion mass. When using the method 1, the integrands corresponding to the kernel 2 and 3 are less peaked at short distances, approach zero faster at long distances and remain positive. When using Method 2, the integrand for both kernels 2 and 3 are identical but also more long range. Since this setup is considerably cheaper for practical lattice QCD calculations, one can attempt to correct for finite-size effects on this contribution by computing the pion-transition form factor on the same set of ensembles, as done in ref. [19]. See ref. [36] for a practical implementation.

8.2.2 The lepton-loop contribution to a_μ^{LbL}

The lepton-loop contribution to a_μ^{LbL} is estimated using the expression of $\widehat{\Pi}$ derived in section 7.3 with $m_l/m_\mu = 1/2, 1, 2$ where m_l is the mass of the lepton in the loop. The

m_l/m_μ	a_μ^{LbL} (exact)	a_μ^{LbL}	precision	deviation
1/2	1229.07	1257.5(6.2)(2.4)	0.5%	2.3%
1	464.97	470.6(2.3)(2.1)	0.7%	1.2%
2	150.31	150.4(0.7)(1.7)	1.2%	0.06%

Table 3. Results, precision and deviation of the lepton-loop contribution to a_μ^{LbL} (in units of 10^{-11}) computed in the continuum with kernel $\overline{\mathcal{L}}^{(0)}$ compared to the known results [81, 82]. The first uncertainty originates from the three-dimensional numerical integration, the second from the extrapolation of the integrand to small $|y|$.

results are summarized in table 3 and the shape of the integrand, as a function of $|y|$, is shown in figure 8. For $m_l = m, 2m$ we reproduce the analytically known results for a_μ^{LbL} in QED [81, 82] with a precision of about 1%. As can be seen from the plots, the integrand is quite steep close to the origin and we probe the QED kernel at short distances. We observe that the height of the peak grows for smaller masses of the lepton in the loop. For $m_l = m/2$ this rise to the peak is very steep, and we observe a 2.3% deviation from the exact result. It thus appears difficult to obtain a_μ^{LbL} at the percent level with our implementation of the QED kernel for such a long-range contribution. As for the pion, the integrand resulting from the standard kernel also exhibits a long negative tail. Again, the kernel 2 and 3 are peaked at short ranges when using Method 1, a feature that does not hold when switching to Method 2.

8.2.3 The charged-pion loop contribution to a_μ^{HLbL}

Using the master formula (2.29) with kernel $\mathcal{L}^{(2)}$ defined in eq. (8.1) and $i\widehat{\Pi}$ given by eqs. (7.87), (7.95) and (7.96), we compute the contribution of a physical-mass charged pion to a_μ^{HLbL} in the scalar QED framework. After the x integral has been performed, no contributing delta-function contributions are left, so that the integrand can be displayed straightforwardly; see figure 9. With $a_\mu^{\mathrm{HLbL}} = -43.9 \times 10^{-11}$ we reproduce the result $-43.86(5) \times 10^{-11}$ obtained analytically in ref. [83] with a rapidly converging series expansion in $(m/m_{\pi^+})^2 = 0.573092$ at the per-mille level.

8.3 The lepton-loop on the lattice

We will now show the results of performing a full lattice calculation of the lepton loop contribution using both Methods 1 and 2. This was a first step towards the full lattice QCD calculations, and an important benchmark of our implementation of the position-space approach.

The correlation function is computed on a L^4 lattice using unit gauge links, (anti-)periodic boundary conditions in (time-)space and Wilson fermions. For a fixed vertex position y, the sums over the sites x and z in eq. (2.29) are performed explicitly. After which we have a one-dimensional integral that can be sampled sufficiently finely using the variable $|y|$, for all values of $y = (n, n, n, n)$ with $0 < n < L/2$. We also consider both the
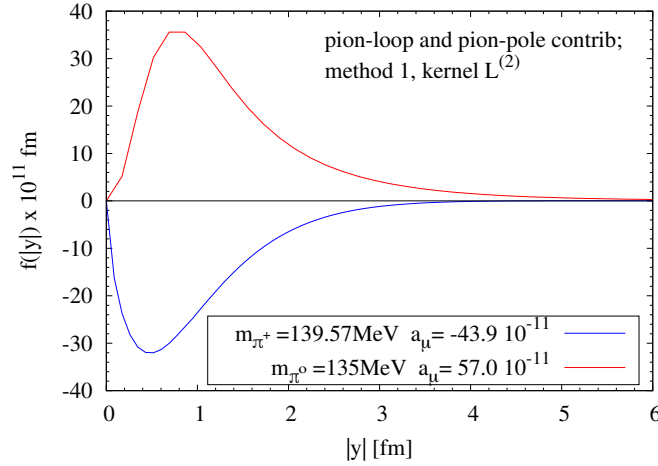
Figure 9. The integrand with respect to the variable $|y|$ leading to a_μ^{HLbL} for the charged-pion loop computed in scalar QED, together (for comparison) with the integrand for the neutral pion-pole computed with a VMD form factor. The integrals over $|x|$ and $\cos\beta$ have already been performed at this stage. Here Method 1 is used with kernel $\mathcal{L}^{(2)}$.

local (l) and the conserved (c) vector currents, which have different discretization effects,

$$j_\mu^{(l)}(x) = \overline{\psi}(x)\gamma_\mu \mathcal{Q}\psi_j(x)\,, \tag{8.10a}$$

$$j_\mu^{(c)}(x) = \frac{1}{2}\left(\overline{\psi}(x+a\hat{\mu})(1+\gamma_\mu)U_\mu^\dagger(x)\mathcal{Q}\psi(x) - \overline{\psi}(x)(1-\gamma_\mu)U_\mu(x)\mathcal{Q}\psi(x+a\hat{\mu})\right)\,. \tag{8.10b}$$

Here, $\mathcal{Q}$ is the lepton charge in units of e. Let m_0 be the bare subtracted lepton mass, related to the hopping parameter κ_ℓ via $am_0 = (1/\kappa_\ell - 1/\kappa_{\mathrm{cr}})/2$ with $\kappa_{\mathrm{cr}} = 1/8$. In the free theory, the local vector current has the advantage of being automatically O(a)-improved, if one uses as multiplicative renormalization factor $(1 + b_{\mathrm{V}}am_0)$ with $b_{\mathrm{V}} = 1$ [84]. While no multiplicative renormalization of the conserved vector current is needed, an additive improvement term with a coefficient $c_{\mathrm{V}} = 1/2$ is required to remove 'on-shell' O(a) lattice artifacts, but not included here (see e.g. [85]). Indeed, for both current discretizations, additional lattice artifacts scaling linearly with the lattice spacing are expected to arise from the region where two or more currents are separated by a distance on the order of the lattice spacing. Our line of constant physics is defined by a constant renormalized mass of the lepton in the loop, $m_\ell = \mathrm{cst}$. Including O(a) effects, one has $m_\ell = Z_{\mathrm{m}}\, m_0(1 + b_{\mathrm{m}}am_0)$, with $Z_{\mathrm{m}} = 1$ and $b_{\mathrm{m}} = -1/2$ [84], so that the bare subtracted quark mass has to be adjusted in the simulation. Finally, we are working with the QCD code and the result must be divided by $N_c = 3$, the number of colors.
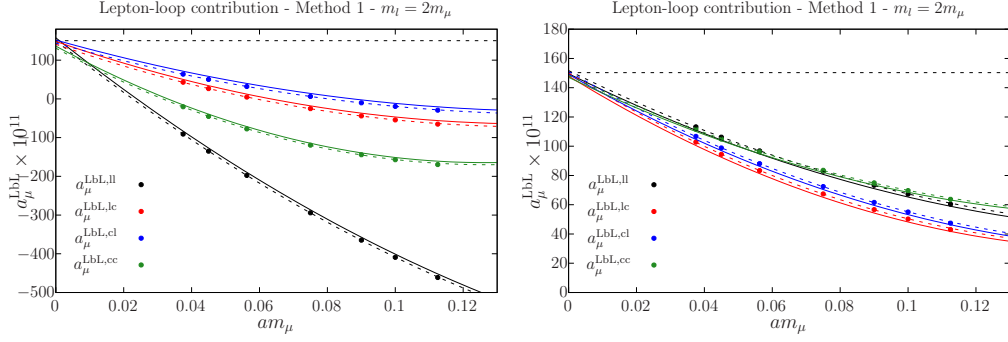
Figure 10. Continuum extrapolation of the lepton-loop contribution using the kernel $\overline{\mathcal{L}}^{(0)}$ (left panel) and $\overline{\mathcal{L}}^{(2)}$ (right panel) using Method 1. We use $m_l = 2m_\mu$. The colors correspond to different discretizations of the correlation function. The horizontal dashed line represents the exact result.

$m_l = 2m_\mu$	ll	lc	cl	cc
Kernel $\overline{\mathcal{L}}^{(0)}$	157.8	148.5	152.0	136.3
Kernel $\overline{\mathcal{L}}^{(2)}$	149.5	147.9	149.1	147.1

Table 4. Results for a_μ^{LbL} in units of 10^{-11} from the lepton loop of mass $m_l = 2m_\mu$ obtained with Method 1 by extrapolating the lattice results displayed in figure 10 to the continuum. Two different kernels and four different discretizations of $i\widehat{\Pi}$ are used. The exact result is $a_\mu^{\mathrm{LbL}} = 150.31$ [81, 82].

We have used seven lattices, with the same physical volume $L\,m_l = 7.2$, and the continuum extrapolation is performed assuming the simple functional form

$$a_\mu^{\mathrm{LbL}}(a) = a_\mu^{\mathrm{LbL}}(0) + \alpha\,a + \beta\,a^2\,, \tag{8.11}$$

where only the four lattices with the smallest lattice spacings are included in the fit. The result using the first strategy with $m_l = 2m_\mu$ is shown in figure 10 for the kernel $\overline{\mathcal{L}}^{(0)}$ (left panel) and for the subtracted kernel $\overline{\mathcal{L}}^{(2)}$ (right panel);

Note the very different ranges on the y-axis. In both cases, we use four different discretizations of the correlation function (all combinations of local and conserved vector currents at sites x and z). The continuum extrapolation, at fixed volume, is given by the dashed lines. To estimate the correction due to finite-size effects, a new set of two lattices, with larger volumes, are used. The finite-size effect correction is assumed to be independent of the lattice spacing and is estimated as the difference between the small and the large volumes at a given lattice spacing. The corrected results are finally given by the plain lines. One observes much smaller discretization effects for the kernel $\overline{\mathcal{L}}^{(2)}$ in the right panel where one only has to extrapolate $a_\mu^{\mathrm{LbL}} \times 10^{11}$ from about 100 to 140, compared to rather large extrapolations with kernel $\overline{\mathcal{L}}^{(0)}$ in the left panel (even from negative values). The results of the continuum extrapolations are collected in table 4. The same observation applies to the following two figures. We also note that very similar results are obtained with the kernel $\overline{\mathcal{L}}^{(3)}$.
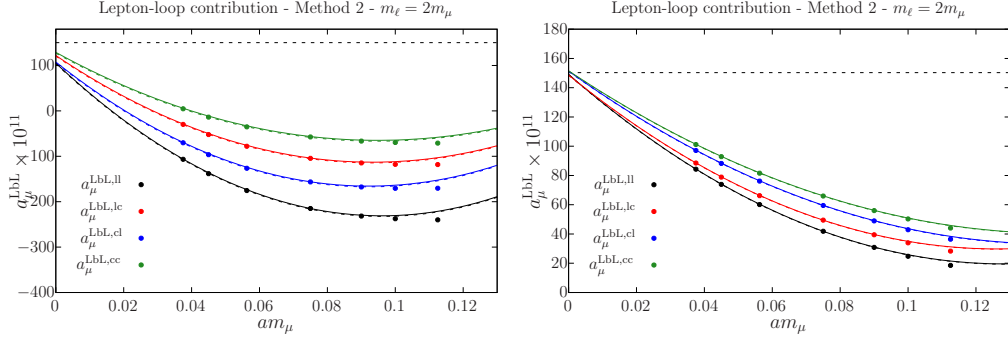
Figure 11. Continuum extrapolation of the lepton loop contribution for the two kernels $\overline{\mathcal{L}}^{(0)}$ (left panel) and $\overline{\mathcal{L}}^{(2)}$ (right panel) using Method 2. We use $m_l = 2m_\mu$. The colors correspond to different discretizations of the correlation function. The horizontal dashed line represents the exact result.
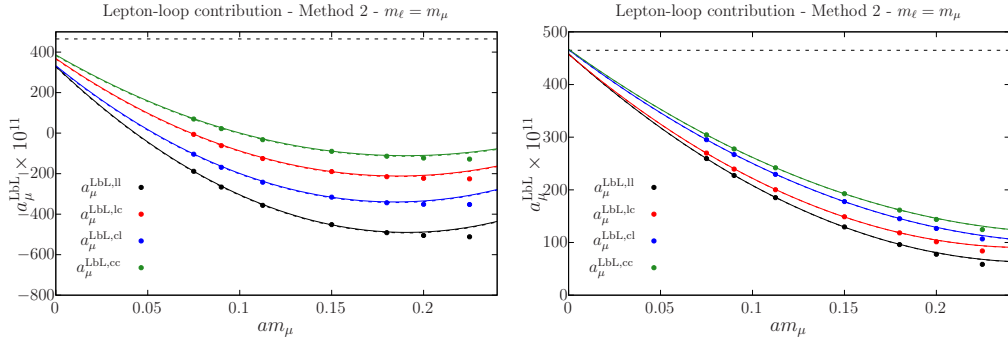
Figure 12. Same as figure 11 but with $m_l = m_\mu$.

The results using Method 2 are shown in figures 11 and 12 for $m_l = 2m_\mu$ and $m_l = m_\mu$ respectively. As before, the left panel corresponds to the standard kernel $\overline{\mathcal{L}}^{(0)}$ and the right panel to the subtraction $\overline{\mathcal{L}}^{(2)}$. Again, the continuum extrapolation is much easier using the subtracted kernel. The resuls of the continuum extrapolations are collected in table 5. Further results for the lepton loop, computed on the lattice with the kernel $\bar{\mathcal{L}}^{(\Lambda)}$, can be found in appendix B of ref. [51].

8.4 Overview of lattice QCD results for the quark-connected contribution

In this section, we briefly review a subset of the results obtained to date for the hadronic-light-by-light contribution a_μ^{HLbL} using the QED kernel derived above, restricting ourselves to the quark-connected contribution. The relevant publications are [36, 37, 51], and some preliminary results can also be found in the earlier proceedings contributions [43, 86]. All these calculations have been performed on gauge ensembles provided by the Coordinated Lattice Simulations (CLS) initiative [87]. The ensembles were generated using three flavours of non-perturbatively O(a)-improved Wilson fermions and with the tree-level O(a^2)-improved Symanzik gauge action.

Reference [51] focuses on QCD with degenerate u, d, s quark, corresponding to $m_\pi = m_K \simeq 420\,\mathrm{MeV}$. It contains results for the connected contribution obtained either with

$m_l = 2m_\mu$	ll	lc	cl	cc
Kernel $\overline{\mathcal{L}}^{(0)}$	105.2	122.1	107.7	129.0
Kernel $\overline{\mathcal{L}}^{(2)}$	149.1	148.6	151.3	151.5
$m_l = m_\mu$	ll	lc	cl	cc
Kernel $\overline{\mathcal{L}}^{(0)}$	329.3	368.3	333.0	386.2
Kernel $\overline{\mathcal{L}}^{(2)}$	458.2	457.3	466.1	466.9

Table 5. Results for a_μ^{LbL} in units of 10^{-11} from the lepton loop of mass $m_l = 2m_\mu$ or $m_l = m_\mu$ obtained with Method 2 by extrapolating the lattice results displayed in figures 11 and 12 to the continuum. Two different kernels and four discretizations of $i\widehat{\Pi}$ employing different combinations of local (l) and conserved (c) vector currents are used. The exact results are $a_\mu^{\mathrm{LbL}} = 150.31$ and 464.97 respectively [81, 82].

Method 1 or Method 2. Focussing first on Method 1 with the kernel choice $\overline{\mathcal{L}}^{(\Lambda=0.16)}$, the difference in the integrand between choosing a conserved or a local lattice vector current at vertex x was tested and found to be modest.[13] The cutoff effect on a_μ^{HLbL} for an ensemble with lattice spacing of $0.076\,\mathrm{fm}$ turned out to be on the order of 10%, with a significant uncertainty on this estimate. Finite-size effects were probed directly by comparing two ensembles differing only by their volume, $m_\pi L = 4.4$ and 6.4, and their size found to be roughly consistent with the finite-size effects expected for the π^0 pole contribution. As for Method 2, the kernel $\overline{\mathcal{L}}^{(\Lambda=0.40)}$ was found to be a good choice, and the use of local and conserved currents was investigated as well. The final choice fell on four local currents, although the final integrand with respect to the variable $|y|$ was found to be similar if the current at vertex z was replaced by a conserved current. The size of both cutoff effects and finite-size effects was similar to Method 1. Hence, given the lower computational cost of Method 2, the latter method was selected for all subsequent calculations.

Figure 13 shows the integrand for the quark-connected contribution within Method 1 obtained in lattice QCD with degenerate u, d, s quarks. It is compared to predictions based on the calculations of section 7: the quark loop with a 'constituent mass' of $350\,\mathrm{MeV}$, the π^0 and η pole contributions, as well as the charged pion loop. For the latter two contributions, a modification of the prediction applicable to the full HLbL amplitude must be applied in order to account for the fact that only the quark-connected contribution is considered. This leads to an enhancement of the combined π^0 and η contribution by a factor of three [53, 89]. The combined contribution of pion and kaon loops, computed in the framework of scalar QED, must instead be divided by a factor of three [51] to match the contribution of quark-connected diagrams. Figure 13 illustrates that a semi-quantitative understanding of the integrand can be gained via these fairly simple calculations.

Analogous plots (based on Method 2 with $\Lambda = 0.40$) at lighter pion masses can be found in [36], for which similar qualitative observations can be made. The π^0 pole contribution becomes increasingly dominant as the pion mass is lowered towards its physical value. In

---

[13]See figure 8 of ref. [51]. The difference is about 10% around the peak of the integrand, at $|y| \simeq 0.4\,\mathrm{fm}$, and not statistically significant for $|y| > 0.6\,\mathrm{fm}$.
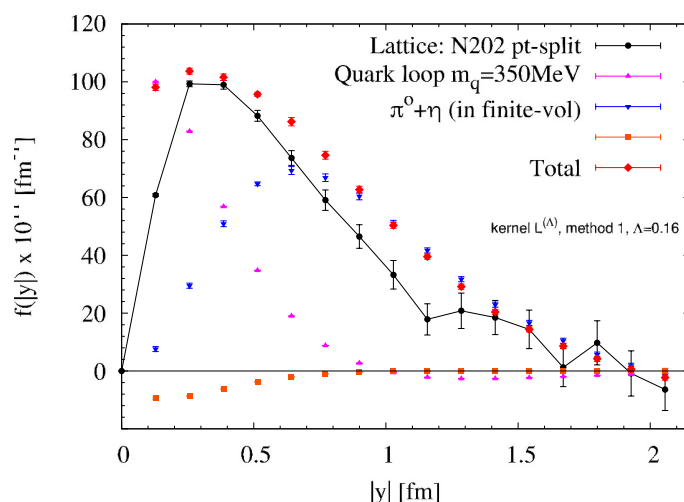
Figure 13. Integrand for the connected contribution using Method 1 with $\overline{\mathcal{L}}^{(\Lambda=0.16)}$ on ensemble N202 of size $48^3 \times 128$, lattice spacing $0.064\,\mathrm{fm}$ [88] with $m_\pi = m_K = 421\,\mathrm{MeV}$. The lattice data use a point-split current at x. The integrand is compared to the prediction for the pole contributions of the π^0 and η mesons with a VMD transition form factor, which is expected to provide a good approximation to the tail. In addition, an attempt to describe the short-distance contribution with a constituent-quark loop with a quark mass of $350\,\mathrm{MeV}$ is made. Figure reproduced from [51].

the case of a heavy quark propagating in the loop [37], the upward trend as a function of the lattice spacing is seen most clearly. The latter calculation allowed for a state-of-the-art estimate of the charm-quark contribution to a_μ^{HLbL}.

9 Conclusions

In this paper we have presented extensive details of our calculation of the 'QED kernel' needed in the Lorentz-covariant coordinate-space method for computing the hadronic light-by-light contribution to the muon $(g-2)$ in lattice QCD. At the core of this QED kernel is the amplitude represented by the graph of figure 3. It is an unusual amplitude in particle physics in that it involves both the plane-wave propagation of the muon in the initial and final state, and the emission by the muon of massless particles (photons) propagating to definite coordinate-space positions. It is thereby a mixed momentum-space and coordinate-space amplitude. We remark that such mixed amplitudes, although quite complex, may have further interesting applications in quantum-field theoretic calculations [58, 59, 90].

We were able to carry out the calculation analytically up to and including the averaging over the direction of the muon momentum. Numerical methods were used only in the final convolution integral, which can be interpreted as yielding the static potential generated by a certain (analytically known) electric charge distribution in four space dimensions. While the angular integral of this final convolution can perhaps still be handled analytically, and we have made some progress in this direction [91], one angular integral still had to be performed numerically in our two implementations of sections 4 and 5.

For the practical purpose of computing a_μ^{HLbL} on the lattice, we have tested the robustness of the numerics by reproducing a number of known light-by-light contributions, typically at the one-percent level. Such a precision is sufficient for the foreseeable future, given that the current precision goal for a_μ^{HLbL} is to reach the 10% level. As noted in the introduction, our implementation of the QED kernel has already been applied in lattice QCD calculations of a_μ^{HLbL} [36, 37, 51]. Given the phenomenological importance of the muon $(g-2)$, the present paper serves to document and underpin a central aspect of these results.

The idea of treating photon propagators in the continuum, infinite-volume theory has been applied in other contexts as well, most recently in ref. [92]. One simpler application is the fully covariant coordinate-space method for the HVP contribution to the muon $(g-2)$ [93]. Another interesting application concerns the calculation of the QED self-energy of stable hadrons without power-law finite-size effects [94]. Further applications will probably follow in the future.

Acknowledgments

A The tensors $T^{\mathrm{A}}_{\alpha\beta\delta}(x, y)$ in terms of the weight functions

In this appendix, we consider the weight functions $\bar{\mathfrak{g}}^{(0)}$, $\bar{\mathfrak{g}}^{(1)}$, $\bar{\mathfrak{g}}^{(2)}$, $\bar{\mathfrak{l}}^{(1)}$, $\bar{\mathfrak{l}}^{(2)}$, $\bar{\mathfrak{l}}^{(3)}$ as being functions of $(|x|, \hat{c}_\beta \equiv \hat{x} \cdot \hat{y}, |y|)$ and use the notation $\partial^{[j]}$ to denote the derivative of a weight

function with respect to its j'th argument. The chain rule for $T^{(\mathrm{I})}_{\alpha\beta\delta}(x,y)$ reads

$$
\begin{aligned}
T^{\mathrm{I}}_{\alpha\beta\delta}(x,y) &= \delta_{\beta\delta}\frac{x_\alpha}{|x|}\Big\{\partial^{[1]}\bar{\mathfrak{g}}^{(1)} + \partial^{[1]}\bar{\mathfrak{g}}^{(2)} - \frac{\hat{c}_\beta}{|x|}\Big(\partial^{[2]}\bar{\mathfrak{g}}^{(1)} + \partial^{[2]}\bar{\mathfrak{g}}^{(2)}\Big)\Big\} \\
&+ \delta_{\beta\delta}\frac{y_\alpha}{|x||y|}\Big\{\partial^{[2]}\bar{\mathfrak{g}}^{(1)} + \partial^{[2]}\bar{\mathfrak{g}}^{(2)}\Big\} \\
&+ (\delta_{\alpha\delta}x_\beta + \delta_{\alpha\beta}x_\delta)\frac{1}{|x|}\Big\{\partial^{[1]}\bar{\mathfrak{g}}^{(1)} + \Big(\frac{1}{|y|} - \frac{\hat{c}_\beta}{|x|}\Big)\partial^{[2]}\bar{\mathfrak{g}}^{(1)}\Big\} \\
&+ \delta_{\alpha\delta}\frac{y_\beta}{|y|}\Big\{\partial^{[3]}\bar{\mathfrak{g}}^{(1)} + \Big(\frac{1}{|x|} - \frac{\hat{c}_\beta}{|y|}\Big)\partial^{[2]}\bar{\mathfrak{g}}^{(1)}\Big\} \\
&+ \delta_{\alpha\beta}\frac{y_\delta}{|x|}\Big\{\partial^{[1]}\bar{\mathfrak{g}}^{(2)} + \Big(\frac{1}{|y|} - \frac{\hat{c}_\beta}{|x|}\Big)\partial^{[2]}\bar{\mathfrak{g}}^{(2)}\Big\} \\
&+ \frac{x_\alpha x_\beta x_\delta}{x^2}\Big\{\partial^{[1]}\partial^{[1]}\bar{\mathfrak{g}}^{(1)} + \Big(\frac{1}{|y|} - 2\frac{\hat{c}_\beta}{|x|}\Big)\partial^{[1]}\partial^{[2]}\bar{\mathfrak{g}}^{(1)} - \frac{\hat{c}_\beta}{|x|}\Big(\frac{1}{|y|} - \frac{\hat{c}_\beta}{|x|}\Big)\partial^{[2]}\partial^{[2]}\bar{\mathfrak{g}}^{(1)} \\
&\qquad\qquad - \frac{1}{|x|}\partial^{[1]}\bar{\mathfrak{g}}^{(1)} + \frac{1}{|x|}\Big(\frac{3\hat{c}_\beta}{|x|} - \frac{1}{|y|}\Big)\partial^{[2]}\bar{\mathfrak{g}}^{(1)}\Big\} \\
&+ \frac{y_\alpha y_\beta y_\delta}{|x| y^2}\Big\{\partial^{[2]}\partial^{[3]}\bar{\mathfrak{g}}^{(2)} + \Big(\frac{1}{|x|} - \frac{\hat{c}_\beta}{|y|}\Big)\partial^{[2]}\partial^{[2]}\bar{\mathfrak{g}}^{(2)} - \frac{1}{|y|}\partial^{[2]}\bar{\mathfrak{g}}^{(2)}\Big\} \\
&+ \frac{x_\alpha x_\beta y_\delta}{|x|^2}\Big\{\partial^{[1]}\partial^{[1]}\bar{\mathfrak{g}}^{(2)} + \Big(\frac{1}{|y|} - 2\frac{\hat{c}_\beta}{|x|}\Big)\partial^{[1]}\partial^{[2]}\bar{\mathfrak{g}}^{(2)} - \frac{\hat{c}_\beta}{|x|}\Big(\frac{1}{|y|} - \frac{\hat{c}_\beta}{|x|}\Big)\partial^{[2]}\partial^{[2]}\bar{\mathfrak{g}}^{(2)} \\
&\qquad\qquad - \frac{1}{|x|}\partial^{[1]}\bar{\mathfrak{g}}^{(2)} + \frac{1}{|x|}\Big(\frac{3\hat{c}_\beta}{|x|} - \frac{1}{|y|}\Big)\partial^{[2]}\bar{\mathfrak{g}}^{(2)}\Big\} \\
&+ \frac{y_\alpha y_\beta x_\delta}{|x||y|^2}\Big\{\partial^{[2]}\partial^{[3]}\bar{\mathfrak{g}}^{(1)} + \Big(\frac{1}{|x|} - \frac{\hat{c}_\beta}{|y|}\Big)\partial^{[2]}\partial^{[2]}\bar{\mathfrak{g}}^{(1)} - \frac{1}{|y|}\partial^{[2]}\bar{\mathfrak{g}}^{(1)}\Big\} \\
&+ \frac{y_\alpha x_\beta x_\delta}{|x|^2|y|}\Big\{\partial^{[1]}\partial^{[2]}\bar{\mathfrak{g}}^{(1)} + \Big(\frac{1}{|y|} - \frac{\hat{c}_\beta}{|x|}\Big)\partial^{[2]}\partial^{[2]}\bar{\mathfrak{g}}^{(1)} - \frac{1}{|x|}\partial^{[2]}\bar{\mathfrak{g}}^{(1)}\Big\} \\
&+ \frac{x_\alpha y_\beta y_\delta}{|x||y|}\Big\{\partial^{[1]}\partial^{[3]}\bar{\mathfrak{g}}^{(2)} - \frac{\hat{c}_\beta}{|x|}\partial^{[2]}\partial^{[3]}\bar{\mathfrak{g}}^{(2)} + \Big(\frac{1}{|x|} - \frac{\hat{c}_\beta}{|y|}\Big)\partial^{[1]}\partial^{[2]}\bar{\mathfrak{g}}^{(2)} \\
&\qquad\qquad - \frac{\hat{c}_\beta}{|x|}\Big(\frac{1}{|x|} - \frac{\hat{c}_\beta}{|y|}\Big)\partial^{[2]}\partial^{[2]}\bar{\mathfrak{g}}^{(2)} + \frac{1}{|x|}\Big(\frac{\hat{c}_\beta}{|y|} - \frac{1}{|x|}\Big)\partial^{[2]}\bar{\mathfrak{g}}^{(2)}\Big\} \\
&+ \frac{x_\alpha y_\beta x_\delta}{|x||y|}\Big\{\partial^{[1]}\partial^{[3]}\bar{\mathfrak{g}}^{(1)} - \frac{\hat{c}_\beta}{|x|}\partial^{[2]}\partial^{[3]}\bar{\mathfrak{g}}^{(1)} + \Big(\frac{1}{|x|} - \frac{\hat{c}_\beta}{|y|}\Big)\Big(\partial^{[1]}\partial^{[2]}\bar{\mathfrak{g}}^{(1)} - \frac{\hat{c}_\beta}{|x|}\partial^{[2]}\partial^{[2]}\bar{\mathfrak{g}}^{(1)}\Big) \\
&\qquad\qquad + \frac{1}{|x|}\Big(\frac{\hat{c}_\beta}{|y|} - \frac{1}{|x|}\Big)\partial^{[2]}\bar{\mathfrak{g}}^{(1)}\Big\} \\
&+ \frac{y_\alpha x_\beta y_\delta}{|x|^2|y|}\Big\{\partial^{[1]}\partial^{[2]}\bar{\mathfrak{g}}^{(2)} + \Big(\frac{1}{|y|} - \frac{\hat{c}_\beta}{|x|}\Big)\partial^{[2]}\partial^{[2]}\bar{\mathfrak{g}}^{(2)} - \frac{1}{|x|}\partial^{[2]}\bar{\mathfrak{g}}^{(2)}\Big\}.
\end{aligned}
\tag{A.1}
$$

Similarly, the chain rule for $T^{\mathrm{II}}_{\alpha\beta\delta}$ and $T^{\mathrm{III}}_{\alpha\beta\delta}$ read

$$
\frac{1}{m} T^{\mathrm{II}}_{\alpha\beta\delta}(x,y) = \delta_{\beta\delta} \frac{x_\alpha}{|x|} \left\{ \frac{1}{4} \left(\partial^{[1]} \bar{\mathfrak{g}}^{(0)} - \frac{\hat{c}_\beta}{|x|} \partial^{[2]} \bar{\mathfrak{g}}^{(0)} \right) - \frac{x^2}{4} \left(\partial^{[1]} \bar{\mathfrak{l}}^{(1)} - \frac{\hat{c}_\beta}{|x|} \partial^{[2]} \bar{\mathfrak{l}}^{(1)} \right) \right.
$$

$$
\left. - \frac{y^2}{4} \left(\partial^{[1]} \bar{\mathfrak{l}}^{(2)} - \frac{\hat{c}_\beta}{|x|} \partial^{[2]} \bar{\mathfrak{l}}^{(2)} \right) - \frac{|x||y|\hat{c}_\beta}{2} \left(\partial^{[1]} \bar{\mathfrak{l}}^{(3)} - \frac{\hat{c}_\beta}{|x|} \partial^{[2]} \bar{\mathfrak{l}}^{(3)} \right) - \frac{|x|}{2} \bar{\mathfrak{l}}^{(1)} \right\}
$$

$$
+ \delta_{\beta\delta} \frac{y_\alpha}{|x||y|} \left\{ \frac{1}{4} \partial^{[2]} \bar{\mathfrak{g}}^{(0)} - \frac{x^2}{4} \partial^{[2]} \bar{\mathfrak{l}}^{(1)} - \frac{y^2}{4} \partial^{[2]} \bar{\mathfrak{l}}^{(2)} - \frac{|x||y|\hat{c}_\beta}{2} \partial^{[2]} \bar{\mathfrak{l}}^{(3)} - \frac{|x||y|}{2} \bar{\mathfrak{l}}^{(3)} \right\}
$$

$$
+ (\delta_{\alpha\beta} x_\delta + \delta_{\alpha\delta} x_\beta) \left\{ \bar{\mathfrak{l}}^{(1)} \right\}
$$

$$
+ (\delta_{\alpha\beta} y_\delta + \delta_{\alpha\delta} y_\beta) \left\{ \bar{\mathfrak{l}}^{(3)} \right\}
$$

$$
+ \frac{x_\alpha x_\beta x_\delta}{|x|} \left\{ \partial^{[1]} \bar{\mathfrak{l}}^{(1)} - \frac{\hat{c}_\beta}{|x|} \partial^{[2]} \bar{\mathfrak{l}}^{(1)} \right\}
$$

$$
+ \frac{y_\alpha y_\beta y_\delta}{|x||y|} \left\{ \partial^{[2]} \bar{\mathfrak{l}}^{(2)} \right\}
$$

$$
+ \frac{y_\alpha x_\beta x_\delta}{|x||y|} \left\{ \partial^{[2]} \bar{\mathfrak{l}}^{(1)} \right\}
$$

$$
+ \frac{x_\alpha y_\beta x_\delta}{|x|} \left\{ \partial^{[1]} \bar{\mathfrak{l}}^{(3)} - \frac{\hat{c}_\beta}{|x|} \partial^{[2]} \bar{\mathfrak{l}}^{(3)} \right\}
$$

$$
+ \frac{x_\alpha x_\beta y_\delta}{|x|} \left\{ \partial^{[1]} \bar{\mathfrak{l}}^{(3)} - \frac{\hat{c}_\beta}{|x|} \partial^{[2]} \bar{\mathfrak{l}}^{(3)} \right\}
$$

$$
+ \frac{x_\alpha y_\beta y_\delta}{|x|} \left\{ \partial^{[1]} \bar{\mathfrak{l}}^{(2)} - \frac{\hat{c}_\beta}{|x|} \partial^{[2]} \bar{\mathfrak{l}}^{(2)} \right\}
$$

$$
+ \frac{y_\alpha x_\beta y_\delta}{|x||y|} \left\{ \partial^{[2]} \bar{\mathfrak{l}}^{(3)} \right\}
$$

$$
+ \frac{y_\alpha y_\beta x_\delta}{|x||y|} \left\{ \partial^{[2]} \bar{\mathfrak{l}}^{(3)} \right\} \tag{A.2}
$$

and

$$
\frac{1}{m} T^{\mathrm{III}}_{\alpha\beta\delta}(x,y) = (\delta_{\beta\delta} x_\alpha + \delta_{\alpha\beta} x_\delta) \left\{ \bar{\mathfrak{l}}^{(1)} + \bar{\mathfrak{l}}^{(3)} \right\}
$$

$$
+ (\delta_{\beta\delta} y_\alpha + \delta_{\alpha\beta} y_\delta) \left\{ \bar{\mathfrak{l}}^{(2)} + \bar{\mathfrak{l}}^{(3)} \right\}
$$

$$
+ \delta_{\alpha\delta} \frac{x_\beta}{|x|} \left\{ \frac{1}{4} \left(\partial^{[1]} \bar{\mathfrak{g}}^{(0)} + \left(\frac{1}{|y|} - \frac{\hat{c}_\beta}{|x|} \right) \partial^{[2]} \bar{\mathfrak{g}}^{(0)} \right) \right.
$$

$$
- \frac{x^2}{4} \left(\partial^{[1]} \bar{\mathfrak{l}}^{(1)} + \left(\frac{1}{|y|} - \frac{\hat{c}_\beta}{|x|} \right) \partial^{[2]} \bar{\mathfrak{l}}^{(1)} \right)
$$

$$
- \frac{y^2}{4} \left(\partial^{[1]} \bar{\mathfrak{l}}^{(2)} + \left(\frac{1}{|y|} - \frac{\hat{c}_\beta}{|x|} \right) \partial^{[2]} \bar{\mathfrak{l}}^{(2)} \right)
$$

$$
\left. - \frac{|x||y|\hat{c}_\beta}{2} \left(\partial^{[1]} \bar{\mathfrak{l}}^{(3)} + \left(\frac{1}{|y|} - \frac{\hat{c}_\beta}{|x|} \right) \partial^{[2]} \bar{\mathfrak{l}}^{(3)} \right) - \frac{|x|}{2} \left(\bar{\mathfrak{l}}^{(1)} + \bar{\mathfrak{l}}^{(3)} \right) \right\}
$$

$$
+ \delta_{\alpha\delta} \frac{y_\beta}{|y|} \left\{ \frac{1}{4} \left(\partial^{[3]} \bar{\mathfrak{g}}^{(0)} + \left(\frac{1}{|x|} - \frac{\hat{c}_\beta}{|y|} \right) \partial^{[2]} \bar{\mathfrak{g}}^{(0)} \right) \right.
$$

$$
- \frac{x^2}{4} \left(\partial^{[3]} \bar{\mathfrak{l}}^{(1)} + \left(\frac{1}{|x|} - \frac{\hat{c}_\beta}{|y|} \right) \partial^{[2]} \bar{\mathfrak{l}}^{(1)} \right)
$$

$$-\frac{y^2}{4}\left(\partial^{[3]}\bar{\mathfrak{l}}^{(2)}+\left(\frac{1}{|x|}-\frac{\hat{c}_\beta}{|y|}\right)\partial^{[2]}\bar{\mathfrak{l}}^{(2)}\right)$$

$$-\frac{|x||y|\hat{c}_\beta}{2}\left(\partial^{[3]}\bar{\mathfrak{l}}^{(3)}+\left(\frac{1}{|x|}-\frac{\hat{c}_\beta}{|y|}\right)\partial^{[2]}\bar{\mathfrak{l}}^{(3)}\right)-\frac{|y|}{2}\left(\bar{\mathfrak{l}}^{(2)}+\bar{\mathfrak{l}}^{(3)}\right)\Bigg\}$$

$$+\frac{x_\alpha x_\beta x_\delta}{|x|}\left\{\partial^{[1]}\bar{\mathfrak{l}}^{(1)}+\left(\frac{1}{|y|}-\frac{\hat{c}_\beta}{|x|}\right)\partial^{[2]}\bar{\mathfrak{l}}^{(1)}\right\}$$

$$+\frac{y_\alpha y_\beta y_\delta}{|y|}\left\{\partial^{[3]}\bar{\mathfrak{l}}^{(2)}+\left(\frac{1}{|x|}-\frac{\hat{c}_\beta}{|y|}\right)\partial^{[2]}\bar{\mathfrak{l}}^{(2)}\right\}$$

$$+\frac{x_\alpha y_\beta x_\delta}{|y|}\left\{\partial^{[3]}\bar{\mathfrak{l}}^{(1)}+\left(\frac{1}{|x|}-\frac{\hat{c}_\beta}{|y|}\right)\partial^{[2]}\bar{\mathfrak{l}}^{(1)}\right\}$$

$$+\frac{y_\alpha x_\beta x_\delta}{|x|}\left\{\partial^{[1]}\bar{\mathfrak{l}}^{(3)}+\left(\frac{1}{|y|}-\frac{\hat{c}_\beta}{|x|}\right)\partial^{[2]}\bar{\mathfrak{l}}^{(3)}\right\}$$

$$+\frac{x_\alpha x_\beta y_\delta}{|x|}\left\{\partial^{[1]}\bar{\mathfrak{l}}^{(3)}+\left(\frac{1}{|y|}-\frac{\hat{c}_\beta}{|x|}\right)\partial^{[2]}\bar{\mathfrak{l}}^{(3)}\right\}$$

$$+\frac{y_\alpha x_\beta y_\delta}{|x|}\left\{\partial^{[1]}\bar{\mathfrak{l}}^{(2)}+\left(\frac{1}{|y|}-\frac{\hat{c}_\beta}{|x|}\right)\partial^{[2]}\bar{\mathfrak{l}}^{(2)}\right\}$$

$$+\frac{y_\alpha y_\beta x_\delta}{|y|}\left\{\partial^{[3]}\bar{\mathfrak{l}}^{(3)}+\left(\frac{1}{|x|}-\frac{\hat{c}_\beta}{|y|}\right)\partial^{[2]}\bar{\mathfrak{l}}^{(3)}\right\}$$

$$+\frac{x_\alpha y_\beta y_\delta}{|y|}\left\{\partial^{[3]}\bar{\mathfrak{l}}^{(3)}+\left(\frac{1}{|x|}-\frac{\hat{c}_\beta}{|y|}\right)\partial^{[2]}\bar{\mathfrak{l}}^{(3)}\right\}. \tag{A.3}$$

B   Derivatives of the integrands for the six weight functions with respect to $|x|$

In this appendix, we provide the expressions of the $|x|$-derivatives of the relevant sums (see eqs. (3.66)–(3.68) as well as eqs. (5.24)–(5.31)) entering the expression for the six weight functions parametrizing the QED kernel.

A few notational remarks are in order. In this appendix, we write the argument of z_n as the four-vector u instead of u^2 and use the notation $z'_n \equiv \frac{\partial}{\partial|u|}z_n$, not $\frac{\partial}{\partial|u|^2}$. Also, we set $v = x - u$. The argument of the Gegenbauer polynomials C_n and their derivatives is always $(\hat{u}\cdot\widehat{x-u})$.

We obtain

$$\frac{\partial}{\partial|x|}\sigma_0 = \frac{|x|-|u|\hat{c}_1}{|u-x|}\sum_{n=0}^{\infty}z_n(u)z'_n(v)\frac{C_n}{n+1} \tag{B.1}$$

$$+\frac{|u||x|\hat{s}_1^2}{|x-u|^3}\sum_{n=0}^{\infty}z_n(u)z_n(v)\frac{C'_n}{n+1},$$

$$\frac{\partial\sigma_3}{\partial|x|} = \frac{\hat{c}_1}{|x|}\sum_{n=0}^{\infty}\Big\{z_n(u)\Big[-\frac{z_{n+1}(v)}{|x|}+\frac{|x|-|u|\hat{c}_1}{|x-u|}z'_{n+1}(v)\Big]\frac{C_{n+1}}{n+2} \tag{B.2}$$

$$+z_{n+1}(u)\Big[-\frac{z_n(v)}{|x|}+\frac{|x|-|u|\hat{c}_1}{|x-u|}z'_n(v)\Big]\frac{C_n}{n+1}\Big\}$$

$$+\frac{\hat{s}_1^2}{|x-u|^2}\sum_{n=0}^{\infty}\Big\{\Big(\Big[|u|\hat{c}_1-\frac{(|x|-|u|\hat{c}_1)}{n+1}\Big]\frac{z_n(u)z_{n+1}(v)}{|x-u|}+\frac{|x|-|u|\hat{c}_1}{n+1}z_n(u)z'_{n+1}(v)\Big)\frac{C'_{n+1}}{n+2}$$

$$+ \left(\left[|u|\hat{c}_1 + \frac{|x| - |u|\hat{c}_1}{n+2} \right] \frac{z_{n+1}(u)z_n(v)}{|x-u|} - \frac{|x| - |u|\hat{c}_1}{n+2} z_{n+1}(u)z_n'(v) \right) \frac{C_n'}{n+1} \right\}$$

$$+ \frac{|x||u|\hat{s}_1^4}{|x-u|^4} \sum_{n=0}^{\infty} \frac{1}{(n+1)(n+2)} \left\{ z_n(u)z_{n+1}(v)C_{n+1}'' - z_{n+1}(u)z_n(v)C_n'' \right\},$$

$$\frac{1}{\hat{s}_1^2} \frac{\partial}{\partial |x|} \sigma_2 = -\frac{|x| - |u|\hat{c}_1}{|x-u|} \sum_{n=0}^{\infty} \left\{ \frac{z_n(u)z_{n+1}'(v)}{n+2} C_{n+1} + \frac{z_{n+1}(u)z_n'(v)}{n+1} C_n \right\} \tag{B.3}$$

$$+ \frac{x^2 |u|\hat{c}_1\hat{s}_1^2}{|x-u|^4} \sum_{n=0}^{\infty} \frac{1}{(n+1)(n+2)} \left\{ z_n(u)z_{n+1}(v) C_{n+1}'' - z_{n+1}(u)z_n(v)C_n'' \right\}$$

$$+ \frac{1}{|x-u|^3} \sum_{n=0}^{\infty} \frac{1}{(n+1)(n+2)} \Big\{$$

$$\Big[|x||x-u|\hat{c}_1(|x| - |u|\hat{c}_1)z_{n+1}'(v) + |u|\Big(|u|\hat{c}_1 - |x|\hat{c}_1^2 - (n+1)|x|\hat{s}_1^2\Big)z_{n+1}(v)\Big]z_n(u)C_{n+1}'$$

$$- \Big[|x||x-u|\hat{c}_1(|x| - |u|\hat{c}_1)z_n'(v) + |u|\Big(|u|\hat{c}_1 - |x|\hat{c}_1^2 + (n+2)|x|\hat{s}_1^2\Big)z_n(v)\Big]z_{n+1}(u)C_n' \Big\},$$

$$\frac{\partial}{\partial |x|} \sigma_1 = -\frac{|x|}{2} \sum_{n=0}^{\infty} z_n(u)z_n(v) \frac{C_n}{n+1} \tag{B.4}$$

$$- \frac{x^2}{4} \frac{|x| - |u|\hat{c}_1}{|x-u|} \sum_{n=0}^{\infty} z_n(u)z_n'(v) \frac{C_n}{n+1}$$

$$+ \frac{u^2}{4} \frac{|x| - |u|\hat{c}_1}{|x-u|} \sum_{n=0}^{\infty} z_n'(v)\Big(z_{n-2}(u) + (2-\delta_{n0})z_n(u) + z_{n+2}(u)\Big) \frac{C_n}{n+1}$$

$$+ \frac{(x-u)^2}{4} \frac{|x| - |u|\hat{c}_1}{|x-u|} \sum_{n=0}^{\infty} z_n(u)\Big(z_{n-2}'(v) + (2-\delta_{n0})z_n'(v) + z_{n+2}'(v)\Big) \frac{C_n}{n+1}$$

$$+ \frac{(|x| - |u|\hat{c}_1)}{2} \sum_{n=0}^{\infty} z_n(u)\Big(z_{n-2}(v) + (2-\delta_{n0})z_n(v) + z_{n+2}(v)\Big) \frac{C_n}{n+1}$$

$$+ \frac{|u|(|x| - |u|\hat{c}_1)}{4|x-u|} \sum_{n=0}^{\infty} \Big\{ \Big(z_n(u)z_{n+2}(v) + 2z_n(u)z_n(v) + z_{n+2}(u)z_n(v)\Big)\frac{C_{n+1}}{n+2}$$

$$+ \Big(z_{n-2}(u)z_n(v) + 2z_n(u)z_n(v) + z_n(u)z_{n-2}(v)\Big)\frac{C_{n-1}}{n} \Big\}$$

$$+ \frac{|u|}{4}(|x| - |u|\hat{c}_1) \sum_{n=0}^{\infty} \Big\{ \Big(z_n(u)z_{n+2}'(v) + 2z_n(u)z_n'(v) + z_{n+2}(u)z_n'(v)\Big)\frac{C_{n+1}}{n+2}$$

$$+ \Big(z_{n-2}(u)z_n'(v) + 2z_n(u)z_n'(v) + z_n(u)z_{n-2}'(v)\Big)\frac{C_{n-1}}{n} \Big\}$$

$$+ \frac{|x||u|\hat{s}_1^2}{|x-u|^3} \Big\{ -\frac{x^2}{4} \sum_{n=0}^{\infty} z_n(u)z_n(v)\frac{C_n'}{n+1}$$

$$+ \frac{u^2}{4} \sum_{n=0}^{\infty} z_n(v)\Big(z_{n-2}(u) + (2-\delta_{n0})z_n(u) + z_{n+2}(u)\Big)\frac{C_n'}{n+1}$$

$$+ \frac{(x-u)^2}{4} \sum_{n \geq 0} z_n(u)\Big(z_{n-2}(v) + (2-\delta_{n0})z_n(v) + z_{n+2}(v)\Big)\frac{C_n'}{n+1}$$

$$+ \frac{|u||x-u|}{4} \sum_{n=0}^{\infty} \Big\{ \Big(z_n(u)z_{n+2}(v) + 2z_n(u)z_n(v) + z_{n+2}(u)z_n(v)\Big)\frac{C_{n+1}'}{n+2}$$

$$+ \Big(z_{n-2}(u)z_n(v) + 2z_n(u)z_n(v) + z_n(u)z_{n-2}(v)\Big)\frac{C_{n-1}'}{n} \Big\} \Big\},$$

$$\frac{\partial s_1}{\partial |x|} = \frac{u^2}{4} \frac{|x| - |u|\hat{c}_1}{|x - u|} \sum_{n=0}^{\infty} \Big(z_{n-2}(u) + (1 - \delta_{n0}) z_n(u) + z_{n+2}(u) \Big) z_n'(v) \frac{C_n}{n+1} \tag{B.5}$$

$$+ \frac{|u|^3 |x| \hat{s}_1^2}{4|x - u|^3} \sum_{n=0}^{\infty} \Big(z_{n-2}(u) + (1 - \delta_{n0}) z_n(u) + z_{n+2}(u) \Big) z_n(v) \frac{C_n'}{n+1},$$

$$\frac{\partial s_2}{\partial |x|} = \frac{|x| - |u|\hat{c}_1}{2} \sum_{n=0}^{\infty} z_n(u) \Big(z_{n-2}(v) + (1 - \delta_{n0}) z_n(v) + z_{n+2}(v) \Big) \frac{C_n}{n+1} \tag{B.6}$$

$$+ \frac{|x - u|(|x| - |u|\hat{c}_1)}{4} \sum_{n=0}^{\infty} z_n(u) \Big(z_{n-2}'(v) + (1 - \delta_{n0}) z_n'(v) + z_{n+2}'(v) \Big) \frac{C_n}{n+1}$$

$$+ \frac{|x||u|\hat{s}_1^2}{4|x - u|} \sum_{n=0}^{\infty} z_n(u) \Big(z_{n-2}(v) + (1 - \delta_{n0}) z_n(v) + z_{n+2}(v) \Big) \frac{C_n'}{n+1},$$

$$\frac{\partial \sigma_4}{\partial |x|} = \frac{1}{|u|} \Big(-\frac{2|u|}{x^2} \hat{c}_1 \sigma_1 + (2\frac{|u|}{|x|}\hat{c}_1 - 1)\frac{\partial \sigma_1}{\partial |x|} + \frac{\partial s_2}{\partial |x|} - \frac{\partial s_1}{\partial |x|} \Big), \tag{B.7}$$

$$\frac{\partial \sigma_5}{\partial |x|} = \frac{1}{u^2} \Big(\frac{|u|}{|x|^3}(-2|u|(1 + 2\hat{c}_1^2) + 3|x|\hat{c}_1)\sigma_1 + \frac{|u|}{x^2}(|u|(1 + 2\hat{c}_1^2) - 3|x|\hat{c}_1)\frac{\partial \sigma_1}{\partial |x|} \tag{B.8}$$

$$- 3\frac{|u|}{x^2}\hat{c}_1(s_2 - s_1) + 3\frac{|u|}{|x|}\hat{c}_1(\frac{\partial s_2}{\partial |x|} - \frac{\partial s_1}{\partial |x|}) + 3\frac{\partial s_1}{\partial |x|} \Big).$$

C Expansion of the kernel for small arguments

This appendix provides the relevant expressions to obtain the QED weight functions and the full kernel at $x = 0$ or at $y = 0$. In the following, we refer to various functions defined mainly in subsection 5.2.

C.1 The regime of small $|x|$

In this subsection, the argument of the z_n is always u^2 if not explicitly specified. As in appendix B, z_n' means $\frac{\partial}{\partial |u|} z_n$, not the derivative with respect to u^2. As for the sums σ_k ($1 \le k \le 5$), we recall that their generic arguments are $(|x|, \hat{c}_1 \equiv \hat{x} \cdot \hat{u}, |u|)$.

We begin by giving the first terms of the Taylor expansion of the sums σ_k that enter the calculation of the QED weight functions $\bar{\mathfrak{g}}^{(0)}, \bar{\mathfrak{g}}^{(1)}, \bar{\mathfrak{g}}^{(2)}, \bar{\mathfrak{l}}^{(1)}, \bar{\mathfrak{l}}^{(2)}, \bar{\mathfrak{l}}^{(3)}$. In several cases, we express the result in terms of auxiliary sums collected below in eqs. (C.15)–(C.22). We obtain

$$\sigma_0\big|_{x=0} = \sum_{n=0}^{\infty} (-1)^n z_n^2, \tag{C.1}$$

$$\sigma_3\big|_{x=0} = \hat{s}_1^2 \sum_{n=0}^{\infty} (-1)^n \Big(1 + \frac{2n}{3} \Big) \frac{z_n z_{n+1}}{|u|} + \hat{c}_1^2 \sum_{n=0}^{\infty} (-1)^n \Big(z_n z_{n+1}' - z_{n+1} z_n' \Big), \tag{C.2}$$

$$\lim_{|x| \to 0} \frac{\sigma_1}{x^2} = \frac{4\hat{c}_1^2 - 1}{12} \sigma_1^{(2,2)}(u), \tag{C.3}$$

$$\lim_{|x| \to 0} \frac{\sigma_2}{|x|} = \hat{c}_1 \hat{s}_1^2 \sigma_2^{(1,2)}(u), \tag{C.4}$$

$$\lim_{|x| \to 0} \frac{\sigma_4}{|x|} = -\frac{2}{3} \hat{c}_1 \hat{s}_1^2 \sigma_4^{(1,2)}(u), \tag{C.5}$$

$$\sigma_5\big|_{x=0} = \frac{2}{3} \hat{s}_1^4 \sigma_5^{(0,2)}(u). \tag{C.6}$$

In addition, the following intermediate results are needed,

$$\lim_{|x|\to 0} \frac{s_2 - s_1}{|x|} = -\frac{|u|\hat{c}_1}{2}\sigma_1^{(2,2)}(u), \tag{C.7}$$

$$s_1\big|_{x=0} = \frac{u^2}{4}\sigma_1^{(2,2)}(u). \tag{C.8}$$

For some of the sums, we will need the expansion to one order higher. In particular, we record

$$\frac{1}{2}\frac{\partial^2(s_2 - s_1)}{\partial|x|^2}\Big|_{x=0} = \frac{1}{4}\sigma_1^{(2,2)}(u) + \frac{|u|\hat{c}_1^2}{2}\sigma_{s_1}^{(1,1)}(u), \tag{C.9}$$

$$\frac{\partial s_1}{\partial|x|}\Big|_{x=0} = -\frac{\hat{c}_1 u^2}{4}\,\sigma_{s_1}^{(1,1)}(u), \tag{C.10}$$

as well as the results

$$\frac{\partial\sigma_3}{\partial|x|}\Big|_{x=0} = \hat{c}_1^3\sum_{n=0}^{\infty}(-1)^n\left(-\frac{z_n z_{n+1}'' - z_{n+1}z_n''}{2}\right) \tag{C.11}$$

$$+\hat{c}_1\hat{s}_1^2\sum_{n=0}^{\infty}(-1)^n\left(\frac{(2n+3)z_n z_{n+1}}{2u^2} - \frac{(2n+9)z_n z_{n+1}'}{6|u|} + \frac{(3-2n)z_{n+1}z_n'}{6|u|}\right),$$

$$\frac{1}{6}\frac{\partial^3\sigma_1}{\partial|x|^3}\Big|_{x=0} = 2\Big(C_1(\hat{c}_1)\,\hat{t}_{\sigma_1}^{(3,1)}(u) + C_3(\hat{c}_1)\,\hat{u}_{\sigma_1}^{(3,1)}(u)\Big), \tag{C.12}$$

$$\frac{1}{2}\frac{\partial^2\sigma_2}{\partial|x|^2}\Big|_{x=0} = \hat{s}_1^4\sum_{n=0}^{\infty}(-1)^n\left(-\frac{(2n+3)z_n z_{n+1}}{6u^2} + \frac{z_n z_{n+1}' - z_{n+1}z_n'}{2|u|}\right) \tag{C.13}$$

$$+\hat{s}_1^2\hat{c}_1^2\sum_{n=0}^{\infty}(-1)^n\left(\frac{(2n+3)z_n z_{n+1}}{3u^2} - \frac{(n+3)z_n z_{n+1}'}{3|u|} - \frac{nz_{n+1}z_n'}{3|u|}\right.$$

$$\left. +\frac{z_n z_{n+1}'' - z_{n+1}z_n''}{2}\right),$$

$$\frac{\partial\sigma_5}{\partial|x|}\Big|_{x=0} = \frac{2\hat{c}_1\hat{s}_1^4}{3}\,\sigma_5^{(1,3)}(u). \tag{C.14}$$

The auxiliary sums appearing in the results above are defined as follows,

$$\sigma_1^{(2,2)}(u) = \sum_{n=0}^{\infty}(-1)^n z_n\Big((1-\delta_{n0})z_n + 2z_{n+2}\Big) = 3u^2 b(u^2), \tag{C.15}$$

$$\sigma_2^{(1,2)}(u) = \sum_{n=0}^{\infty}(-1)^n\left(z_{n+1}z_n' - z_n z_{n+1}' + (1+\frac{2n}{3})\frac{z_n z_{n+1}}{|u|}\right), \tag{C.16}$$

$$\sigma_4^{(1,2)}(u) = \sigma_1^{(2,2)}(u), \tag{C.17}$$

$$\sigma_5^{(0,2)}(u) = \sigma_1^{(2,2)}(u), \tag{C.18}$$

$$\sigma_{s_1}^{(1,1)}(u) = \sum_{n=0}^{\infty}(-1)^n\Big[(1-\delta_{n0})z_n z_n' + z_n z_{n+2}' + z_{n+2}z_n'\Big], \tag{C.19}$$

$$\hat{t}_{\sigma_1}^{(3,1)}(u) = -\frac{1}{24|u|}\sigma_1^{(2,2)}(u) - \frac{1}{48}\sigma_{s_1}^{(1,1)}(u), \tag{C.20}$$

$$\hat{u}_{\sigma_1}^{(3,1)}(u) = \frac{1}{48}\sigma_5^{(1,3)}(u), \tag{C.21}$$

$$\sigma_5^{(1,3)}(u) = \frac{\sigma_1^{(2,2)}(u)}{|u|} - \sigma_{s_1}^{(1,1)}(u). \tag{C.22}$$

We recall that $b(u^2)$ was first introduced in eqs. (3.61)–(3.62).

C.1.1 The scalar weight function

The behavior of $\bar{\mathfrak{g}}^{(0)}$ around $x = 0$ is determined by a small number of coefficients $\alpha_{m\pm}^{(0)}$; see eq. (5.15). All $\alpha_{m\pm}^{(0)}$ vanish at $|x| = 0$, except

$$\alpha_{0-}^{(0)}(0, |y|) = \frac{1}{2}\sum_{n=0}^{\infty}(-1)^n \int_0^{|y|} d|u| \, |u|^3 \, z_n^2 \tag{C.23}$$

and $\alpha_{0+}^{(0)}$; the latter, whose integral is infrared divergent at large $|u|$, is however not needed. As for the $|x|$-derivative of the coefficients at the origin, they all vanish except

$$\frac{\partial \alpha_{1+}^{(0)}}{\partial |x|}\bigg|_{|x|=0} = \lim_{|x|\to 0}\alpha_{1+}^{(0)}(|x|,|y|)/|x| = -\frac{1}{8}\sum_{n=0}^{\infty}(-1)^n\int_{|y|}^{\infty}d|u|\, z_n z_n' \tag{C.24}$$

$$= \frac{1}{16}\sum_{n=0}^{\infty}(-1)^n z_n (y^2)^2,$$

$$\frac{\partial \alpha_{1-}^{(0)}}{\partial |x|}\bigg|_{|x|=0} = \lim_{|x|\to 0}\alpha_{1-}^{(0)}(|x|,|y|)/|x| = -\frac{1}{8}\sum_{n=0}^{\infty}(-1)^n\int_0^{|y|}d|u|\, |u|^4 \, z_n z_n' \tag{C.25}$$

$$= \frac{1}{2}\alpha_{0-}^{(0)}(|x|=0,|y|) - |y|^4 \lim_{|x|\to 0}\alpha_{1+}^{(0)}(|x|,|y|)/|x|.$$

Combining these observations, one finds for the actually needed derivatives of the scalar weight function

$$\frac{\partial}{\partial|x|}\bar{\mathfrak{g}}^{(0)}\bigg|_{x=0} = 2\hat{c}_\beta\Big(\frac{1}{|y|^3}\frac{\alpha_{1-}^{(0)}(|x|,|y|)}{|x|} + |y|\frac{\alpha_{1+}^{(0)}(|x|,|y|)}{|x|}\Big)_{x=0}, \tag{C.26}$$

$$\frac{\partial}{\partial\hat{c}_\beta}\bar{\mathfrak{g}}^{(0)}\bigg|_{x=0} = 2|x|\Big(\frac{1}{|y|^3}\frac{\alpha_{1-}^{(0)}(|x|,|y|)}{|x|} + |y|\frac{\alpha_{1+}^{(0)}(|x|,|y|)}{|x|}\Big)_{x=0} + \mathrm{O}(x^2), \tag{C.27}$$

$$\frac{\partial}{\partial|y|}\bar{\mathfrak{g}}^{(0)}\bigg|_{x=0} = -\frac{2}{|y|^3}\alpha_{0-}^{(0)}(|x|=0,|y|). \tag{C.28}$$

From eqs. (C.26)–(C.27) one sees that

$$\frac{\partial}{\partial|x|}\bar{\mathfrak{g}}^0 - \frac{\hat{c}_\beta}{|x|}\frac{\partial}{\partial\hat{c}_\beta}\bar{\mathfrak{g}}^0 = \mathrm{O}(|x|).$$

This and further similar relations for the other weight functions will be exploited to arrive at the final expressions of the tensors $T_{\alpha\beta\delta}^{\mathrm{A}}(x,y)$, eqs. (C.56)–(C.58) below.

C.1.2 The vector weight functions

In the Taylor expansion of a QED weight function $\bar{\mathfrak{g}}^{(k)}$, we denote by $\bar{\mathfrak{g}}^{(k,n)}$ the term of order $|x|^n$. For $\bar{\mathfrak{g}}^{(2)}$, one finds $\bar{\mathfrak{g}}^{(2,0)} = 0$ and

$$\bar{\mathfrak{g}}^{(2,1)} = -\frac{|x|\hat{c}_\beta}{12}\left[\frac{1}{|y|^5}\int_0^{|y|} d|u|\,|u|^5\,\sigma_2^{(1,2)}(u) + |y|\int_{|y|}^\infty \frac{d|u|}{|u|}\,\sigma_2^{(1,2)}(u)\right], \qquad (C.29)$$

and

$$\bar{\mathfrak{g}}^{(2,2)} = -\frac{x^2}{6}\left[\frac{1}{|y|^4}\int_0^{|y|} d|u|\,|u|^4\sigma_2^{(2,1)}(u) + \int_{|y|}^\infty d|u|\,\sigma_2^{(2,1)}(u)\right] \qquad (C.30)$$

$$-\frac{x^2}{30}(6\hat{c}_\beta^2 - 1)\left[\frac{1}{|y|^6}\int_0^{|y|} d|u|\,|u|^6\sigma_2^{(2,3)}(u) + |y|^2\int_{|y|}^\infty \frac{d|u|}{|u|^2}\,\sigma_2^{(2,3)}(u)\right],$$

$$\sigma_2^{(2,1)}(u) = \frac{-1}{48u^2}\sum_{n=0}^\infty (-1)^n\left\{|u|z_{n+1}\Big((2n+15)z_n' + 3|u|z_n''\Big)\right. \qquad (C.31)$$

$$\left. + z_n\Big((9+6n)z_{n+1} + |u|((2n-9)z_{n+1}' - 3|u|z_{n+1}'')\Big)\right\},$$

$$\sigma_2^{(2,3)}(u) = \frac{5}{96u^2}\sum_{n=0}^\infty (-1)^n\left\{|u|z_{n+1}\Big((3-2n)z_n' - 3|u|z_n''\Big)\right. \qquad (C.32)$$

$$\left. + z_n\Big((9+6n)z_{n+1} + |u|(3|u|z_{n+1}'' - (9+2n)z_{n+1}')\Big)\right\}.$$

Similarly for $\bar{\mathfrak{g}}^{(3)}$:

$$\bar{\mathfrak{g}}^{(3,0)} = \frac{1}{2}\left[\frac{1}{|y|^2}\int_0^{|y|} d|u|\,|u|^3\sigma_3^{(0,0)}(u) + \int_{|y|}^\infty d|u|\,|u|\,\sigma_3^{(0,0)}(u)\right] \qquad (C.33)$$

$$+\frac{4\hat{c}_\beta^2 - 1}{6}\left[\frac{1}{|y|^4}\int_0^{|y|} d|u|\,|u|^5\,\sigma_3^{(0,2)}(u) + y^2\int_{|y|}^\infty \frac{d|u|}{|u|}\,\sigma_3^{(0,2)}(u)\right],$$

$$\sigma_3^{(0,0)}(u) = \frac{1}{8|u|}\sum_{n=0}^\infty (-1)^n\left\{-|u|z_{n+1}z_n' + z_n((2n+3)z_{n+1} + |u|z_{n+1}')\right\}, \qquad (C.34)$$

$$\sigma_3^{(0,2)}(u) = -\frac{1}{8}\sigma_2^{(1,2)}(u) \qquad (C.35)$$

(with $\sigma_2^{(1,2)}(u)$ defined in eq. (C.16)), as well as

$$\bar{\mathfrak{g}}^{(3,1)} = \frac{|x|\hat{c}_\beta}{2}\left[\frac{1}{|y|^3}\int_0^{|y|} d|u|\,|u|^4\,\sigma_3^{(1,1)}(u) + |y|\int_{|y|}^\infty d|u|\,\sigma_3^{(1,1)}(u)\right] \qquad (C.36)$$

$$+\frac{|x|\hat{c}_\beta(2\hat{c}_\beta^2 - 1)}{2}\left[\frac{1}{|y|^5}\int_0^{|y|} d|u|\,|u|^6\,\sigma_3^{(1,3)}(u) + |y|^3\int_{|y|}^\infty \frac{d|u|}{|u|^2}\,\sigma_3^{(1,3)}(u)\right],$$

$$\sigma_3^{(1,1)}(u) = \frac{1}{48u^2}\sum_{n=0}^\infty (-1)^n\left\{|u|z_{n+1}((3-2n)z_n' + 3|u|z_n'')\right. \qquad (C.37)$$

$$\left. + z_n((6n+9)z_{n+1} - |u|((2n+9)z_{n+1}' + 3|u|z_{n+1}''))\right\},$$

$$\sigma_3^{(1,3)}(u) = -\frac{1}{5}\sigma_2^{(2,3)}(u) \qquad (C.38)$$

(with $\sigma_2^{(2,3)}(u)$ given in eq. (C.32)). These results imply, for the actually needed weight function $\bar{\mathfrak{g}}^{(1)}$,

$$\bar{\mathfrak{g}}^{(1,0)} = \frac{1}{2}\left[\frac{1}{|y|^2}\int_0^{|y|} d|u|\,|u|^3 \sigma_3^{(0,0)}(u) + \int_{|y|}^\infty d|u|\,|u|\,\sigma_3^{(0,0)}(u)\right] \tag{C.39}$$

$$+ \frac{1}{48}\left[\frac{1}{|y|^4}\int_0^{|y|} d|u|\,|u|^5 \sigma_2^{(1,2)}(u) + y^2 \int_{|y|}^\infty \frac{d|u|}{|u|}\,\sigma_2^{(1,2)}(u)\right],$$

$$\bar{\mathfrak{g}}^{(1,1)} = |x|\hat{c}_\beta\left[\frac{1}{2}\left(\frac{1}{|y|^3}\int_0^{|y|} d|u|\,|u|^4\,(\sigma_3^{(1,1)}(u) + \frac{1}{3}\sigma_2^{(2,1)}(u)) + |y|\int_{|y|}^\infty d|u|\,(\sigma_3^{(1,1)}(u) + \frac{1}{3}\sigma_2^{(2,1)}(u))\right)\right.$$

$$\left.+ \frac{1}{15}\left(\frac{1}{|y|^5}\int_0^{|y|} d|u|\,|u|^6\,\sigma_2^{(2,3)}(u) + |y|^3\int_{|y|}^\infty \frac{d|u|}{|u|^2}\,\sigma_2^{(2,3)}(u)\right)\right]. \tag{C.40}$$

C.1.3 The tensor weight functions

Similar to above, in the Laurent series of a QED weight function $\bar{\mathfrak{l}}^{(k)}$, we denote by $\bar{\mathfrak{l}}^{(k,n)}$ the term of order $|x|^n$. First, using the same notation for the auxiliary weight function $\bar{v}^{(1)}$, we find

$$\bar{v}^{(1,2)} = \frac{x^2(4\hat{c}_\beta^2 - 1)}{72}\left(\frac{1}{|y|^4}\int_0^{|y|} d|u|\,|u|^5\,\sigma_1^{(2,2)}(u) + y^2 \int_{|y|}^\infty \frac{d|u|}{|u|}\,\sigma_1^{(2,2)}(u)\right), \tag{C.41}$$

$$\bar{v}^{(1,3)} = \frac{|x|^3 C_1(\hat{c}_\beta)}{2}\left(\frac{1}{|y|^3}\int_0^{|y|} d|u|\,|u|^4\,\hat{t}_{\sigma_1}^{(3,1)}(u) + |y|\int_{|y|}^\infty d|u|\,\hat{t}_{\sigma_1}^{(3,1)}(u)\right) \tag{C.42}$$

$$+ \frac{|x|^3 C_3(\hat{c}_\beta)}{4}\left(\frac{1}{|y|^5}\int_0^{|y|} d|u|\,|u|^6\,\hat{u}_{\sigma_1}^{(3,1)}(u) + |y|^3\int_{|y|}^\infty \frac{d|u|}{|u|^2}\,\hat{u}_{\sigma_1}^{(3,1)}(u)\right).$$

We can now proceed to determining the first two non-trivial terms for weight function $\bar{\mathfrak{l}}^{(4)}$,

$$\bar{\mathfrak{l}}^{(4,1)} = \frac{|x|\,\hat{c}_\beta}{9}\left[\frac{1}{|y|^3}\int_0^{|y|} d|u|\,|u|^5\,\sigma_4^{(1,2)}(u) + |y|^3\int_{|y|}^\infty \frac{d|u|}{|u|}\,\sigma_4^{(1,2)}(u)\right], \tag{C.43}$$

$$\bar{\mathfrak{l}}^{(4,2)} = \frac{-x^2}{3}\left(\frac{1}{y^2}\int_0^{|y|} d|u|\,|u|^4\sigma_4^{(2,1)}(u) + y^2\int_{|y|}^\infty d|u|\,\sigma_4^{(2,1)}(u)\right) \tag{C.44}$$

$$- \frac{x^2(6\hat{c}_\beta^2 - 1)}{15}\left(\frac{1}{|y|^4}\int_0^{|y|} d|u|\,|u|^6\,\sigma_4^{(2,3)}(u) + |y|^4\int_{|y|}^\infty \frac{d|u|}{|u|^2}\sigma_4^{(2,3)}(u)\right),$$

$$\sigma_4^{(2,1)}(u) = -4\hat{t}_{\sigma_1}^{(3,1)}(u), \tag{C.45}$$

$$\sigma_4^{(2,3)}(u) = -\frac{5}{24}\sigma_5^{(1,3)}(u). \tag{C.46}$$

Next come the first two terms for weight function $\bar{\mathfrak{l}}^{(2)}$,

$$\bar{\mathfrak{l}}^{(2,0)} = \frac{1}{18}\left(\frac{1}{|y|^6}\int_0^{|y|} d|u|\,|u|^5\,\sigma_5^{(0,2)}(u) + \int_{|y|}^\infty \frac{d|u|}{|u|}\,\sigma_5^{(0,2)}(u)\right), \tag{C.47}$$

$$\bar{\mathfrak{l}}^{(2,1)} = \frac{|x|\hat{c}_\beta}{24}\left(\frac{1}{|y|^7}\int_0^{|y|} d|u|\,|u|^6\sigma_5^{(1,3)}(u) + |y|\int_{|y|}^\infty \frac{d|u|}{|u|^2}\sigma_5^{(1,3)}(u)\right). \tag{C.48}$$

Now from eq. (4.40), we obtain $\bar{\mathfrak{l}}^{(3)}$ via

$$\bar{\mathfrak{l}}^{(3)} = \frac{1}{2x^2y^2}\bar{\mathfrak{l}}^{(4)} - \frac{|y|}{|x|}\,\hat{c}_\beta\,\bar{\mathfrak{l}}^{(2)}, \tag{C.49}$$

so that the O(1/|x|) contribution cancels out,

$$\overline{\mathfrak{l}}^{(3,-1)} = \frac{1}{2x^2 y^2}\overline{\mathfrak{l}}^{(4,1)} - \frac{|y|}{|x|}\,\hat{c}_\beta\,\overline{\mathfrak{l}}^{(2,0)} = 0. \tag{C.50}$$

The leading contribution is finite,

$$\overline{\mathfrak{l}}^{(3,0)} = \frac{1}{2x^2 y^2}\overline{\mathfrak{l}}^{(4,2)} - \frac{|y|}{|x|}\,\hat{c}_\beta\,\overline{\mathfrak{l}}^{(2,1)} \tag{C.51}$$

$$= \frac{-1}{6}\Bigg[\frac{1}{|y|^4}\int_0^{|y|} d|u|\,|u|^4 \sigma_4^{(2,1)}(u) + \int_{|y|}^\infty d|u|\,\sigma_4^{(2,1)}(u) \tag{C.52}$$

$$+ \frac{1}{24}\Bigg(\frac{1}{|y|^6}\int_0^{|y|} d|u|\,|u|^6 \sigma_5^{(1,3)}(u) + y^2 \int_{|y|}^\infty \frac{d|u|}{|u|^2}\sigma_5^{(1,3)}(u)\Bigg)\Bigg].$$

Similarly, one finds that the O(1/x^2) contribution to (see eq. (4.41))

$$\overline{\mathfrak{l}}^{(1)} = \frac{4}{3x^4}\left(\overline{v}_1 - x^2 y^2\left(\hat{c}_\beta^2 - \frac{1}{4}\right)\overline{\mathfrak{l}}^{(2)} - \frac{3}{2}x^3 y \hat{c}_\beta\,\overline{\mathfrak{l}}^{(3)}\right) \tag{C.53}$$

vanishes,

$$\overline{\mathfrak{l}}^{(1,-2)} = 0. \tag{C.54}$$

For the contribution of order $1/|x|$, it is useful to decompose the expression in the basis of the $C_m(\hat{c}_\beta)$, calculating the coefficient $\overline{\mathfrak{l}}^{(1,-1,m)}$ of $C_m(\hat{c}_\beta)$ using $\overline{\mathfrak{l}}^{(1,-1,m)} = \frac{2}{\pi}\int_0^\pi d\beta\,\sin^2\beta\,C_m(\hat{c}_\beta)\overline{\mathfrak{l}}^{(1,-1)}$. Before forming the linear combination (C.53), we find that there are $m = 1$ and $m = 3$ components, but they cancel in the linear combination, $\overline{\mathfrak{l}}^{(1,-1,1)} = \overline{\mathfrak{l}}^{(1,-1,3)} = 0$, so that

$$\overline{\mathfrak{l}}^{(1,-1)} = 0. \tag{C.55}$$

Thus $\overline{\mathfrak{l}}^{(1)}$ is finite in the limit $|x| \to 0$.

C.1.4 The limit $|x| \to 0$ for the tensors $T^{\mathbf{A}}_{\alpha\beta\delta}(x,y)$

With the help of the chain rules for the tensors $T^{\mathbf{A}}_{\alpha\beta\delta}(x,y)$ given in appendix A, we find the following, finite expressions for these three tensors at $|x| \to 0$,

$$T^{\mathrm{I}}_{\alpha\beta\delta}(0,y) = (\delta_{\alpha\delta}\hat{y}_\beta + \delta_{\beta\delta}\hat{y}_\alpha)\left(\frac{\partial\overline{\mathfrak{g}}^{(1)}}{|x|\partial\hat{c}_\beta}\right) + \delta_{\alpha\beta}y_\delta\left(\frac{\partial^2\overline{\mathfrak{g}}^{(2)}}{\partial|x|^2} - \hat{c}_\beta^2\frac{\partial^2\overline{\mathfrak{g}}^{(2)}}{x^2\partial\hat{c}_\beta^2}\right) \tag{C.56}$$

$$+ \delta_{\alpha\delta}\hat{y}_\beta\left(\frac{\partial\overline{\mathfrak{g}}^{(1)}}{\partial|y|}\right) + (\delta_{\beta\delta}\hat{y}_\alpha + \delta_{\alpha\beta}\hat{y}_\delta)\left(\frac{\partial\overline{\mathfrak{g}}^{(2)}}{|x|\partial\hat{c}_\beta}\right)$$

$$+ \hat{y}_\alpha\hat{y}_\beta\hat{y}_\delta\frac{1}{|x|}\left(\frac{|y|}{|x|}\frac{\partial}{\partial\hat{c}_\beta} + |y|\frac{\partial}{\partial|y|} - 1\right)\frac{\partial\overline{\mathfrak{g}}^{(2)}}{\partial\hat{c}_\beta}\,,$$

$$\frac{1}{m}T^{\mathrm{II}}_{\alpha\beta\delta}(0,y) = \left(\delta_{\alpha\beta}y_\delta + \delta_{\alpha\delta}y_\beta - \frac{y_\alpha}{2}\delta_{\beta\delta}\right)\overline{\mathfrak{l}}^{(3)} + \left(y_\beta y_\delta - \frac{y^2}{4}\delta_{\beta\delta}\right)\hat{y}_\alpha\left(\frac{\partial\overline{\mathfrak{l}}^{(2)}}{|x|\partial\hat{c}_\beta}\right) \tag{C.57}$$

$$+ \frac{\delta_{\beta\delta}}{4}\hat{y}_\alpha\left(\frac{\partial\overline{\mathfrak{g}}^{(0)}}{|x|\partial\hat{c}_\beta}\right),$$

$$\frac{1}{m}T^{\mathrm{III}}_{\alpha\beta\delta}(0,y) = \left(\delta_{\beta\alpha}y_\delta + \delta_{\beta\delta}y_\alpha - \frac{y_\beta}{2}\delta_{\alpha\delta}\right)\left(\overline{\mathfrak{l}}^{(2)} + \overline{\mathfrak{l}}^{(3)}\right) \tag{C.58}$$

$$+ \left(y_\alpha y_\delta - \frac{y^2}{4}\delta_{\alpha\delta}\right)\hat{y}_\beta\left(\frac{\partial\overline{\mathfrak{l}}^{(2)}}{|x|\partial\hat{c}_\beta} + \frac{\partial\overline{\mathfrak{l}}^{(2)}}{\partial|y|}\right) + \frac{\delta_{\alpha\delta}}{4}\hat{y}_\beta\left(\frac{\partial\overline{\mathfrak{g}}^{(0)}}{|x|\partial\hat{c}_\beta} + \frac{\partial\overline{\mathfrak{g}}^{(0)}}{\partial|y|}\right).$$

The right-hand side should be evaluated in the limit $|x| \to 0$. Using the results respectively in eqs. (C.29), (C.40), (C.30), (C.39), (C.51), (C.48), (C.27) and (C.47), (C.51), (C.48), (C.27), (C.28) the evaluation of the three tensors is easily performed. We remark that the $\hat{c}_\beta$ dependence cancels everywhere, in particular in the second term of eq. (C.56), which contains an explicit factor of $\hat{c}_\beta^2$.

C.2 The regime of small $|y|$

In the following, we give without further comment the relevant expressions for the weight functions in the limit of $|y| \to 0$.

C.2.1 The scalar weight function

$$\left. \frac{\partial \bar{\mathfrak{g}}^{(0)}}{\partial |x|} \right|_{y=0} = \frac{1}{\pi} \int_0^\infty d|u|\,|u| \int_0^\pi d\phi_1\,\hat{s}_1^2\,\frac{\partial \sigma_0}{\partial |x|}(|x|,\hat{c}_1,|u|) = \frac{\partial \alpha_{0+}^{(0)}(|x|,0)}{\partial |x|}, \tag{C.59}$$

$$\left. \frac{\partial \bar{\mathfrak{g}}^{(0)}}{\partial \hat{c}_\beta} \right|_{y=0} = \frac{|y|}{\pi} \int_0^\infty d|u| \int_0^\pi d\phi_1\,\hat{s}_1^2\,C_1(\hat{c}_1)\,\sigma_0(|x|,\hat{c}_1,|u|) = 2|y|\alpha_{1+}^{(0)}(|x|,0), \tag{C.60}$$

$$\left. \frac{\partial \bar{\mathfrak{g}}^{(0)}}{\partial |y|} \right|_{y=0} = C_1(\hat{c}_\beta)\,\alpha_{1+}^{(0)}(|x|,0). \tag{C.61}$$

C.2.2 The vector weight functions

$$\left. \bar{\mathfrak{g}}^{(1)} \right|_{y=0} = \frac{1}{2\pi} \int_0^\infty d|u|\,|u| \int_0^\pi d\phi_1\,\hat{s}_1^2\,\sigma_3(|x|,\hat{c}_1,|u|) = \alpha_{0+}^{(3)}(|x|,0), \tag{C.62}$$

$$\left. \bar{\mathfrak{g}}^{(2)} \right|_{y=0} = \frac{-1}{3\pi} \int_0^\infty d|u| \int_0^\pi d\phi_1\,\hat{s}_1^2\,\sigma_2(|x|,\hat{c}_1,|u|) = 2\,\beta_{1+}^{(2)}(|x|,0), \tag{C.63}$$

$$\left. \frac{\partial \bar{\mathfrak{g}}^{(1)}}{\partial |y|} \right|_{y=0} = C_1(\hat{c}_\beta) \left[-\frac{1}{2|x|} \bar{\mathfrak{g}}^{(2)} \Big|_{y=0} + \frac{1}{2\pi} \int_0^\infty d|u| \int_0^\pi d\phi_1\,\hat{s}_1^2\,\hat{c}_1\,\sigma_3(|x|,\hat{c}_1,|u|) \right] \tag{C.64}$$

$$= C_1(\hat{c}_\beta) \left[-\frac{\beta_{1+}^{(2)}(|x|,0)}{|x|} + \alpha_{1+}^{(3)}(|x|,0) \right]. \tag{C.65}$$

C.2.3 The tensor weight functions

$$\left. \bar{\mathfrak{l}}^{(1)} \right|_{y=0} = \frac{4}{3\pi|x|^4} \int_0^\infty d|u|\,|u| \int_0^\pi d\phi_1\,\hat{s}_1^2\,\sigma_1(|x|,\hat{c}_1,|u|) = \frac{4}{3|x|^4}\alpha_{0+}^{(1)}(|x|,0), \tag{C.66}$$

$$\left. \bar{\mathfrak{l}}^{(3)} \right|_{y=0} = \frac{-1}{3\pi\,x^2} \int_0^\infty d|u| \int_0^\pi d\phi_1\,\hat{s}_1^2\,\sigma_4(|x|,\hat{c}_1,|u|) = \frac{\beta_{1+}^{(4)}(|x|,0)}{x^2}, \tag{C.67}$$

$$\left. \frac{\partial \bar{\mathfrak{l}}^{(1)}}{\partial |y|} \right|_{y=0} = \frac{C_1(\hat{c}_\beta)}{|x|} \left[\frac{4}{3\pi|x|^3} \int_0^\infty d|u| \int_0^\pi d\phi_1\,\hat{s}_1^2\,\hat{c}_1\,\sigma_1(|x|,\hat{c}_1,|u|) - \bar{\mathfrak{l}}^{(3)} \Big|_{y=0} \right] \tag{C.68}$$

$$= C_1(\hat{c}_\beta) \left[\frac{4}{3|x|^4}\alpha_{1+}^{(1)}(|x|,0) - \frac{1}{|x|^3}\beta_{1+}^{(4)}(|x|,0) \right]. \tag{C.69}$$

C.2.4 The limit $|y| \to 0$ for the tensors $T^{\mathrm{A}}_{\alpha\beta\delta}(x, y)$

We find the finite result

$$T^{\mathrm{I}}_{\alpha\beta\delta}(x, 0) = \left(\delta_{\alpha\delta}\hat{x}_\beta + \delta_{\beta\delta}\hat{x}_\alpha + \delta_{\alpha\beta}\hat{x}_\delta - \hat{x}_\alpha\hat{x}_\beta\hat{x}_\delta\right)\left(\frac{\partial\bar{\mathfrak{g}}^{(1)}}{\partial|x|}\right) + \hat{x}_\alpha\hat{x}_\beta x_\delta\left(\frac{\partial^2\bar{\mathfrak{g}}^{(1)}}{\partial|x|^2}\right) \quad \text{(C.70)}$$

$$+ \left(\delta_{\alpha\delta}\hat{x}_\beta + \delta_{\alpha\beta}\hat{x}_\delta - \hat{x}_\alpha\hat{x}_\beta\hat{x}_\delta\right)\left(\frac{\partial\bar{\mathfrak{g}}^{(1)}}{|y|\partial\hat{c}_\beta}\right) + \hat{x}_\alpha\hat{x}_\beta x_\delta\left(\frac{\partial^2\bar{\mathfrak{g}}^{(1)}}{|y|\partial|x|\partial\hat{c}_\beta}\right)$$

$$+ \delta_{\beta\delta}\,\hat{x}_\alpha\left(\frac{\partial\bar{\mathfrak{g}}^{(2)}}{\partial|x|}\right),$$

$$\frac{1}{m}T^{\mathrm{II}}_{\alpha\beta\delta}(x, 0) = \frac{\delta_{\beta\delta}\,\hat{x}_\alpha}{4}\left(\frac{\partial\bar{\mathfrak{g}}^{(0)}}{\partial|x|}\right) \quad \text{(C.71)}$$

$$+ \left(\delta_{\alpha\beta}x_\delta + x_\beta\delta_{\alpha\delta} - \frac{x_\alpha}{2}\delta_{\beta\delta}\right)\bar{\mathfrak{l}}^{(1)} + \left(x_\beta x_\delta - \frac{x^2}{4}\delta_{\beta\delta}\right)\hat{x}_\alpha\left(\frac{\partial\bar{\mathfrak{l}}^{(1)}}{\partial|x|}\right),$$

$$\frac{1}{m}T^{\mathrm{III}}_{\alpha\beta\delta}(x, 0) = \frac{\delta_{\alpha\delta}}{4}\,\hat{x}_\beta\left(\frac{\partial\bar{\mathfrak{g}}^{(0)}}{\partial|x|} + \frac{\partial\bar{\mathfrak{g}}^{(0)}}{|y|\partial\hat{c}_\beta}\right) \quad \text{(C.72)}$$

$$+ \left(\delta_{\alpha\beta}x_\delta + x_\alpha\delta_{\beta\delta} - \frac{x_\beta}{2}\delta_{\alpha\delta}\right)\left(\bar{\mathfrak{l}}^{(1)} + \bar{\mathfrak{l}}^{(3)}\right)$$

$$+ \left(x_\alpha x_\delta - \frac{x^2}{4}\delta_{\alpha\delta}\right)\hat{x}_\beta\left(\frac{\partial\bar{\mathfrak{l}}^{(1)}}{\partial|x|} + \frac{\partial\bar{\mathfrak{l}}^{(1)}}{|y|\partial\hat{c}_\beta}\right),$$

where the right-hand side should be evaluated in the limit $|y| \to 0$. Using the results above in this subsection, this evaluation is easily performed.

D Contribution of the scalar function $S(x, y)$ to the QED kernel: large-$|y|$ asymptotics

The scalar weight function is given by

$$S(x, y) = \int_{u, \text{IR−reg.}} G_0(y - u)s(x, u), \quad \text{(D.1)}$$

with $s(x, u) \sim |u|^{-2}$ at large $|u|$, see eq. (3.51). Thus the y-dependence of $S(x, y)$ corresponds to the static potential induced (in four space dimensions) by a charge distribution given by $s(x, u)$, x playing the role of a fixed position vector. The function $S(x, y)$ itself is logarithmically infrared-divergent, however $-\frac{\partial}{\partial|y|}S(x, y)$, which corresponds to the radial electric field, is finite. The electric field generated by a charge distribution falling like $|u|^{-2}$ is of order $|y|^{-1}$, in any number of dimensions greater than two. This is easiest obtained by applying Gauss' law to a sphere of radius $|y|$ and one finds

$$-\frac{\partial}{\partial|y|}S(x, y) \stackrel{|y|\to\infty}{=} \frac{1}{384\pi^2 m^2|y|}, \quad \text{(D.2)}$$

independent of x, which is kept fixed. Although we have obtained this from the region of large u, it is clear that the integral over $|u|$ from 0 to a finite $|u|_{\max}$ cannot generate an electric field falling off as slowly as $|y|^{-1}$; instead it generates an $\mathrm{O}(|y|^{-3})$ field.

We now proceed to determining the leading behavior of $\frac{\partial}{\partial|x|}S(x,y)$ and $\frac{\partial}{\partial\hat{c}_\beta}S(x,y)$ at large $|y|$. For this purpose it is useful to write (similarly to eq. (3.60))

$$s(x,u) - s(0,u) = \sum_{n\geq 0}(-1)^n z_n(u^2)\Big[z_n((x-u)^2)(-1)^n\frac{C_n(\hat{u}\cdot\widehat{x-u})}{n+1} - z_n(u^2)\Big], \quad \text{(D.3)}$$

and to realize that the expression inside the square bracket has the asymptotic large-$|u|$ behavior $\frac{\hat{u}\cdot x}{4\pi^2 m\,(n+1)u^2}$. The series is then still absolutely convergent and one finds

$$s(x,u) - s(0,u) \overset{|u|\to\infty}{=} \frac{1}{192\pi^2 m^2|u|^3}\,x\cdot\hat{u}. \quad \text{(D.4)}$$

Thus we get, using eq. (D.1) and the multipole expansion (3.16)–(3.17) of the photon propagator $G_0(y-u)$,

$$\frac{\partial\bar{\mathfrak{g}}^{(0)}}{\partial|x|} = \frac{\hat{c}_\beta}{768\pi^2 m^2|y|}, \quad \text{(D.5)}$$

$$\frac{\partial\bar{\mathfrak{g}}^{(0)}}{\partial\hat{c}_\beta} = \frac{|x|}{768\pi^2 m^2|y|}. \quad \text{(D.6)}$$

Therefore the scalar contribution to the tensors $T^{\text{II}}_{\alpha\beta\delta}(x,y)$ and $T^{\text{III}}_{\alpha\beta\delta}(x,y)$ is respectively

$$\frac{m}{4}\delta_{\beta\delta}\partial^{(x)}_\alpha S(x,y) \overset{|y|\to\infty}{=} \frac{\delta_{\beta\delta}\,\hat{y}_\alpha}{3072\pi^2 m|y|}\left(1 + \text{O}\left((m|y|)^{-1}\right)\right), \quad \text{(D.7)}$$

$$\frac{m}{4}\delta_{\alpha\delta}(\partial^{(x)}_\beta + \partial^{(y)}_\beta)S(x,y) \overset{|y|\to\infty}{=} \frac{-\delta_{\alpha\delta}\,\hat{y}_\beta}{3072\pi^2 m|y|}\left(1 + \text{O}\left((m|y|)^{-1}\right)\right). \quad \text{(D.8)}$$

We note that this result is consistent with the scalar contribution to the rank-three tensors satisfying eq. (2.50).

E   Our version of the kernel code

Our implementation of the QED kernel `KQED` can be found in [96], it is licensed under version 3 of the GNU public license [97]. The library is built using GNU automake and is intended to be linked as a static library. An example for integrating the lepton loop using `hcubature` [80] can be found in the companion code `KAMU` [98], which illustrates how to link to `KQED` and initialize it.

`KQED` includes a look-up-table of the Chebyshev coefficients as a file in single precision, which is entirely read upon initialization (and the crc32c of it is computed for correctness), although all computations are performed in double precision. The code can be compiled with `OpenMP` to use multi-threading whereby the kernel at coordinates x and y can be called safely within a parallel region. The code makes heavy use of AVX/FMA intrinsics to speed up the calculation of the various terms $S(x,y), V_\delta(x,y)$, and $T_{\beta\delta}(x,y)$, particularly in the Clenshaw recurrences (eqs. (6.2), (6.3) and (6.4)). Where possible, loop-fusion is performed on all necessary weight-function derivatives (see section 6), as well as an internal re-mapping of neighboring elements on the grid to SIMD lanes.

The code compiles a binary which performs some simple unit tests and provides a stress-test for the time taken to compute a fixed number of expensive kernel calls. A script is also included in the package to regression-test the kernel against various x and y, and to check the multi-threading equivalence. Heavily loop-unrolled and optimised versions of the subtracted kernels (with 4 arbitrary Λ terms eq. (8.4)) are available as this was one of the most costly parts of our calculation in [36, 51] and [37].

Open Access. This article is distributed under the terms of the Creative Commons Attribution License ([CC-BY 4.0](#)), which permits any use, distribution and reproduction in any medium, provided the original author(s) and source are credited. SCOAP^3 supports the goals of the International Year of Basic Sciences for Sustainable Development.

References

[1] Muon g-2 collaboration, *Measurement of the Positive Muon Anomalous Magnetic Moment to 0.46 ppm*, *Phys. Rev. Lett.* **126** (2021) 141801 [arXiv:2104.03281] [InSPIRE].

[2] Muon g-2 collaboration, *Final Report of the Muon E821 Anomalous Magnetic Moment Measurement at BNL*, *Phys. Rev. D* **73** (2006) 072003 [hep-ex/0602035] [InSPIRE].

[3] T. Aoyama et al., *The anomalous magnetic moment of the muon in the Standard Model*, *Phys. Rept.* **887** (2020) 1 [arXiv:2006.04822] [InSPIRE].

[4] T. Aoyama, M. Hayakawa, T. Kinoshita and M. Nio, *Complete Tenth-Order QED Contribution to the Muon g-2*, *Phys. Rev. Lett.* **109** (2012) 111808 [arXiv:1205.5370] [InSPIRE].

[5] T. Aoyama, T. Kinoshita and M. Nio, *Theory of the Anomalous Magnetic Moment of the Electron*, *Atoms* **7** (2019) 28 [InSPIRE].

[6] A. Czarnecki, W.J. Marciano and A. Vainshtein, *Refinements in electroweak contributions to the muon anomalous magnetic moment*, *Phys. Rev. D* **67** (2003) 073006 [*Erratum ibid.* **73** (2006) 119901] [hep-ph/0212229] [InSPIRE].

[7] C. Gnendiger, D. Stöckinger and H. Stöckinger-Kim, *The electroweak contributions to $(g-2)_\mu$ after the Higgs boson mass measurement*, *Phys. Rev. D* **88** (2013) 053005 [arXiv:1306.5546] [InSPIRE].

[8] M. Davier, A. Hoecker, B. Malaescu and Z. Zhang, *Reevaluation of the hadronic vacuum polarisation contributions to the Standard Model predictions of the muon $g-2$ and $\alpha(m_Z^2)$ using newest hadronic cross-section data*, *Eur. Phys. J. C* **77** (2017) 827 [arXiv:1706.09436] [InSPIRE].

[9] A. Keshavarzi, D. Nomura and T. Teubner, *Muon $g-2$ and $\alpha(M_Z^2)$: a new data-based analysis*, *Phys. Rev. D* **97** (2018) 114025 [arXiv:1802.02995] [InSPIRE].

[10] G. Colangelo, M. Hoferichter and P. Stoffer, *Two-pion contribution to hadronic vacuum polarization*, *JHEP* **02** (2019) 006 [arXiv:1810.00007] [InSPIRE].

[11] M. Hoferichter, B.-L. Hoid and B. Kubis, *Three-pion contribution to hadronic vacuum polarization*, *JHEP* **08** (2019) 137 [arXiv:1907.01556] [InSPIRE].

[12] M. Davier, A. Hoecker, B. Malaescu and Z. Zhang, *A new evaluation of the hadronic vacuum polarisation contributions to the muon anomalous magnetic moment and to $\boldsymbol{\alpha(m_Z^2)}$*, *Eur. Phys. J. C* **80** (2020) 241 [*Erratum ibid.* **80** (2020) 410] [arXiv:1908.00921] [InSPIRE].

[13] A. Keshavarzi, D. Nomura and T. Teubner, *g − 2 of charged leptons, $\alpha(M_Z^2)$, and the hyperfine splitting of muonium*, *Phys. Rev. D* **101** (2020) 014029 [arXiv:1911.00367] [INSPIRE].

[14] A. Kurz, T. Liu, P. Marquard and M. Steinhauser, *Hadronic contribution to the muon anomalous magnetic moment to next-to-next-to-leading order*, *Phys. Lett. B* **734** (2014) 144 [arXiv:1403.6400] [INSPIRE].

[15] K. Melnikov and A. Vainshtein, *Hadronic light-by-light scattering contribution to the muon anomalous magnetic moment revisited*, *Phys. Rev. D* **70** (2004) 113006 [hep-ph/0312226] [INSPIRE].

[16] P. Masjuan and P. Sanchez-Puertas, *Pseudoscalar-pole contribution to the $(g_\mu − 2)$: a rational approach*, *Phys. Rev. D* **95** (2017) 054026 [arXiv:1701.05829] [INSPIRE].

[17] G. Colangelo, M. Hoferichter, M. Procura and P. Stoffer, *Dispersion relation for hadronic light-by-light scattering: two-pion contributions*, *JHEP* **04** (2017) 161 [arXiv:1702.07347] [INSPIRE].

[18] M. Hoferichter et al., *Dispersion relation for hadronic light-by-light scattering: pion pole*, *JHEP* **10** (2018) 141 [arXiv:1808.04823] [INSPIRE].

[19] A. Gérardin, H.B. Meyer and A. Nyffeler, *Lattice calculation of the pion transition form factor with $N_f = 2 + 1$ Wilson quarks*, *Phys. Rev. D* **100** (2019) 034520 [arXiv:1903.09471] [INSPIRE].

[20] J. Bijnens, N. Hermansson-Truedsson and A. Rodríguez-Sánchez, *Short-distance constraints for the HLbL contribution to the muon anomalous magnetic moment*, *Phys. Lett. B* **798** (2019) 134994 [arXiv:1908.03331] [INSPIRE].

[21] G. Colangelo et al., *Longitudinal short-distance constraints for the hadronic light-by-light contribution to $(g − 2)_\mu$ with large-N_c Regge models*, *JHEP* **03** (2020) 101 [arXiv:1910.13432] [INSPIRE].

[22] T. Blum et al., *Hadronic Light-by-Light Scattering Contribution to the Muon Anomalous Magnetic Moment from Lattice QCD*, *Phys. Rev. Lett.* **124** (2020) 132002 [arXiv:1911.08123] [INSPIRE].

[23] G. Colangelo et al., *Remarks on higher-order hadronic corrections to the muon g−2*, *Phys. Lett. B* **735** (2014) 90 [arXiv:1403.7512] [INSPIRE].

[24] P. Athron et al., *New physics explanations of a_μ in light of the FNAL muon g − 2 measurement*, *JHEP* **09** (2021) 080 [arXiv:2104.03691] [INSPIRE].

[25] J.S. Schwinger, *On Quantum electrodynamics and the magnetic moment of the electron*, *Phys. Rev.* **73** (1948) 416 [INSPIRE].

[26] S. Borsanyi et al., *Leading hadronic contribution to the muon magnetic moment from lattice QCD*, *Nature* **593** (2021) 51 [arXiv:2002.12347] [INSPIRE].

[27] MUON G-2 collaboration, *Muon (g-2) Technical Design Report*, arXiv:1501.06858 [INSPIRE].

[28] M. Abe et al., *A New Approach for Measuring the Muon Anomalous Magnetic Moment and Electric Dipole Moment*, *PTEP* **2019** (2019) 053C02 [arXiv:1901.03047] [INSPIRE].

[29] M. Aiba et al., *Science Case for the new High-Intensity Muon Beams HIMB at PSI*, arXiv:2111.05788 [INSPIRE].

[30] V. Pauk and M. Vanderhaeghen, *Single meson contributions to the muon's anomalous magnetic moment*, *Eur. Phys. J. C* **74** (2014) 3008 [arXiv:1401.0832] [INSPIRE].

[31] I. Danilkin and M. Vanderhaeghen, *Light-by-light scattering sum rules in light of new data*, *Phys. Rev. D* **95** (2017) 014019 [arXiv:1611.04646] [INSPIRE].

[32] F. Jegerlehner, *The Anomalous Magnetic Moment of the Muon*, *Springer Tracts Mod. Phys.* **274** (2017) 1 [INSPIRE].

[33] M. Knecht, S. Narison, A. Rabemananjara and D. Rabetiarivony, *Scalar meson contributions to a_μ from hadronic light-by-light scattering*, *Phys. Lett. B* **787** (2018) 111 [arXiv:1808.03848] [INSPIRE].

[34] G. Eichmann, C.S. Fischer and R. Williams, *Kaon-box contribution to the anomalous magnetic moment of the muon*, *Phys. Rev. D* **101** (2020) 054015 [arXiv:1910.06795] [INSPIRE].

[35] P. Roig and P. Sanchez-Puertas, *Axial-vector exchange contribution to the hadronic light-by-light piece of the muon anomalous magnetic moment*, *Phys. Rev. D* **101** (2020) 074019 [arXiv:1910.02881] [INSPIRE].

[36] E.-H. Chao et al., *Hadronic light-by-light contribution to $(g-2)_\mu$ from lattice QCD: a complete calculation*, *Eur. Phys. J. C* **81** (2021) 651 [arXiv:2104.02632] [INSPIRE].

[37] E.-H. Chao et al., *The charm-quark contribution to light-by-light scattering in the muon $(g-2)$ from lattice QCD*, *Eur. Phys. J. C* **82** (2022) 664 [arXiv:2204.08844] [INSPIRE].

[38] N. Asmussen et al., *Hadronic Light-by-Light Contribution to the Muon Anomalous Magnetic Moment on the Lattice*, talk by N. Asmussen at the Spring Conference of the Deutsche Physikalische Gesellschaft, Heidelberg, 23–27 March, 2015.

[39] J. Green et al., *Direct calculation of hadronic light-by-light scattering*, *PoS* **LATTICE2015** (2016) 109 [arXiv:1510.08384] [INSPIRE].

[40] N. Asmussen, J. Green, H.B. Meyer and A. Nyffeler, *Position-space approach to hadronic light-by-light scattering in the muon $g-2$ on the lattice*, *PoS* **LATTICE2016** (2016) 164 [arXiv:1609.08454] [INSPIRE].

[41] N. Asmussen, A. Gérardin, H.B. Meyer and A. Nyffeler, *Exploratory studies for the position-space approach to hadronic light-by-light scattering in the muon $g-2$*, *EPJ Web Conf.* **175** (2018) 06023 [arXiv:1711.02466] [INSPIRE].

[42] N. Asmussen et al., *Hadronic light-by-light scattering contribution to the muon $g-2$ on the lattice*, *EPJ Web Conf.* **179** (2018) 01017 [arXiv:1801.04238] [INSPIRE].

[43] N. Asmussen et al., *Developments in the position-space approach to the HLbL contribution to the muon $g-2$ on the lattice*, *PoS* **LATTICE2019** (2019) 195 [arXiv:1911.05573] [INSPIRE].

[44] M. Hayakawa, T. Blum, T. Izubuchi and N. Yamada, *Hadronic light-by-light scattering contribution to the muon g-2 from lattice QCD: Methodology*, *PoS* **LAT2005** (2006) 353 [hep-lat/0509016] [INSPIRE].

[45] S. Chowdhury et al., *Calculating the light by light contribution to the muon anomalous magnetic moment using lattice QED*, *PoS* **LATTICE2008** (2008) 251 [INSPIRE].

[46] T. Blum, S. Chowdhury, M. Hayakawa and T. Izubuchi, *Hadronic light-by-light scattering contribution to the muon anomalous magnetic moment from lattice QCD*, *Phys. Rev. Lett.* **114** (2015) 012001 [arXiv:1407.2923] [INSPIRE].

[47] T. Blum et al., *Lattice Calculation of Hadronic Light-by-Light Contribution to the Muon Anomalous Magnetic Moment*, *Phys. Rev. D* **93** (2016) 014503 [`arXiv:1510.07100`] [inSPIRE].

[48] T. Blum et al., *Connected and Leading Disconnected Hadronic Light-by-Light Contribution to the Muon Anomalous Magnetic Moment with a Physical Pion Mass*, *Phys. Rev. Lett.* **118** (2017) 022005 [`arXiv:1610.04603`] [inSPIRE].

[49] T. Blum et al., *Using infinite volume, continuum QED and lattice QCD for the hadronic light-by-light contribution to the muon anomalous magnetic moment*, *Phys. Rev. D* **96** (2017) 034515 [`arXiv:1705.01067`] [inSPIRE].

[50] A. Gérardin, H.B. Meyer and A. Nyffeler, *Lattice calculation of the pion transition form factor $\pi^0 \to \gamma^*\gamma^*$*, *Phys. Rev. D* **94** (2016) 074507 [`arXiv:1607.08174`] [inSPIRE].

[51] E.-H. Chao et al., *Hadronic light-by-light contribution to $(g-2)_\mu$ from lattice QCD with SU(3) flavor symmetry*, *Eur. Phys. J. C* **80** (2020) 869 [`arXiv:2006.16224`] [inSPIRE].

[52] J. Green et al., *Lattice QCD calculation of hadronic light-by-light scattering*, *Phys. Rev. Lett.* **115** (2015) 222003 [`arXiv:1507.01577`] [inSPIRE].

[53] A. Gérardin et al., *Hadronic light-by-light scattering amplitudes from lattice QCD versus dispersive sum rules*, *Phys. Rev. D* **98** (2018) 074501 [`arXiv:1712.00421`] [inSPIRE].

[54] M. Knecht and A. Nyffeler, *Hadronic light by light corrections to the muon g-2: The Pion pole contribution*, *Phys. Rev. D* **65** (2002) 073034 [`hep-ph/0111058`] [inSPIRE].

[55] G.F. Sterman, *An Introduction to Quantum Field Theory*, Cambridge University Press (1993).

[56] J. Aldins, T. Kinoshita, S.J. Brodsky and A.J. Dufner, *Photon-photon scattering contribution to the sixth order magnetic moments of the muon and electron*, *Phys. Rev. D* **1** (1970) 2378 [inSPIRE].

[57] E. Mendels, *Feynman Diagrams Without Feynman Parameters*, *Nuovo Cim. A* **45** (1978) 87 [inSPIRE].

[58] S. Groote, J.G. Korner and A.A. Pivovarov, *On the evaluation of a certain class of Feynman diagrams in x-space: Sunrise-type topologies at any loop order*, *Annals Phys.* **322** (2007) 2374 [`hep-ph/0506286`] [inSPIRE].

[59] S. Groote and J.G. Körner, *Coordinate space calculation of two- and three-loop sunrise-type diagrams, elliptic functions and truncated Bessel integral identities*, *Nucl. Phys. B* **938** (2019) 416 [`arXiv:1804.10570`] [inSPIRE].

[60] K. Johnson, M. Baker and R. Willey, *Selfenergy of the electron*, *Phys. Rev.* **136** (1964) B1111 [inSPIRE].

[61] K. Johnson, R. Willey and M. Baker, *Vacuum polarization in quantum electrodynamics*, *Phys. Rev.* **163** (1967) 1699 [inSPIRE].

[62] J.L. Rosner, *Higher-order contributions to the divergent part of Z(3) in a model quan tum electrodynamics*, *Annals Phys.* **44** (1967) 11 [inSPIRE].

[63] M.J. Levine and R. Roskies, *Hyperspherical approach to quantum electrodynamics - sixth-order magnetic moment*, *Phys. Rev. D* **9** (1974) 421 [inSPIRE].

[64] M.J. Levine, E. Remiddi and R. Roskies, *Analytic contributions to the g factor of the electron in sixth order*, *Phys. Rev. D* **20** (1979) 2068 [inSPIRE].

[65] W. Celmaster and R.J. Gonsalves, *Fourth Order QCD Contributions to the e+ e- Annihilation Cross-Section*, *Phys. Rev. D* **21** (1980) 3112 [INSPIRE].

[66] A.E. Terrano, *A Method for Feynman Diagram Evaluation*, *Phys. Lett. B* **93** (1980) 424 [INSPIRE].

[67] K.G. Chetyrkin, A.L. Kataev and F.V. Tkachov, *New Approach to Evaluation of Multiloop Feynman Integrals: The Gegenbauer Polynomial x Space Technique*, *Nucl. Phys. B* **174** (1980) 345 [INSPIRE].

[68] K.G. Chetyrkin, A.L. Kataev and F.V. Tkachov, *Progress In Multiloop Renormalization Group Calculations*, preprint IYaI-P-0200 (1981).

[69] R.Z. Roskies, M.J. Levine and E. Remiddi, *Analytic evaluation of sixth order contributions to the electron's g factor*, *Adv. Ser. Direct. High Energy Phys.* **7** (1990) 162 [INSPIRE].

[70] F. Jegerlehner and A. Nyffeler, *The Muon g-2*, *Phys. Rept.* **477** (2009) 1 [arXiv:0902.3360] [INSPIRE].

[71] R. Barbieri and E. Remiddi, *Electron and Muon 1/2(g-2) from Vacuum Polarization Insertions*, *Nucl. Phys. B* **90** (1975) 233 [INSPIRE].

[72] N.N. Bogolyubov and D.V. Shirkov, *Introduction to the theory of quantized fields*, Wiley-Interscience, New York (1959) [INSPIRE].

[73] M. Abramowitz and I.A. Stegun eds., *Handbook of Mathematical Functions*, Dover Publications, New York (1965).

[74] F.W.J. Olver and L.C. Maximon, *Chapter 10 Bessel Functions*, https://dlmf.nist.gov/10.

[75] I.S. Gradshteyn and I.M. Ryzhik, *Table of Integrals, Series, and Products*, Elsevier Science (2014).

[76] G.N. Watson, *A Treatise on the Theory of Bessel Functions*, Cambridge University Press (1944).

[77] A.P. Prudnikov, Yu.A. Brychkov and O.I. Marichev, *Integrals and Series. Volume 2: Special functions*, Gordon and Breach Science Publishers (1986).

[78] N. Asmussen, *Position-Space Approach to the Hadronic Light-by-Light Scattering Contribution to the Anomalous Magnetic Moment of the Muon on the Lattice*, Ph.D. thesis, Johannes Gutenberg University Mainz (2018).

[79] *Numerical Recipes in C: The Art of Scientific Computing*, 2nd edition, Cambridge University Press (1992).

[80] S.G. Johnson, *Cubature*, version 1.02 https://github.com/stevengj/cubature.

[81] M. Passera, private communication.

[82] S. Laporta and E. Remiddi, *The Analytical value of the electron light-light graphs contribution to the muon (g-2) in QED*, *Phys. Lett. B* **301** (1993) 440 [INSPIRE].

[83] J.H. Kuhn, A.I. Onishchenko, A.A. Pivovarov and O.L. Veretin, *Heavy mass expansion, light by light scattering and the anomalous magnetic moment of the muon*, *Phys. Rev. D* **68** (2003) 033018 [hep-ph/0301151] [INSPIRE].

[84] S. Sint and P. Weisz, *Further results on O(a) improved lattice QCD to one loop order of perturbation theory*, *Nucl. Phys. B* **502** (1997) 251 [hep-lat/9704001] [INSPIRE].

[85] A. Gerardin, T. Harris and H.B. Meyer, *Nonperturbative renormalization and O(a)-improvement of the nonsinglet vector current with $N_f = 2 + 1$ Wilson fermions and tree-level Symanzik improved gauge action*, *Phys. Rev. D* **99** (2019) 014519 [arXiv:1811.08209] [INSPIRE].

[86] N. Asmussen, A. Gérardin, A. Nyffeler and H.B. Meyer, *Hadronic light-by-light scattering in the anomalous magnetic moment of the muon*, *SciPost Phys. Proc.* **1** (2019) 031 [arXiv:1811.08320] [INSPIRE].

[87] M. Bruno et al., *Simulation of QCD with $N_f = 2 + 1$ flavors of non-perturbatively improved Wilson fermions*, *JHEP* **02** (2015) 043 [arXiv:1411.3982] [INSPIRE].

[88] M. Bruno, T. Korzec and S. Schaefer, *Setting the scale for the CLS $2 + 1$ flavor ensembles*, *Phys. Rev. D* **95** (2017) 074504 [arXiv:1608.08900] [INSPIRE].

[89] J. Bijnens and J. Relefors, *Pion light-by-light contributions to the muon $g − 2$*, *JHEP* **09** (2016) 113 [arXiv:1608.01454] [INSPIRE].

[90] J. Parrino, *The Two-Loop Vacuum Polarization in Euclidean Coordinate Space*, Master Thesis, Joh. Gutenberg Universität Mainz (Nov. 2019).

[91] Ch. L. Schröder, *The Gegenbauer polynomial coordinate space technique applied to massive Feynman integrals*, B.Sc. Thesis, Joh. Gutenberg Universität Mainz (Aug. 2019).

[92] V. Biloshytskyi et al., *Forward light-by-light scattering and electromagnetic correction to hadronic vacuum polarization*, *JHEP* **03** (2023) 194 [arXiv:2209.02149] [INSPIRE].

[93] H.B. Meyer, *Lorentz-covariant coordinate-space representation of the leading hadronic contribution to the anomalous magnetic moment of the muon*, *Eur. Phys. J. C* **77** (2017) 616 [arXiv:1706.01139] [INSPIRE].

[94] X. Feng and L. Jin, *QED self energies from lattice QCD without power-law finite-volume errors*, *Phys. Rev. D* **100** (2019) 094509 [arXiv:1812.09817] [INSPIRE].

[95] M. Luscher and S. Schaefer, *Lattice QCD with open boundary conditions and twisted-mass reweighting*, *Comput. Phys. Commun.* **184** (2013) 519 [arXiv:1206.2809] [INSPIRE].

[96] *KQED*, https://github.com/RJHudspith/KQED.

[97] *GNU General Public License*, https://www.gnu.org/licenses/gpl-3.0.en.html.

[98] *KAMU*, https://github.com/RJHudspith/KAMU.